In the name of Allah, the Most Beneficent, the Most Merciful

Wiener-Hopf Analysis of EM-Wave Diffraction by a Finite Plate in Cold Plasma

By

Sajjad Hussain

Department of Mathematics
Quaid-i-Azam University
Islamabad, Pakistan
2020

Wiener-Hopf Analysis of EM-Wave Diffraction by a Finite Plate in Cold Plasma

By

Sajjad Hussain

Supervised By

Prof. Dr. Muhammad Ayub

Department of Mathematics
Quaid-i-Azam University
Islamabad, Pakistan
2020

Wiener-Hopf Analysis of EM-Wave Diffraction by a Finite Plate in Cold Plasma

By

Sajjad Hussain

A THESIS SUBMITTED IN THE PARTIAL FULFILLMENT OF THE REQUIREMENT FOR THE

DEGREE OF

DOCTOR OF PHILOSOPHY
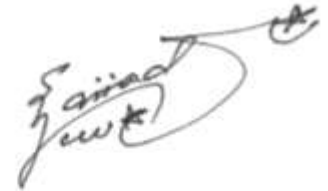
IN

MATHEMATICS

Supervised By

Prof. Dr. Muhammad Ayub

Department of Mathematics
Quaid-i-Azam University
Islamabad, Pakistan
2020

Author's Declaration

I, **Sajjad Hussain,** hereby state that my Ph. D thesis titled **Wiener-Hopf Analysis of EM-Wave Diffraction by a Finite Plate in Cold Plasma** is my own work and has not been submitted previously by me for taking any degree from the Quaid-i-Azam University Islamabad, Pakistan or anywhere else in the country/world.

At any time if my statement is found to be incorrect even after my graduate the university has the right to withdraw my Ph. D degree.
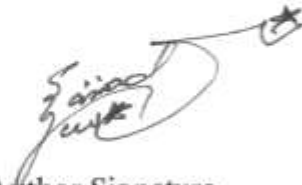
Name of Student: **Sajjad Hussain**

Date: **09 Dec 2020**

Plagiarism Undertaking

I solemnly declare that research work presented in the thesis titled "**Wiener-Hopf Analysis of EM-Wave Diffraction by a Finite Plate in Cold Plasma**" is solely my research work with no significant contribution from any other person. Small contribution/help wherever taken has been duly acknowledged and that complete thesis has been written by me.

I understand the zero tolerance policy of the HEC and **Quaid-i-Azam University** towards plagiarism. Therefore, I as an Author of the above titled thesis declare that no portion of my thesis has been plagiarized and any material used as reference is properly referred/cited.

I undertake that if I am found guilty of any formal plagiarism in the above titled thesis even afterward of Ph. D degree, the University reserves the rights to withdraw/revoke my Ph. D degree and that HEC and the University has the right to publish my name on the HEC/University Website on which names of students are placed who submitted plagiarized thesis.

Student/Author Signature

Name: **Sajjad Hussain**

Wiener-Hopf Analysis of EM-Wave Diffraction by a Finite Plate in Cold Plasma
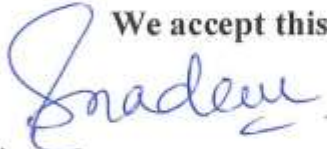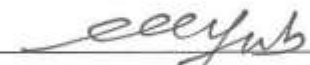
By

Sajjad Hussain

CERTIFICATE

A THESIS SUBMITTED IN THE PARTIAL FULFILLMENT OF THE
REQUIREMENTS FOR THE DEGREE OF THE

DOCTOR OF PHILOSOPHY IN MATHEMATICS

We accept this thesis as conforming to the required standard

1. _____

Prof. Dr. Sohail Nadeem
(Chairman)

2. _____

Prof. Dr. Muhammad Ayub
(Supervisor)

3. _____

Dr. Rahmat Ellahi
(External Examiner)

4. _____

Dr. Nasir Ali
(External Examiner)

Department of Mathematics & Statistics,
Faculty of Basics Applied Sciences,
International Islamic University, Islamabad.

Department of Mathematics & Statistics,
Faculty of Basics Applied Sciences,
International Islamic University, Islamabad.

Department of Mathematics
Quaid-I-Azam University
Islamabad, Pakistan
2020

Certificate of Approval

This is to certify that the research work presented in this thesis entitled **Wiener-Hopf Analysis of EM-Wave Diffraction by a Finite Plate in Cold Plasma** was conducted by **Mr. Sajjad Hussain** under the kind supervision of **Prof. Dr. Muhammad Ayub**. No part of this thesis has been submitted anywhere else for any other degree. This thesis is submitted to the Department of Mathematics, Quaid-i-Azam University, Islamabad in partial fulfillment of the requirements for the degree of Doctor of Philosophy in field of Mathematics from Department of Mathematics, Quaid-i-Azam University Islamabad, Pakistan.

Student Name: **Sajjad Hussain**   Signature:_____

External committee:

a) **External Examiner 1**:   Signature:_____
   Name: **Dr. Rahmat Ellahi**
   Designation: Associate Professor
   Office Address: Department of Mathematics & Statistics, Faculty of Basics Applied Sciences, International Islamic University, Islamabad.

b) **External Examiner 2**:   Signature:_____
   Name: **Dr. Nasir Ali**
   Designation: Associate Professor
   Office Address: Department of Mathematics & Statistics, Faculty of Basics Applied Sciences, International Islamic University, Islamabad.

c) **Internal Examiner**   Signature:_____
   Name: **Prof. Dr. Muhammad Ayub**
   Designation: Professor
   Office Address: Department of Mathematics, Quaid-i-Azam University, Islamabad.

Supervisor Name: Signature:_____
Prof. Dr. Muhammad Ayub

Name of Dean/ HOD   Signature:_____

Prof. Dr. Sohail Nadeem

Acknowledgement

*All praises and glories be to **Allah, the Creator,** Who created everything from spinning electrons to spiraling galaxies with astonishing beauty and symmetry. Thank Allah Almighty for His uncountable blessings on **Ummat-e-Musalma** due to **Ahl-e-Bait, Panjtan Pak** and all **Sahaba-e-Karaam,** Who urge us to unveil the truth behind the natural phenomenon which gives us motivation for research.*

*I would also like to express my heartiest gratitude to my worthy supervisor **Sir Professor Dr. Muhammad Ayub** (Passionate and Great Mathematician) for his constant guidance, support, valuable discussions, and inspiring attitude throughout my research work. Here I especially like to mention that he has been very kind to me, without his motivational encouragement I would never be able to complete this dissertation. It was a great privilege and honor for me to work under his kind supervision. I thank him for housing me as a research student and providing me with all his valuable ideas and time.*

*At this great occasion, I can never forget my teachers what they have taught me, especially the thought provoking lectures and inspiring personality of **Prof. Dr. Tasawar Hayat** (Distinguished National Professor), **Prof. Dr. Sohail Nadeem, Prof. Dr. Tariq Shah, Dr. Umar Hayat, Dr. Amjad Hussain, Dr. Khalid Saifullah, Dr. Munir, Mr. Mehdi, Mr. Arif Javed, Mr. Arshad, Mr. Muhammad Ilyas, Mr. Tariq, Mr. Sajjad and Mr. Saadat Rafique.***

*I want to convey my deepest thanks and compliments by the core of heart to my beloved father **Haji Ahmed.** Despite facing many hardships, he supported and encouraged me continuously for completion of my Ph. D degree. And especially to my beloved mother **Rashmina Kousar** whose support has been as important for me as my father's. I can never forget their sacrifice for me. Their unconditional love for me is priceless.*

*It is honor for me to mention the great personalities and heroes who have been a source of inspiration. These great personalities and heroes are **Quaid-e-Azam Muhammad Ali Jinnah, Dr. Allama Muhammad Iqbal, Abdul Sattar Edhi, Allama Khadim Hussain Rizvi, Tariq Aziz** and **martyrs of Islam** and **Pakistan.** I would also like to pay special thanks to my **grandparents,** maternal uncles **Tanveer Hussain (Late), Muhammad Rafique, Muhammad Shafique,***

At the end I would like to mention what my heartbeat sounds,

★ *Shukriya Pakistan,* ★

★ *Muskra Pakistan.* ★

Sajjad Hussain

I dedicate this thesis to my beloved

⭐ *Holy Prophet (SAW)* ⭐

⭐ *Mola Ali (A.S)* ⭐

⭐ *Pakistan* ⭐

⭐ *Parents* ⭐

&

⭐ *Supervisor* ⭐

Preface

Propagation of electromagnetic (EM) waves play a vital role in communication system. The ultraviolet radiations impinging on earth's atmosphere ionize a fraction of neutral atmosphere which results into a mixture of charged particles (i.e. ions and electrons) as well as neutral particles. Since the collisions in the region of earth's atmosphere above 80 km from earth, are very rare, therefore, under such conditions the recombination rate of charged species is very slow resulting a permanent ionized medium, named as ionosphere. A cold plasma may correspond to ionosphere under the presence of earth's magnetic field where the effect of finite temperature and pressure variations are ignored. The ionosphere of plasma is highly magnetized under earth's magnetic field; therefore, it can be treated as an anisotropic medium. Also, since the cold plasma can be considered as a model for the ionosphere, it is possible to investigate the diffraction mechanisms of the complex scatterers in the ionosphere such as airplanes or satellites. Measurements based on the artificial satellites moving in the ionosphere around the earth, communicating to earth station are affected drastically as the communicating signals radiated by satellite and diffracted by some obstacle get modified on interaction with ionosphere plasma (cold plasma) and also because of the nature of material of the body i.e. electric and magnetic susceptibilities or impedance. To quantify the results arising due to the effectiveness of cold plasma and nature of the material on the diffraction of electromagnetic waves, some theoretical models have been devised in the present thesis. Thesis is summarized in the order below.

Chapter one contains literature survey of previous research study by the researchers, some basic description of plane wave, Fourier transform, cold plasma, analytic continuation, method of

stationary phase (an asymptotic method) and a short note on Wiener-Hopf technique for general readers.

Chapter two addresses diffraction of electromagnetic plane wave by a finite plate in the cold plasma. Helmholtz equation is derived with the combined use of Maxwell's equations and electric field components in terms of magnetic field with cold plasma effects. Dirichlet boundary conditions assumed along the plate. Fourier transform is applied on the problem and using the general theory of Wiener-Hopf procedure is used to obtain the Wiener-hopf equation. The required diffracted field is obtained by inverse Fourier transform and then by the method of stationary phase. Graphs are plotted to analyze that how the separated field (diffracted field by finite plate) is affected by physical parameters in the presence and absence of cold plasma. The contents of this chapter are published in **Physics of Wave Phenomena 26 (2018) 342-350.**

Chapter three explores the diffracted electromagnetic plane wave by a finite plate in the cold plasma. Helmholtz equation is derived with the combined use of Maxwell's equations and electric field components in terms of magnetic field with cold plasma effects. Neumann boundary conditions assumed along the plate. Fourier transform is applied on the problem and using the general theory of Wiener-Hopf procedure is used to obtain the Wiener-Hopf equation. The required diffracted field is obtained by inverse Fourier transform and then by the method of stationary phase. Graphs are plotted to analyze that how the separated field (diffracted field by finite plate) is affected by physical parameters in the presence and absence of cold plasma. The contents of this chapter are published in **Plasma Physics Reports 46 (2020) 1-9.**

Chapter four examines the diffracted electromagnetic plane wave by a finite plate in the cold plasma. Impedance is assumed on upper and lower surface of the plate. Therefore, Leontovich

boundary conditions are considered to study the effects of impedance on separated field. Helmholtz equation is derived with the combined use of Maxwell's equations and electric field components in terms of magnetic field with cold plasma effects. Fourier transform is applied on the problem and using the general theory of Wiener-Hopf procedure is used to obtain the Wiener-Hopf equations. The required diffracted field is obtained by inverse Fourier transform and then by the method of stationary phase. Graphs are plotted to analyze that how the separated field (diffracted field by finite plate) is affected by physical parameters in the presence and absence of cold plasma.

Chapter five describes the diffracted electromagnetic plane wave by a symmetric finite plate in the cold plasma. Impedance on upper and lower surface of the plate is taken into an account. Leontovich boundary conditions are used to analyze the effects of impedance on the diffracted field by symmetric plate of finite length. Helmholtz equation is derived with the combined use of Maxwell's equations and electric field components in terms of magnetic field with cold plasma effects. Fourier transform is applied on the problem and using the general theory of Wiener-Hopf procedure is used to obtain the Wiener-Hopf equations. The required diffracted field is obtained by inverse Fourier transform and then by the method of stationary phase. Graphs are plotted to analyze that how the separated field (diffracted field by finite plate) is affected by physical parameters in the presence and absence of cold plasma.

Chapter six presents the diffracted electromagnetic plane wave by a slit of finite width in the cold plasma. Surface Helmholtz equation is derived with the combined use of Maxwell's equations and electric field components in terms of magnetic field with cold plasma effects. Fourier transform is applied on the problem and using the general theory of Wiener-Hopf procedure is used to obtain the Wiener-Hopf equations. The required diffracted field is obtained by inverse

Fourier transform and then by the method of stationary phase. Graphs are plotted to analyze that how the separated field (diffracted field by finite plate) is affected by physical parameters in the presence and absence of cold plasma.

Contents

Nomenclature

$\bar{\varepsilon}$	dielectric permittivity tensor
$\varepsilon_1,\ \varepsilon_2,\ \varepsilon_z$	elements of dielectric permittivity tensor
ω	operating frequency
ω_p	plasma frequency
ω_c	cyclotron frequency
e	electric charge
N_e	electron density
H_{dc}	magnitude of dc magnetic field vector
H_z	magnetic field perpendicular to the plane
η_s	surface impedance
η_0	free surface impedance
ε_0	electric permittivity in vacuum
μ_0	magnetic permeability
l	length parameter for plate and width parameter for slit
k_{eff}	propagation constant
k	wave-number
θ_0	angle of incidence
θ	observation angle
EM	electromagnetic

Chapter 1

Related literature survey and Basic laws

Review of previous related studies for diffraction of electromagnetic waves by semi-infinite, finite plates, slit and other different obstacles is made. Methodology of solution is briefly discussed.

1.1   Background

The scattering of waves by semi-infinite plane, infinite plane, finite plane, slits of finite width, gratings and periodic surfaces has always been a great interest of analysis for researchers in the field of optics and electromagnetic theory. Regarding the scattering analysis, various analytical and numerical techniques have been established so far and many different structures have been assumed as an obstacle to study the diffraction phenomena. The scattering and diffraction problems are tackled most efficiently by using the number of methods of research. Poincare [1] and Sommerfeld [2] studied the half-plane problems which explored the new ideas for extensive study of scattering of sound and electromagnetic waves. The Wiener-Hopf technique [3,4] as a function of group theoretic approach for analysis of propagation of waves and scattering problems related to canonical geometries was studied rigorously. Riemann-Hilbert method had been considered in the theory of diffraction and propagation of

electromagnetic waves [5]. The mode-matching method had been applied for the analysis of electromagnetic wave scattering [6]. Several classical problems based on the analysis of line-source and point-source diffraction of electromagnetic waves had been investigated which presented a canonical problem corresponding to the model for GTD (geometrical theory diffraction). Kobayashi [7] studied and then investigated the diffracted wave by a strip in using Wiener-Hopf technique to evaluate the exact and asymptotic solutions. A brief historical perspective of Wiener-Hopf technique may be found in [8]. Diffraction phenomena of the plane waves by a finite plate under the assumption of impedance on both sides of the surface of plate was investigated using Wiener-Hopf technique [9].

The models proposed to elaborate the diffraction phenomena of electromagnetic (EM) waves by an infinite slit in the conductible screen have been brought under the rigorous investigation through mathematical analysis. Morse and Rubenstein [10] used the method of separation of variables for investigation of acoustic waves diffracted by slits and ribbon. Clemmow [11] proposed a mathematical model for diffraction by slit in which he derived a dual integral equation using spectrum description of electromagnetic (EM) fields. He assumed the width of slit much larger or greater than the wavelength giving the two complementary cases under the approximate analysis. Hongo [12] investigated the diffraction phenomena due to parallel slits in the conducting screen in which he used the Kobayashi potential technique. Imran et al. extended the Hongo's work to the slits in an impedance plane. He used the Kobayashi potential technique to investigate the problem rigorously [13].

The EM-waves (electromagnetic waves) propagating across an ionized gas has got the significant attention of researchers for many years. The scientists have studied extensively on the radio waves or signals reflected from and transmitted through the ionosphere [14-16]. It is known that plasma is such an ionized gas which is electrically neutral and consists of substantially the same electron and ion densities. The study of the problems modeled for the antenna characteristics, propagation of waves through the plasma and radar cross section are of great importance. The wave propagation

and antenna characteristics of artificial satellites play a vital role in communicating the signals between the earth station and vehicles. The frequent existence of dc magnetic field in plasma allows it to behave as an anisotropic, the best example is here that the earth magnetic field is effective in cold plasma. The small and negligible effect of pressure variations and finite temperature make plasma as a cold plasma. While analyzing the diffraction problem, researchers thought to investigate the effects of cold plasma. Keeping focus on that idea, scientists worked on the scattering of electromagnetic for different structures in the presence of cold plasma. The diffracted electromagnetic plane wave by a half-plane with impedance had been studied to investigate the effects of cold plasma using Wiener-Hopf technique [17]. Khan et al. analyzed the diffracted E-polarized plane wave by parallel plate wave-guide with imposition of impedance immersed in cold plasma, Wiener-Hopf technique along with mode matching analysis was used [18]. Ayub et al. investigated the affecting cold plasma on the dominant TEM-wave radiated by parallel plate wave-guide with imposition of impedance, radiator behaving as a horn type launcher of surface wave and a horn with impedance loaded [19]. The diffraction of EM-plane wave by a finite plate under the effects of cold plasma was investigated using Wiener-Hopf technique by assuming Dirichlet conditions on the plate [20].

1.2   Plane Wave

The waves of the following form

$$\psi(x, y, z, t) = \mathfrak{Re} \left\{ \psi_0 \exp(\pm \iota \vec{k} \cdot \vec{r} - \iota \omega t) \right\}, \tag{1.1}$$

are called plane waves of homogeneous waves. The sign of plus the exponent presents the wave propagating in the direction of $\vec{k} = [k_x, k_y, k_z]$ which are denoted outgoing waves. On the other hand, the sign of minus indicates the incoming waves which propagate in the opposite direction of $\vec{k}$.

1.3 Cold Plasma (Non-thermal Plasma)

Plasma being a fourth or gaseous state of matter is an ionized gas which is electrically neutral medium and contains substantially the same densities of ions and electrons. If the effects of variations of the finite pressure force and temperature are taken to be small and ignored then plasma is termed as cold plasma. For example, cold plasma can be found in the flow discharge in a fluorescent tube.

1.4 Fourier Transform

This method of complex integral transformation is a mathematical tool which helps in solving the differential equations. This mathematical tool can be utilized for majority of the problems of finite and infinite domain. First suppose that s is real then usual Fourier integral transform of $f(x)$ for all $x \in \Re$ can be defined as

$$F(s) = \int_{-\infty}^{\infty} f(x)e^{\iota s x}dx, \tag{1.2}$$

and inversion can be defined as

$$f(x) = \frac{1}{2\pi} \int_{-\infty}^{\infty} F(\alpha)e^{-\iota \alpha x}ds. \tag{1.3}$$

Now suppose that $\alpha = \sigma + \iota\tau$ is a complex variable. We can define generalized Fourier transform under suitable conditions on f. By starting with half-range transforms, if $|f(x)| < A_1 e^{\tau_- x}$ as $x \to \infty$ and $f(x) = 0$ for $x < 0$, where $A_1 > 0$ and τ_- are constants, then we have following function

$$F_+(\alpha) = \int_{0}^{\infty} f(x)e^{\iota \alpha x}dx, \tag{1.4}$$

which is analytic in the region $\tau > \tau_-$ of complex $s-$plane. Now the inverse Fourier transform of $F_+(\alpha)$ can found as

$$f(x) = \frac{1}{2\pi} \int_C F_+(\alpha) e^{-\iota s x} ds, \tag{1.5}$$

where C is a path of integration lying in the region of analyticity on which σ varies from $-\infty$ to ∞.

Similarly, if $f(x) = 0$ for $x > 0$ and $|f(x)| < A_2 e^{\tau_+ x}$ as $x \to -\infty$, where $A_2 > 0$ and τ_+ are constants, then

$$F_-(\alpha) = \int_{-\infty}^{0} f(x) e^{\iota s x} dx, \tag{1.6}$$

which is analytic in the region $\tau < \tau_+$ of complex $s-$plane. Now the inverse Fourier transform of $F_-(\alpha)$ can found as

$$f(x) = \frac{1}{2\pi} \int_C F_-(s) e^{-\iota \alpha x} ds, \tag{1.7}$$

where C is a path of integration lying in the region of analyticity on which σ varies from $-\infty$ to ∞. If the above results for half range transforms are combined as

$$|f(x)| < \begin{cases} A_1 e^{\tau_- x} & \text{as } x \to \infty \\ A_2 e^{\tau_+ x} & \text{as } x \to -\infty \end{cases} \tag{1.8}$$

with $\tau_- < \tau_+$, then Fourier transform for full-range defined by (1.2) is an analytic function of s in the band of analyticity (strip) $\tau_- < \tau < \tau_+$ and inverse Fourier transform is defined by (1.3) with path of integration lying within the band of analyticity.

1.5   Analytic Continuation

If $f(z)$ is an analytic function in a domain $\mathfrak{D}$ and $F(z)$ is analytic in a domain $\mathfrak{D}'$ such that $F(z) = f(z)$ in $\mathfrak{D}$ and $\mathfrak{D} \subset \mathfrak{D}'$, then F is said to be an analytic continuation

of f.

Now we can say that analytic continuation is a process of extending an analytic function defined in a domain to a larger domain. For example, the geometric series at zero is given by

$$f(z) = 1 + z + z^2 + z^3 \cdots, \tag{1.9}$$

which is convergent in the open disk as $\mathfrak{D} = \{|z| < 1\}$. Multiplication of (1.1) by z and subtraction of result from (1.9) gives

$$(1-z)f(z) = 1 \quad \Rightarrow f(z) = \frac{1}{1-z}. \tag{1.10}$$

Now we write (1.10) as

$$F(z) = \frac{1}{1-z}, \tag{1.11}$$

which is analytic in $\mathfrak{D}' = \mathcal{C}\backslash\{1\}$. Since $\{|z| < 1\} \subset \mathfrak{C}\backslash\{1\}$ i.e. $\mathfrak{D} \subset \mathfrak{D}'$ and $F(z) = f(z)$ therefore, $F(z)$ is analytic continuation of $f(z)$.

1.6 Method of Stationary Phase

Consider a function of the form

$$f(x) = \int_a^b e^{\iota x h(t)} g(t) dt, \tag{1.12}$$

where $h(t)$ is a real function (known as phase function) and $g(t)$ can be complex or real function and integration is along the real axis over the interval (a, b). The stationary phase method helps in finding an asymptotic representation of (1.12). Assume that there is one point $t_0 \in (a, b)$ such that $h'(t_0) = 0$ but $h''(t_0) \neq 0$. In accordance with the idea of the method of stationary phase, we assume that only the neighborhood of the point t_0 is of significance, and we write

$$\iota x h(t) \cong \iota x \left\{ h(t_0) + \frac{1}{2} h''(t_0)(t - t_0)^2 \right\}. \tag{1.13}$$

10

Then

$$f(x) \sim \int_{-\infty}^{\infty} g(t_0) \exp\left[\iota x \left\{ h(t_0) + \frac{1}{2} h''(t_0)(t - t_0)^2 \right\}\right] dt \qquad (1.14)$$

This gives

$$f(x) \sim \left[\frac{2\pi}{x|h''(t_0)|}\right]^{1/2} g(t_0) \exp\left[\iota x h(t_0) \pm \iota \frac{\pi}{4}\right] \qquad (1.15)$$

where the sign of $+$ or $-$ corresponds to $h''(t_0) > 0$ or $h''(t_0) < 0$, respectively. For deep analysis about this method, see [21, 22]

1.7   Wiener-Hopf technique

This technique was initially utilized to solve the integral equation which presents most of physical problems. An integral equation of that form is given by

$$\int_0^{\infty} K(x - y)f(y)dy = g(x), \quad 0 < x < \infty \qquad (1.16)$$

where the kernel difference $k(x - y)$ and $g(x)$ are known functions while the $f(x)$ is the function to be evaluated. The readers interested to know about this technique generally, can study the salient points which are briefly outlined here. To proceed the method, domain of integral equation is extended to negative real values of x that is

$$\int_0^{\infty} k(x - y)f(y)dy = \begin{cases} g(x), & 0 < x < \infty \\ h(x), & -\infty < x < 0 \end{cases} \qquad (1.17)$$

where $h(x)$ is an unknown function. Applying the Fourier transform on (1.17) we get the Wiener-Hopf functional equation

$$G_+(\alpha) + H_-(\alpha) = K(\alpha)F_+(\alpha) \qquad (1.18)$$

in which $G_+(\alpha)$ and $K(\alpha)$ are half-range and full-range Fourier transform of known functions $g(x)$ and $k(x)$, respectively whereas the quantities $H_-(\alpha)$ and $F_+(\alpha)$ are

half-range Fourier transform of unknown functions $h(x)$ and $f(x)$, respectively. The right side of (1.18) is product form which comes from original integral operator being a convolution type. The subscripts $+, -$ indicate the region of analyticity for their respective functions. The functions with subscript $+$ are analytic in the upper half of complex $\alpha-$plane and those with subscript $-$ are analytic in the lower half of complex $\alpha-$plane and they overlap to form a strip or band of analyticity in which all these functions are analytic. The Wiener-Hopf procedure depends on the product factorization of transformed kernel function $K(\alpha)$, in the form

$$K(\alpha) = K_+(\alpha)K_-(\alpha). \tag{1.19}$$

Use (1.19) enables to re-write (1.18) as

$$\frac{G_+(\alpha)}{K_-(\alpha)} + \frac{H_-(\alpha)}{K_-(\alpha)} = K_+(\alpha)F_+(\alpha). \tag{1.20}$$

Note that right hand side is analytic in its indicated region of analyticity. For left hand side, first term needs to be tackled therefore, defining the sum-factorization for first term on the left hand side, in the form of

$$\frac{G_+(\alpha)}{K_-(\alpha)} = L_+(\alpha) + L_-(\alpha). \tag{1.21}$$

Inserting (1.21) in (1.20) and re-expressing the resulting equation as

$$L_-(\alpha) + \frac{H_-(\alpha)}{K_-(\alpha)} = K_+(\alpha)F_+(\alpha) - L_+(\alpha), \tag{1.22}$$

in which left hand side shows analytic behavior in the lower-half of complex $\alpha-$plane and right hand side shows analytic behavior in the overlapping upper-half plane of complex $\alpha-$plane. Analytic continuation allows to equate both sides of (1.22) to an entire function, $\mathfrak{J}(\alpha)$, say. $\mathfrak{J}(\alpha)$ may be evaluated or specified under the physical constraints on the behavior of functions $f(x)$, $g(x)$, $h(x)$ as $x \to 0$ and their corresponding transformed functions in (1.22) as $|\alpha| \to \infty$, and hence, $F_+(\alpha)$ and $H_-(\alpha)$

12

are uniquely evaluated. The inverse Fourier transform finally results the required unknown function $f(x)$.

Chapter 2

Analysis of Diffracted Wave by a Finite Plate with Dirichlet Conditions in Cold Plasma

This chapter addresses the investigation of electromagnetic plane wave diffraction by a conducting plate of finite length in cold plasma. The boundary value problem along with Fourier transform for the corresponding is used to formulate Wiener-Hopf equation which is then solved by using Wiener-Hopf procedure in a standard way. The separated field is evaluated for an anisotropic medium using asymptotic expansion and modified stationary phase method. The results for the isotropic medium can be achieved by taking $\varepsilon_1 \longrightarrow 1$, $\varepsilon_2 \longrightarrow 0$. Graphical results are discussed for separated field against observation angle for various physical parameters in isotropic and anisotropic media.

2.1 Modelling of the Helmholtz Equation

The dielectric permittivity tensor evaluated for cold plasma is presented by

$$\bar{\varepsilon} = \begin{pmatrix} \varepsilon_1 & -\iota\varepsilon_2 & 0 \\ \iota\varepsilon_2 & \varepsilon_1 & 0 \\ 0 & 0 & \varepsilon_z \end{pmatrix}, \tag{2.1}$$

with

$$\varepsilon_1 = 1 - \left(\frac{\omega_p}{\omega}\right)^2 \left[1 - \left(\frac{\omega_c}{\omega}\right)^2\right]^{-1}, \ \varepsilon_2 = \left(\frac{\omega_p}{\omega}\right)^2 \left[\frac{\omega}{\omega_c} - \frac{\omega_c}{\omega}\right]^{-1}, \tag{2.2}$$

and

$$\varepsilon_z = 1 - \left(\frac{\omega_p}{\omega}\right)^2, \tag{2.3}$$

where

$$\omega_p^2 = \frac{N_e e^2}{m\varepsilon_0}, \qquad \omega_c = \frac{|e|\,\mu_0 H_{dc}}{m_e}. \tag{2.4}$$

Maxwell's equations, which are well-known, are proved to be valid in cold plasma with the dielectric permittivity tensor are used to obtain electric field components in expressions of the magnetic field H_z as given by

$$E_x = \frac{\iota\varepsilon_1}{\omega\varepsilon_0\,(\varepsilon_1^2 - \varepsilon_2^2)} \frac{\partial H_z\,(x,y)}{\partial y} + \frac{\varepsilon_2}{\omega\varepsilon_0\,(\varepsilon_1^2 - \varepsilon_2^2)} \frac{\partial H_z\,(x,y)}{\partial x}, \tag{2.5}$$

and

$$E_y = \frac{\varepsilon_2}{\omega\varepsilon_0\,(\varepsilon_1^2 - \varepsilon_2^2)} \frac{\partial H_z\,(x,y)}{\partial y} - \frac{\iota\varepsilon_1}{\omega\varepsilon_0\,(\varepsilon_1^2 - \varepsilon_2^2)} \frac{\partial H_z\,(x,y)}{\partial x}. \tag{2.6}$$

Then the Helmholtz's equation satisfying H_z can be obtained using Maxwell's equations along with (2.5) and (2.6), as given below:

$$\partial_{xx} H_z\,(x,y) + \partial_{yy} H_z\,(x,y) + k_{eff}^2 H_z\,(x,y) = 0, \tag{2.7}$$
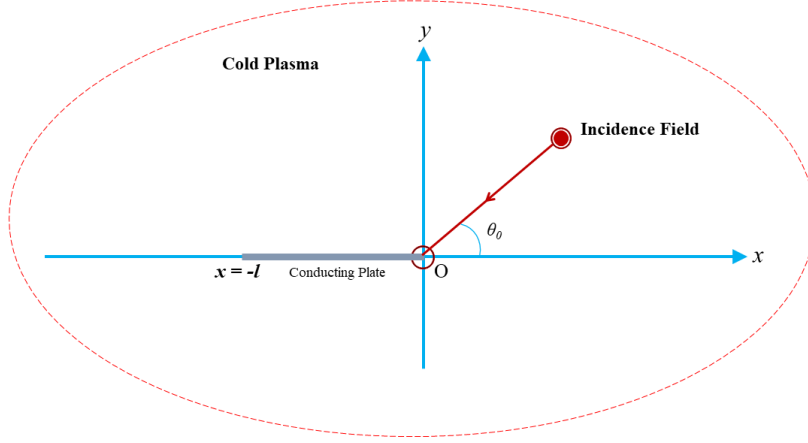
Figure 2.1: **Geometrical description of the model.**

where propagation constant is

$$k_{eff} = k\sqrt{\frac{\varepsilon_1^2 - \varepsilon_2^2}{\varepsilon_1}}, \qquad k = \omega\sqrt{\varepsilon_0\mu_0}. \tag{2.8}$$

Here, k_{eff} is dependent of k, ε_1 and ε_2, time is taken as behaving harmonically as $\exp(-\iota\omega t)$ and will be considered as suppressed throughout the analysis.

2.2 Mathematical Modelling of the Problem

An EM-plane wave incident on a conducting non-symmetric plate of finite length is considered along $y = 0$ with extremities $x = -l$ and $x = 0$ of the plate, as can be seen in Fig. 2.1. The model is proposed for investigation of effects of cold plasma on diffraction phenomena. The total field can be expressed as a sum of $H_z^{inc}(x, y)$ and $H_z(x, y)$

$$H_z^{tot}(x, y) = H_z^{inc}(x, y) + H_z(x, y), \tag{2.9}$$

where $H_z(x, y)$ is the diffracted field and $H_z^{inc}(x, y)$ is the incident field of plane wave making an angle θ_0 with horizontal, which is defined as

$$H_z^{inc}(x, y) = \exp\{-\iota k_{eff}(x\cos\theta_0 + y\sin\theta_0)\}, \tag{2.10}$$

16

where k_{eff} is given in (2.8). Since the medium for present model is taken to be slightly lossy, so for convenience of analyticity, we can consider that $k_{eff} = \mathfrak{Re}\{k_{eff}\} + \iota\mathfrak{Im}\{k_{eff}\}$ has very small positive imaginary part $(0 < \mathfrak{Im}\{k_{eff}\} \ll \mathfrak{Re}\{k_{eff}\})$ and the solution for real of k_{eff} can be attained by assuming $\mathfrak{Im}\{k_{eff}\} \longrightarrow 0$. The boundary value problem (BVP) under consideration is expressed in terms of the magnetic field and it is adequate to denote the diffracted field in different zones. The total field $H_z^{tot}(x, y)$ in the range $x \in (-\infty, \infty)$, satisfying the Helmholtz's equation as

$$\left[\partial_{xx} + \partial_{yy} + k_{eff}^2\right] H_z^{tot}(x, y) = 0. \tag{2.11}$$

The diffracted field satisfying Helmholtz's equation can be extracted from above equation as follows:

$$\left[\partial_{xx} + \partial_{yy} + k_{eff}^2\right] H_z(x, y) = 0. \tag{2.12}$$

Our aim is to determine the diffraction of incident electromagnetic (EM) plane wave by a finite plate in cold plasma. To proceed further suitable boundary conditions are required. Therefore, here for the present model, Dirichlet boundary conditions along the plate assumed as

$$H_z^{tot}(x, 0^\pm) = 0, \quad \text{for } -l \leq x \leq 0, \tag{2.13}$$

and continuity relations are taken into account, which are defined as

$$
\begin{aligned}
H_z^{tot}(x, 0^+) &= H_z^{tot}(x, 0^-), \quad \text{for } -\infty < x < -l, \ x > 0, \\
\partial_y H_z^{tot}(x, 0^+) &= \partial_y H_z^{tot}(x, 0^-), \quad \text{for } -\infty < x < -l, \ x > 0.
\end{aligned}
\tag{2.14}
$$

2.3 Transformation of Problem

Fourier transformation w.r.t x variable for the present model is defined as

$$\mathcal{F}(\alpha, y) = \frac{1}{\sqrt{2\pi}} \int_{-\infty}^{\infty} H_z(x, y) e^{\iota \alpha x} dx$$

$$= \mathcal{F}_+(\alpha, y) + e^{-\iota \alpha l} \mathcal{F}_-(\alpha, y) + \mathcal{F}_l(\alpha, y),$$

(2.15)

where $\alpha = \mathfrak{Re}\{\alpha\} + \iota \mathfrak{Im}\{\alpha\} = \sigma + \iota \tau$. The asymptotic behavior of $H_z(x, y)$ for $x \longrightarrow \pm\infty$ is taken into account which is defined as

$$H_z(x, y) = \begin{cases} O\left(e^{-\mathfrak{Im}\{k_{eff}\}x}\right) & \text{for } x \longrightarrow \infty, \\ O\left(e^{\mathfrak{Im}\{k_{eff}\}x \cos\theta_0}\right) & \text{for } x \longrightarrow -\infty. \end{cases}$$

(2.16)

$\mathcal{F}_+(\alpha, y)$ behaving as a regular function of α lies in the upper-half of the $\alpha-$plane i.e. in the region $\mathfrak{Im}\{-k_{eff}\} < \mathfrak{Im}\{\alpha\}$ and $\mathcal{F}_-(\alpha, y)$ behaving as a regular function of α lies in the lower-half of the $\alpha-$plane i.e. in the region $\mathfrak{Im}\{\alpha\} < \mathfrak{Im}\{k_{eff} \cos\theta_0\}$ and both these regions together form a band of analyticity (i.e. a common region where the upper- and lower-half planes are overlapped, can be seen in Fig. 2.2) and all the functions including $\mathcal{F}_l(\alpha, y)$ are analytic functions of α in that common region i.e. in the region $\mathfrak{Im}\{-k_{eff}\} < \mathfrak{Im}\{\alpha\} < \mathfrak{Im}\{k_{eff} \cos\theta_0\}$, thus, we can define

$$\mathcal{F}_+(\alpha, y) = \frac{1}{\sqrt{2\pi}} \int_0^{\infty} H_z(x, y) e^{\iota \alpha x} dx,$$

(2.17)

$$\mathcal{F}_-(\alpha, y) = \frac{1}{\sqrt{2\pi}} \int_{-\infty}^{-l} H_z(x, y) e^{\iota \alpha(x+l)} dx,$$

(2.18)

$$\mathcal{F}_l(\alpha, y) = \frac{1}{\sqrt{2\pi}} \int_{-l}^{0} H_z(x, y) e^{\iota \alpha x} dx.$$

(2.19)

$$\mathcal{F}^{inc}(\alpha, 0) = \frac{1 - e^{-\iota l\left(\alpha - k_{eff} \cos\theta_0\right)}}{\sqrt{2\pi}\iota\left(\alpha - k_{eff} \cos\theta_0\right)}.$$

(2.20)

Use of Fourier transform for (2.12)-(2.14) yields

$$\left(\frac{d^2}{dy^2} + \gamma^2\right) \mathcal{F}(\alpha, y) = 0, \tag{2.21}$$

where $\gamma(\alpha) = \sqrt{k_{eff}^2 - \alpha^2}$.

$$\mathcal{F}_l\left(\alpha, 0^+\right) = -\mathcal{F}^{inc}(\alpha, 0), \tag{2.22}$$

$$\mathcal{F}_l\left(\alpha, 0^-\right) = -\mathcal{F}^{inc}(\alpha, 0), \tag{2.23}$$

and

$$\begin{aligned}
\mathcal{F}_-\left(\alpha, 0^+\right) &= \mathcal{F}_-\left(\alpha, 0^-\right) = \mathcal{F}_-(\alpha, 0), \\
\mathcal{F}_+\left(\alpha, 0^+\right) &= \mathcal{F}_+\left(\alpha, 0^-\right) = \mathcal{F}_+(\alpha, 0), \\
\partial_y \mathcal{F}_-\left(\alpha, 0^+\right) &= \partial_y \mathcal{F}_-\left(\alpha, 0^-\right) = \partial_y \mathcal{F}_-(\alpha, 0), \\
\partial_y \mathcal{F}_+\left(\alpha, 0^+\right) &= \partial_y \mathcal{F}_+\left(\alpha, 0^-\right) = \partial_y \mathcal{F}_+(\alpha, 0).
\end{aligned} \tag{2.24}$$

2.4 Modelling of Wiener-Hopf Equation

The solution of (2.21) satisfying the radiation conditions is given by

$$\mathcal{F}(\alpha, y) = \begin{cases} A_1(\alpha) e^{-\iota\gamma y} & y \geq 0, \\ A_2(\alpha) e^{\iota\gamma y} & y < 0. \end{cases} \tag{2.25}$$

Now with the aid of (2.15) and (2.22)-(2.25), following Wiener-Hopf functional equation is computed as

$$\mathcal{F}_+(\alpha, 0) + e^{-\iota\alpha l}\mathcal{F}_-(\alpha, 0) + \mathcal{K}(\alpha)\tilde{\mathcal{F}}_l'(\alpha, 0) = \mathcal{A}\mathcal{G}(\alpha), \tag{2.26}$$

where $\mathcal{K}(\alpha)$ is the kernel function and given by

$$\mathcal{K}(\alpha) = \frac{1}{\iota\gamma}, \tag{2.27}$$
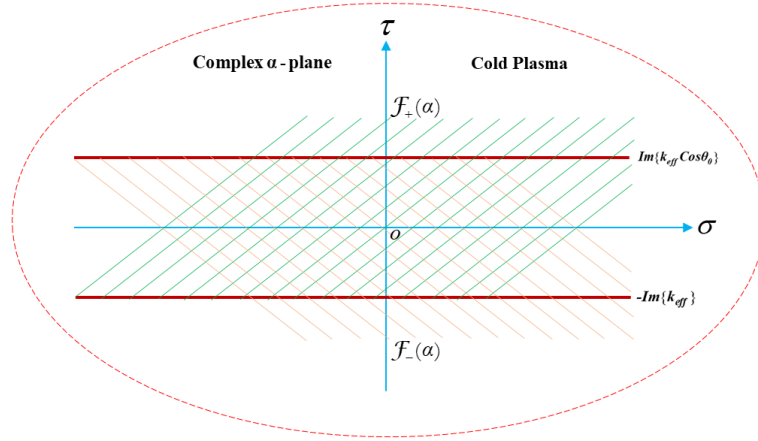
Figure 2.2: **The description of analytic continuation in the complex $\alpha-$plane.**

and

$$\tilde{\mathcal{F}}_l' \left(\alpha, 0 \right) = \frac{1}{2} \left[\mathcal{F}_l' \left(\alpha, 0^+ \right) - \mathcal{F}_l' \left(\alpha, 0^- \right) \right],\tag{2.28}$$

$$\mathcal{A} = -\iota \tag{2.29}$$

$$\mathcal{G}(\alpha) = \frac{1 - e^{-\iota \left(\alpha - k_{eff} \cos \theta_0 \right) l}}{\sqrt{2\pi} \left(\alpha - k_{eff} \cos \theta_0 \right)}.\tag{2.30}$$

2.5   Wiener-Hopf Procedure

The kernel function arising from (2.26), given in (2.27) is factorized as

$$\mathcal{K} \left(\alpha \right) = \frac{1}{\iota \gamma} = \mathcal{K}_+ \left(\alpha \right) \mathcal{K}_- \left(\alpha \right)\tag{2.31}$$

and

$$\gamma \left(\alpha \right) = \gamma_+ \left(\alpha \right) \gamma_- \left(\alpha \right),\tag{2.32}$$

The factors appearing in (2.31) and (2.32) are computed as

$$\mathcal{K}_\pm \left(\alpha \right) = \frac{e^{-\iota \frac{\pi}{4}}}{\sqrt{k_{eff} \pm \alpha}},\tag{2.33}$$

and

$$\gamma_+ \left(\alpha\right) = \sqrt{k_{eff} + \alpha}, \quad \gamma_- \left(\alpha\right) = \sqrt{k_{eff} - \alpha}. \tag{2.34}$$

The factors $\mathcal{K}_+ \left(\alpha\right)$ and $\gamma_+ \left(\alpha\right)$ are regular functions of α in upper-half of the $\alpha-$plane $\mathfrak{Im}\{-k_{eff}\} < \mathfrak{Im}\{\alpha\}$ whereas the factors $\mathcal{K}_- \left(\alpha\right)$ and $\gamma_- \left(\alpha\right)$ regular functions of α in the lower-half of the $\alpha-$plane $\mathfrak{Im}\{\alpha\} < \mathfrak{Im}\{k_{eff} \cos \theta_0\}$. The solution for large $k_{eff} r$ $\left(r = \sqrt{x^2 + y^2}\right)$ may be obtained in an approximate form on the basis of analysis made by using Wiener-Hopf technique. Equating the terms of (2.25) with positive sign on one side of the equation and the terms with negative sign on the other side results into the same function $\mathfrak{J}(\alpha)$, say, which is a polynomial function, thus $\mathfrak{J}(\alpha)$ is an entire function. Analytic continuation (see Fig. 2.2) along with arguments involving extended form of Liouville's theorem allows to equate the function $\mathfrak{J}(\alpha)$ to zero, hence, we obtain the following results

$$\mathcal{F}_+ \left(\alpha, 0\right) = \frac{A\mathcal{K}_+ \left(\alpha\right)}{\sqrt{2\pi}} \left(\mathcal{G}_1 \left(\alpha\right) + \mathcal{T} \left(\alpha\right) \mathcal{C}_1\right), \tag{2.35}$$

$$\mathcal{F}_- \left(\alpha, 0\right) = \frac{A\mathcal{K}_- \left(\alpha\right)}{\sqrt{2\pi}} \left(\mathcal{G}_2 \left(-\alpha\right) + \mathcal{T} \left(-\alpha\right) \mathcal{C}_2\right), \tag{2.36}$$

where

$$\mathcal{G}_1 \left(\alpha\right) = \frac{1}{\left(\alpha - k_{eff} \cos \theta_0\right)} \left(\frac{1}{\mathcal{K}_+ \left(\alpha\right)} - \frac{1}{\mathcal{K}_+ \left(k_{eff} \cos \theta_0\right)}\right) - \exp\left(-\iota l k_{eff} \cos \theta_0\right) \mathcal{R}_1 \left(\alpha\right), \tag{2.37}$$

$$\mathcal{G}_2 \left(\alpha\right) = \frac{\exp\left(\iota l k_{eff} \cos \theta_0\right)}{\left(\alpha + k_{eff} \cos \theta_0\right)} \left(\frac{1}{\mathcal{K}_+ \left(\alpha\right)} - \frac{1}{\mathcal{K}_+ \left(-k_{eff} \cos \theta_0\right)}\right) - \mathcal{R}_2 \left(\alpha\right), \tag{2.38}$$

$$\mathcal{C}_1 = \mathcal{K}_+ \left(k_{eff}\right) \left(\frac{\mathcal{G}_2 \left(k_{eff}\right) + \mathcal{K}_+ \left(k_{eff}\right) \mathcal{G}_1 \left(k_{eff}\right) \mathcal{T} \left(k_{eff}\right)}{1 - \mathcal{K}_+^2 \left(k_{eff}\right) \mathcal{T}^2 \left(k_{eff}\right)}\right), \tag{2.39}$$

$$\mathcal{C}_2 = \mathcal{K}_+ \left(k_{eff}\right) \left(\frac{\mathcal{G}_1 \left(k_{eff}\right) + \mathcal{K}_+ \left(k_{eff}\right) \mathcal{G}_2 \left(k_{eff}\right) \mathcal{T} \left(k_{eff}\right)}{1 - \mathcal{K}_+^2 \left(k_{eff}\right) \mathcal{T}^2 \left(k_{eff}\right)}\right), \tag{2.40}$$

$$\mathcal{R}_{1,2} \left(\alpha\right) = \frac{E_{-1} \left[\mathcal{W}_{-1} \left(-i \left(k_{eff} \pm k_{eff} \cos \theta_0\right) l\right) - \mathcal{W}_{-1} \left(-i \left(k_{eff} + \alpha\right) l\right)\right]}{2\pi i \left(\alpha \mp k_{eff} \cos \theta_0\right)}, \tag{2.41}$$

$$\mathcal{T} \left(\alpha\right) = \frac{1}{2\pi \iota} E_{-1} \mathcal{W}_{-1} \left(-\iota \left(k_{eff} + \alpha\right) l\right), \tag{2.42}$$

21

$$E_{-1} = 2 \exp\left(\iota k_{eff} l\right) (l)^{\frac{1}{2}} (\iota)^{-\frac{1}{2}}, \tag{2.43}$$

and

$$\begin{aligned}
\mathcal{W}_{n-\frac{1}{2}}(s) &= \int_0^\infty \frac{v^n \exp(-v)}{v+s} dv \\
&= \Gamma(n+1) \exp\left(\frac{s}{2}\right) s^{\frac{1}{2}n-\frac{1}{2}} \mathcal{W}_{-\frac{1}{2}(n+1), \frac{1}{2}n}(s),
\end{aligned} \tag{2.44}$$

where $\mathcal{W}_{m,n}$ is called as Whittaker function and $s = -\iota(k_{eff} + \alpha) l$ and $n = \frac{1}{2}$.

From (2.25) and (2.26), the diffracted field in transformed domain is given as follows:

$$\mathcal{F}(\alpha, y) = -\frac{1}{\mathcal{K}(\alpha)} \left[\mathcal{F}_+(\alpha, 0) + \mathcal{F}_l(\alpha, 0) + e^{-\iota \alpha l} \mathcal{F}_-(\alpha, 0) \right] e^{-\iota \gamma |y|}, \tag{2.45}$$

where

$$\mathcal{F}_l(\alpha, 0) = -\mathcal{A}\mathcal{G}(\alpha), \text{ and } \mathcal{A} = -\iota. \tag{2.46}$$

The diffracted field in the $xy-$plane is obtained by inversion of $\mathcal{F}(\alpha, y)$ that is defined as

$$H_z(x, y) = \frac{1}{\sqrt{2\pi}} \int_{-\infty}^\infty \mathcal{F}(\alpha, y) e^{-\iota \alpha x - \iota \gamma |y|} d\alpha. \tag{2.47}$$

Insertion of (2.45) into (2.47) provides the following result

$$H_z(x, y) = -\frac{1}{\sqrt{2\pi}} \int_{-\infty}^\infty \frac{1}{\mathcal{K}(\alpha)} \left[\mathcal{F}_+(\alpha, 0) + \mathcal{F}_l(\alpha, 0) + e^{-\iota \alpha l} \mathcal{F}'_-(\alpha, 0) \right] e^{-\iota \alpha x - \iota \gamma |y|} d\alpha, \tag{2.48}$$

Now the diffracted field $H_z(x, y)$ comprises of two fields $H_z^{sep}(x, y)$ and $H_z^{int}(x, y)$

$$H_z(x, y) = H_z^{sep}(x, y) + H_z^{int}(x, y), \tag{2.49}$$

22

where $H_z^{sep}(x, y)$ is the separated field given as

$$H_z^{sep}(x, y) = -\frac{1}{2\pi} \int\limits_{-\infty}^{\infty} \frac{\mathcal{A}\mathcal{K}_+(\alpha) e^{(-\iota\alpha x - \iota\gamma|y|)}}{\mathcal{K}(\alpha)\mathcal{K}_+(k_{eff}\cos\theta_0)(\alpha - k_{eff}\cos\theta_0)} d\alpha$$
$$+ \frac{1}{2\pi} \int\limits_{-\infty}^{\infty} \frac{\mathcal{A}\exp(-\iota l(\alpha - k_{eff}\cos\theta_0))\mathcal{K}_+(-\alpha) e^{(-\iota\alpha x - \iota\gamma|y|)}}{\mathcal{K}(\alpha)\mathcal{K}_+(-k_{eff}\cos\theta_0)(\alpha - k_{eff}\cos\theta_0)} d\alpha,$$

(2.50)

and $H_z^{int}(x, y)$ is the interacted field given as

$$H_z^{int}(x, y) = \frac{1}{2\pi} \int\limits_{-\infty}^{\infty} \frac{\mathcal{A}}{\mathcal{K}(\alpha)} \begin{pmatrix} \mathcal{K}_+(\alpha)\mathcal{R}_1(\alpha) e^{-\iota l k_{eff}\cos\theta_0} \\ -\mathcal{K}_+(\alpha)\mathcal{T}(\alpha)\mathcal{C}_1 \\ +\mathcal{K}_+(-\alpha)\mathcal{R}_2(-\alpha) e^{-\iota l\alpha} \\ -\mathcal{K}_+(-\alpha)\mathcal{T}(-\alpha)\mathcal{C}_2 e^{-\iota l\alpha} \end{pmatrix} e^{(-\iota\alpha x - \iota\gamma|y|)} d\alpha.$$

(2.51)

The separated field given by (2.50) have two parts, one presenting the diffraction by the edge at $x = 0$ and other presenting the diffraction by edge at $x = -l$. The interaction field given by (2.51) presents the interaction of the edges i.e of the one edge of the plate upon the other.

2.6 Acquirement of Diffracted field

Now, to cope with the integral appearing in the result of diffracted field, asymptotic analysis may be used considering the field in the far field zone. For this purpose, the polar co-ordinates as $x = r\cos\theta$, $|y| = r\sin\theta$ are introduced and following transformation helps in the deformation of contour.

$$\alpha = -k_{eff}\cos(\theta + \iota\zeta) \quad \text{for} \quad 0 < \theta < \pi, \; -\infty < \zeta < \infty.$$

(2.52)

Hence, applying the method of stationary phase, (2.47) takes the following form

$$H_z(x, y) = \frac{\iota k_{eff}}{\sqrt{k_{eff}r}} \mathcal{F}(-k_{eff}\cos\theta, y)\sin\theta \exp\left(\iota k_{eff}r + \iota\frac{\pi}{4}\right).$$

(2.53)

23

Similarly, using the method of stationary phase for integrals in (2.50) and (2.51), we obtain

$$H_z^{sep}(x, y) = -\frac{1}{\sqrt{2\pi}} \frac{\iota k_{eff}}{\sqrt{k_{eff}r}} f_{sep}(-k_{eff}\cos\theta) \sin\theta \exp\left(\iota k_{eff}r + \iota\frac{\pi}{4}\right), \qquad (2.54)$$

$$H_z^{int}(x, y) = -\frac{1}{\sqrt{2\pi}} \frac{\iota k_{eff}}{\sqrt{k_{eff}r}} f_{int}(-k_{eff}\cos\theta) \sin\theta \exp\left(\iota k_{eff}r + \iota\frac{\pi}{4}\right), \qquad (2.55)$$

where

$$f_{sep}(-k_{eff}\cos\theta) = \frac{\mathcal{A}\mathcal{K}_+(-k_{eff}\cos\theta)}{\mathcal{K}(-k_{eff}\cos\theta)\mathcal{K}_+(-k_{eff}\cos\theta_0)(-k_{eff}\cos\theta - k_{eff}\cos\theta_0)}$$
$$- \frac{\mathcal{A}\exp(\iota k_{eff}(\cos\theta + \cos\theta_0)l)\mathcal{K}_+(k_{eff}\cos\theta)}{\mathcal{K}(-k_{eff}\cos\theta)\mathcal{K}_+(k_{eff}\cos\theta_0)(-k_{eff}\cos\theta - k_{eff}\cos\theta_0)}, \qquad (2.56)$$

and

$$f_{int}(-k_{eff}\cos\theta) = \frac{\mathcal{A}}{\mathcal{K}(-k_{eff}\cos\theta)}\begin{pmatrix} \mathcal{K}_+(-k_{eff}\cos\theta)\mathcal{R}_1(-k_{eff}\cos\theta)e^{\iota l k_{eff}\cos\theta_0} \\ +\mathcal{K}_+(k_{eff}\cos\theta)\mathcal{R}_2(k_{eff}\cos\theta)e^{\iota l k_{eff}\cos\theta} \\ -\mathcal{K}_+(-k_{eff}\cos\theta)\mathcal{T}(-k_{eff}\cos\theta)\mathcal{C}_1 \\ -\mathcal{K}_+(k_{eff}\cos\theta)\mathcal{T}(k_{eff}\cos\theta)\mathcal{C}_2 e^{\iota l k_{eff}\cos\theta} \end{pmatrix}. \qquad (2.57)$$

The function given by (2.53) expresses the asymptotic representation of the far field of the diffracted field as $k_{eff}r \longrightarrow \infty$. It can also be described that the asymptotic expansion of $H_z(x, y)$ proves to be valid for any value of observation angle everywhere in the space. Observation depicts that the separated field is actually the diffraction of EM-plane wave by a non-symmetric plate of finite length with edges $x = 0$ and $x = -l$. The separated field is the resultant wave field providing an insight to the physics of the problem. Whereas the interacted field appears due to the interaction of one edge upon the other providing no physics of the problem. The separated field provides the physical perception of diffraction phenomenon at the boundary defined for associated model. Therefore, only the separated field is taken into account while describing the diffraction phenomena at the defined boundary. Furthermore, the

interaction field appears due to dual diffraction by the two edges which has already been counted by the separated field (or diffracted field by a finite length plate). Also, extending the plate length upto infinity discards the involvement of terms appearing due to the interaction and consequently, the separated field appears to be diffracted field. Therefore, only the separated field is focused to discuss graphically in the next section.

2.7   Results and Discussion

In this section, the behavior of separated field versus observation angle θ for different physical parameters such as angle of incidence θ_0, wave-number k, plate length l, permittivity parameters ε_1 and ε_2 in the isotropic medium and anisotropic medium of cold plasma is discussed. In Figs. 2.3, keeping all other parameters fixed, results for separated field for increasing values of θ_0 are presented. The incremental trend of angle of incidence causes the amplification of separated field. It is also observed by comparing Fig. 2.3b with Fig. 2.3a that presence of cold plasma causes a reduction in the amplitude and expansion in the wavelength of separated field, consequently the number of oscillation are lessened. In Figs. 2.4a, 2.4b, the separated field is amplified by increasing the wave-number. The number of oscillations increases for the increment in wave-number that means the wave frequency moves towards the high frequency range. Figs. 2.5a, 2.5b are graphical descriptions of separated field for variation of length of plate l. An amplification in the separated field is noticed for increasing length of plate. The separated field oscillates rapidly on extending the plate length as can be seen in Fig. 2.5a in the absence of cold plasma. On comparative study of separated field plotted with effects cold plasma with that in the absence of cold plasma, it is explored that presence of cold plasma has expanded the wavelength, reduced the amplitude and consequently, the number of oscillation are decreased. This means that presence of cold plasma as prevented the separated field from dispersion. Fig. 2.6 shows the impact of ε_1 on the separated field. The

drastic effects of cold plasma on the amplitude of separated field has been studied. The separated field is amplified by increasing ε_1, it happens due to fixed densities of electrons and ions in cold plasma, an increase in operating frequency ω causes an increase in $\varepsilon_1 \approx 1 - (\omega_p/\omega)^2$ (for high range frequency signal). The electric field of such a high frequency energizes the electrons to oscillate about the cold ionic center, and such oscillating electrons get diffracted rapidly thereby amplifying the separated field. In Fig. 2.7, opposite behavior of separated field is observed for ε_2. The increasing value of ε_2 causes the reduction in signal frequency resulting into decreasing amplitude of separated field by electron oscillation under low frequency. Further, the separated field shows the nulls around observation angle 0 and π.
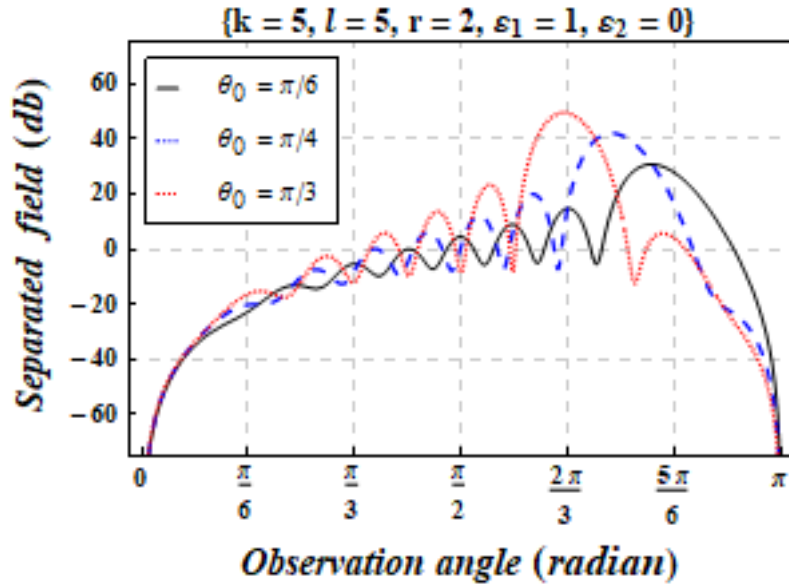
(a)
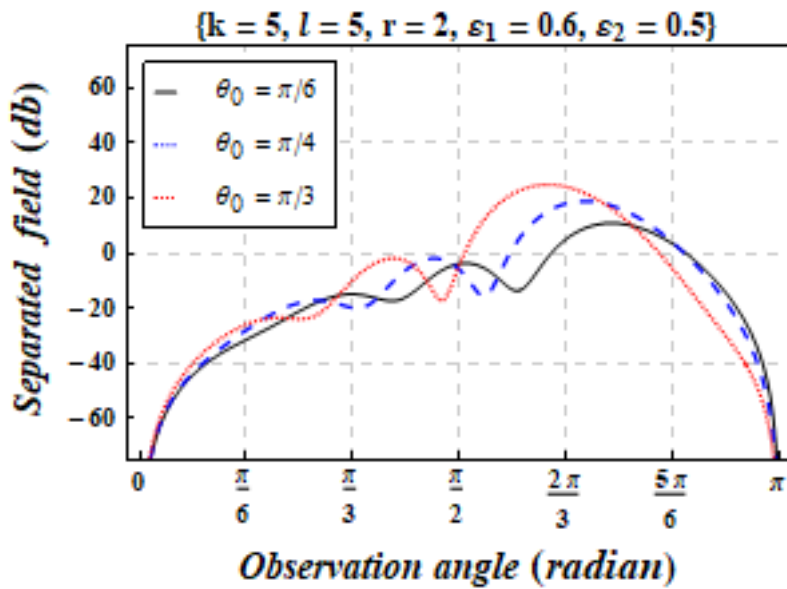
(b)

Figure 2.3: **The separated field for angle of incidence in the absence (a) and presence (b) of cold plasma.**
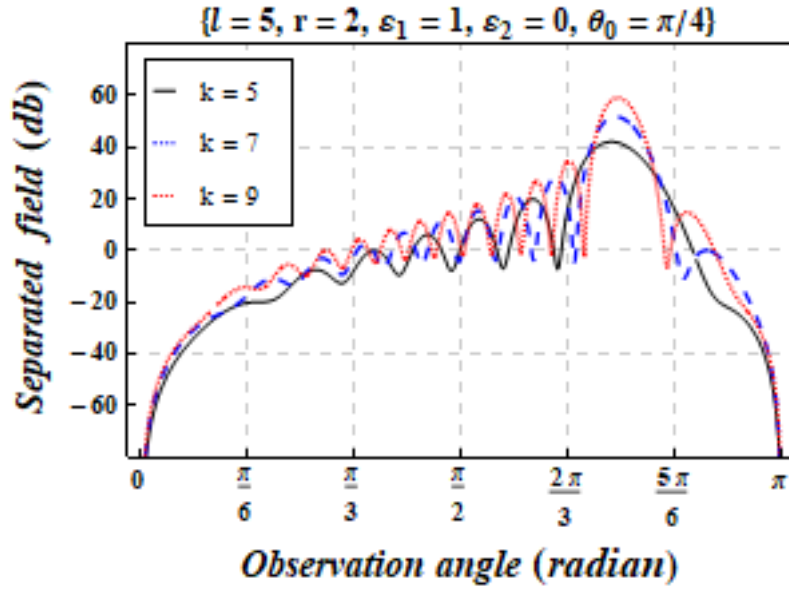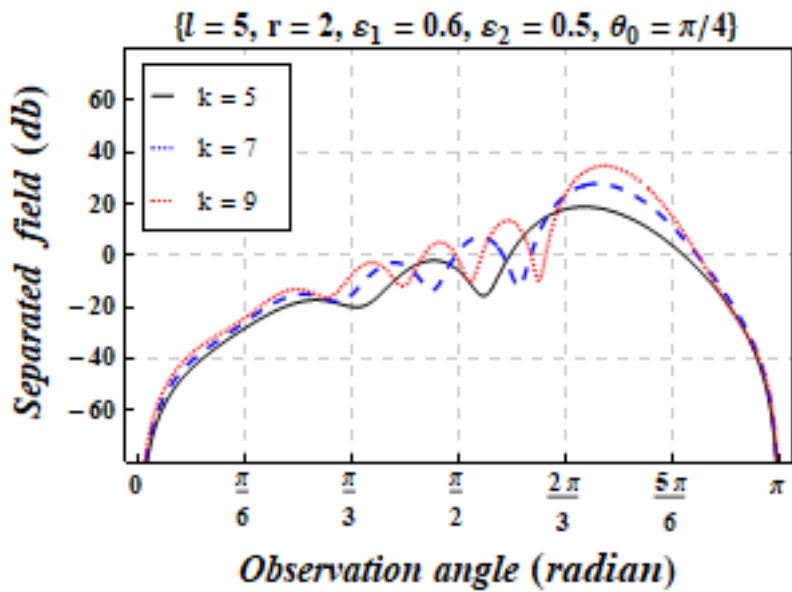
Figure 2.4: **The separated field for wave-number in the absence (a) and presence (b) of cold plasma.**
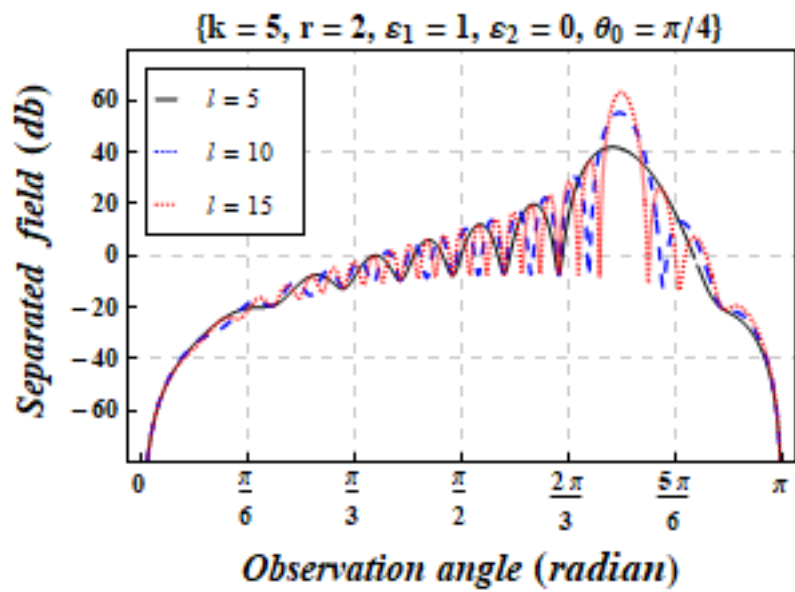
(a)
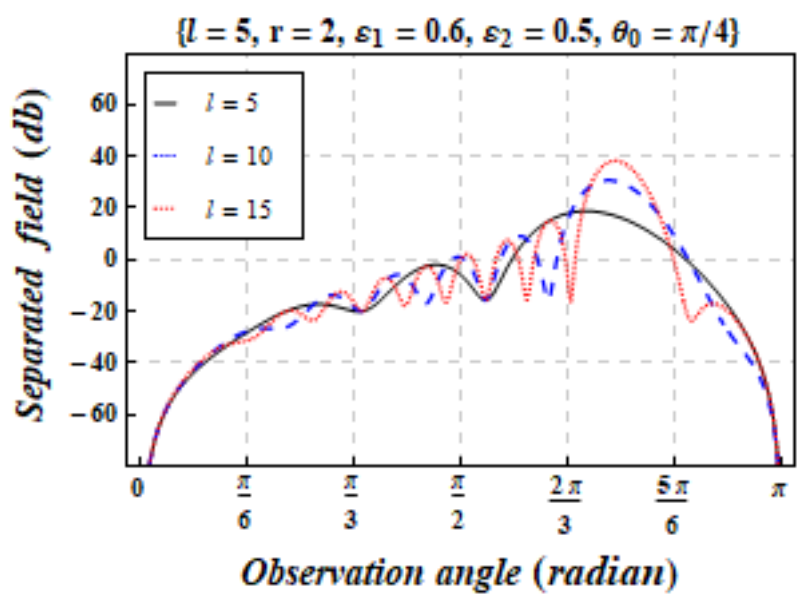
(b)

Figure 2.5: **The separated field for the length of plate in the absence (a) and presence (b) of cold plasma.**
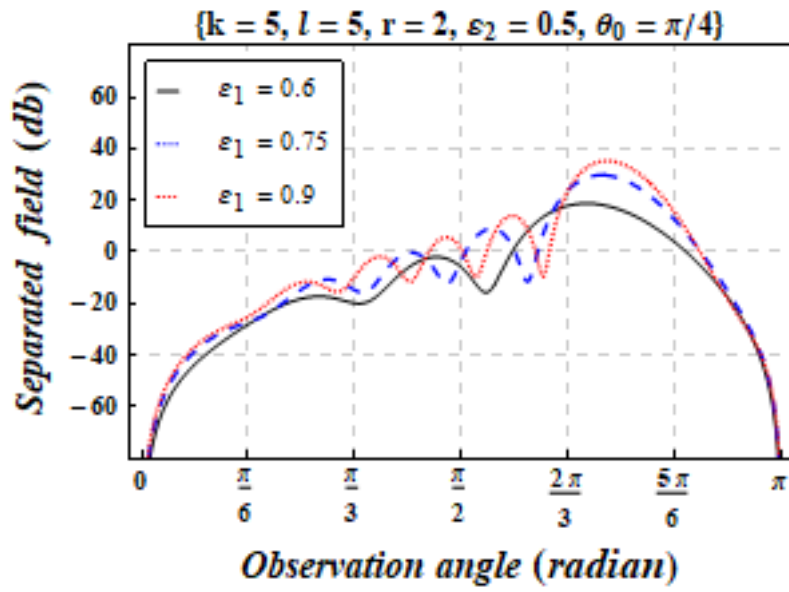
Figure 2.6: **The separated field with ε_1.**
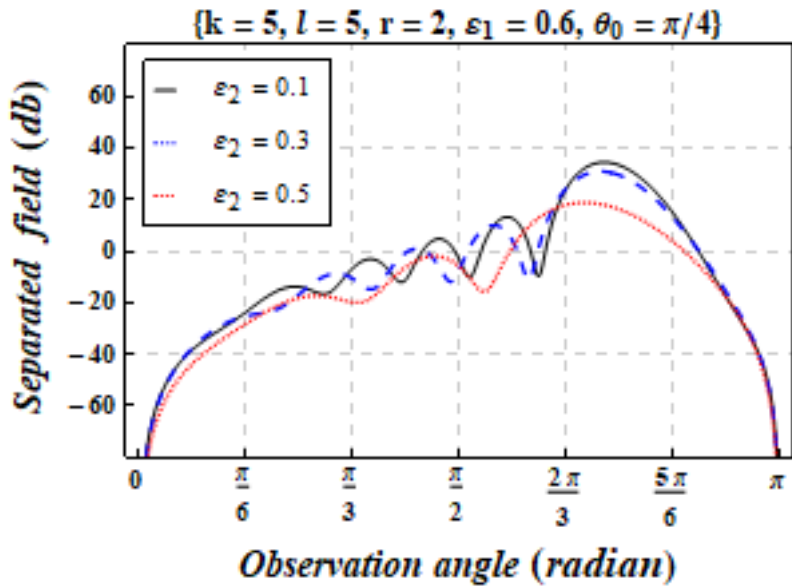
Figure 2.7: **The separated field with ε_2.**

2.8   Conclusions

From above analysis, we conclude that the diffraction of EM-plane wave finite plate under the assumptions of Dirichlet conditions is affected rigorously by physical parameters in the presence of cold plasma. It is noticed that separated field is amplified by different angles of incidence, wave-number, plate length, ε_1 and reduced by ε_2.

Chapter 3

Diffraction Affected by Cold Plasma with Neumann Conditions on Finite Plate

Present chapter elaborates the investigation of diffraction phenomenon of EM-plane wave by a non-symmetric plate of finite length in cold plasma. The Wiener-Hopf equation is formulated with the aid of boundary value problem along with Fourier transform for present model. The theory of Wiener-Hopf procedure is used to cope with resulting equation. Asymptotic expansion and method of stationary phase are used to obtain the result for diffracted field by finite plate (separated field) under the assumption of Neumann boundary conditions in the anisotropic medium. The case of isotropic medium has been discussed by assigning the particular values to elements of permittivity tensor. Impact of physical parameters has been discussed graphically for the isotropic and anisotropic medium.

3.1 Modelling of the Helmholtz Equation

The dielectric permittivity tensor evaluated for cold plasma is expressed as

$$\bar{\varepsilon} = \begin{pmatrix} \varepsilon_1 & -\iota\varepsilon_2 & 0 \\ \iota\varepsilon_2 & \varepsilon_1 & 0 \\ 0 & 0 & \varepsilon_z \end{pmatrix}, \tag{3.1}$$

where ε_1, ε_2 and ε_z are presented as follows:

$$\varepsilon_1 = 1 - \left(\frac{\omega_p}{\omega}\right)^2 \left[1 - \left(\frac{\omega_c}{\omega}\right)^2\right]^{-1}, \quad \varepsilon_2 = \left(\frac{\omega_p}{\omega}\right)^2 \left[\frac{\omega}{\omega_c} - \frac{\omega_c}{\omega}\right]^{-1}, \tag{3.2}$$

$$\varepsilon_z = 1 - \left(\frac{\omega_p}{\omega}\right)^2, \tag{3.3}$$

with

$$\omega_p^2 = \frac{N_e e^2}{m\varepsilon_0}, \quad \omega_c = \frac{|e|\,\mu_0 H_{dc}}{m}. \tag{3.4}$$

The well known Maxwell's equations are proved to be valid in cold plasma with dielectric permittivity tensor given by (3.1). The electric field components in terms of magnetic field obtained by combined use of Maxwell's equation and permittivity tensor (3.1) are described as

$$E_x = \frac{\iota\varepsilon_1}{\omega\varepsilon_0\left(\varepsilon_1^2 - \varepsilon_2^2\right)} \frac{\partial H_z\left(x,y\right)}{\partial y} + \frac{\varepsilon_2}{\omega\varepsilon_0\left(\varepsilon_1^2 - \varepsilon_2^2\right)} \frac{\partial H_z\left(x,y\right)}{\partial x}, \tag{3.5}$$

and

$$E_y = \frac{\varepsilon_2}{\omega\varepsilon_0\left(\varepsilon_1^2 - \varepsilon_2^2\right)} \frac{\partial H_z\left(x,y\right)}{\partial y} - \frac{\iota\varepsilon_1}{\omega\varepsilon_0\left(\varepsilon_1^2 - \varepsilon_2^2\right)} \frac{\partial H_z\left(x,y\right)}{\partial x}. \tag{3.6}$$

Then, the Helmholtz's equation satisfying H_z in cold plasma is obtained by Maxwell's equations along with use of (3.5) and (3.6), as follows :

$$\partial_{xx} H_z\left(x,y\right) + \partial_{yy} H_z\left(x,y\right) + k_{eff}^2 H_z\left(x,y\right) = 0, \tag{3.7}$$
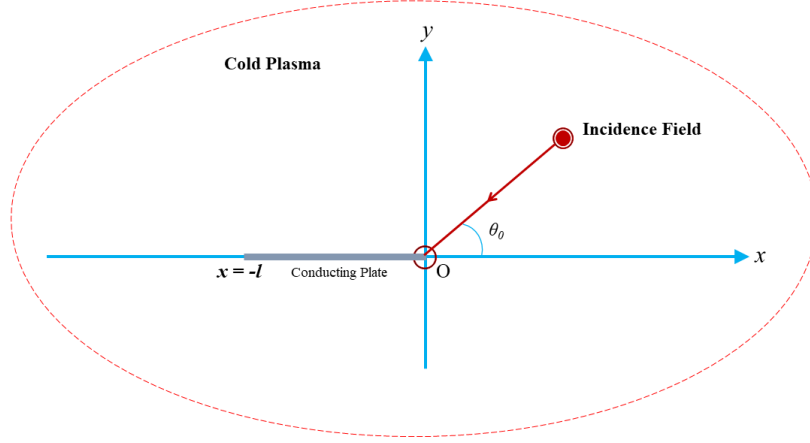
Figure 3.1: **Geometrical description of the model.**

where k_{eff} is the propagation constant which is given as

$$k_{eff} = k\sqrt{\frac{\varepsilon_1^2 - \varepsilon_2^2}{\varepsilon_1}} \quad \text{and} \quad k = \omega\sqrt{\varepsilon_0\mu_0}. \tag{3.8}$$

Here, k_{eff} is dependent of k, ε_1 and ε_2, time is taken as behaving harmonically as $\exp(-\iota\omega t)$ and will be considered as suppressed throughout the analysis.

3.2   Mathematical Modelling of the Problem

Here, for the present model EM-plane wave is considered to be incident on a conductible non-symmetric finite length plate located along $y = 0$ with one end located at origin i.e. at $x = 0$ and other end lies on the negative $x-$axis that is $x = -l$, as displayed in Fig. 3.1. The incident plane wave considered here makes an angle θ_0 with horizontal axis.

The total field for the present model is expressed as

$$H_z^{tot}(x,y) = H_z^{inc}(x,y) + H_z(x,y), \tag{3.9}$$

where H_z^{inc} is the incident field, which is defined by

$$H_z^{inc}(x, y) = \exp\{-\iota k_{eff}(x \cos \theta_0 + y \sin \theta_0)\}, \tag{3.10}$$

where k_{eff} is given in (3.8). For convenience of analysis, medium is considered to be slightly lossy as in $k_{eff} = \mathfrak{Re}\{k_{eff}\} + \iota \mathfrak{Im}\{k_{eff}\}$, $0 < \mathfrak{Im}\{k_{eff}\} \ll \mathfrak{Re}\{k_{eff}\}$ and the solution for real k_{eff} may be achieved by assuming $\mathfrak{Im}\{k_{eff}\} \longrightarrow 0$. The boundary value problem (BVP) under consideration is expressed in terms of the magnetic field and it is adequate to denote the diffracted field in different regions. The total field $H_z^{tot}(x, y)$ in the range $x \in (-\infty, \infty)$, satisfying the Helmholtz's equation is described as

$$\left[\partial_{xx} + \partial_{yy} + k_{eff}^2\right] H_z^{tot}(x, y) = 0. \tag{3.11}$$

The diffracted field satisfying Helmholtz's equation extracted from above equation is expressed as

$$\left[\partial_{xx} + \partial_{yy} + k_{eff}^2\right] H_z(x, y) = 0. \tag{3.12}$$

Our aim is to determine the diffraction of incident electromagnetic (EM) plane wave by a non-symmetric plate of finite length in cold plasma. To proceed further suitable boundary conditions are required. Therefore, for the present model Neumann boundary conditions on the surface of plate are considered, which are defined as

$$\partial_y H_z^{tot}(x, 0^\pm) = 0, \quad \text{for } -l \leq x \leq 0 \tag{3.13}$$

and continuity relations are defined as

$$\begin{aligned} H_z^{tot}(x, 0^+) &= H_z^{tot}(x, 0^-), \quad \text{for } -\infty < x < -l, \ x > 0, \\ \partial_y H_z^{tot}(x, 0^+) &= \partial_y H_z^{tot}(x, 0^-), \quad \text{for } -\infty < x < -l, \ x > 0. \end{aligned} \tag{3.14}$$

3.3 Transformation of Problem

Use of Fourier integral transform for x variable gives the solution of boundary value problem

$$\mathcal{F}(\alpha, y) = \frac{1}{\sqrt{2\pi}} \int\limits_{-\infty}^{\infty} H_z(x, y) e^{\iota \alpha x} dx$$

$$= \mathcal{F}_+(\alpha, y) + e^{-\iota \alpha l} \mathcal{F}_-(\alpha, y) + \mathcal{F}_l(\alpha, y),$$

(3.15)

where $\alpha = \mathfrak{Re}\{\alpha\} + \iota \mathfrak{Im}\{\alpha\} = \sigma + \iota \tau$. The asymptotic behavior of the diffracted field $H_z(x, y)$ for $x \longrightarrow \pm\infty$ is defined as

$$H_z(x, y) = \begin{cases} O\left(e^{-\mathfrak{Im}\{k_{eff}\}x}\right) & \text{for } x \longrightarrow \infty, \\ O\left(e^{\mathfrak{Im}\{k_{eff}\}x \cos\theta_0}\right) & \text{for } x \longrightarrow -\infty. \end{cases}$$

(3.16)

$\mathcal{F}_+(\alpha, y)$ is a regular function of α in upper-half of $\alpha-$plane i.e. in the region $-\mathfrak{Im}\{k_{eff}\} < \mathfrak{Im}\{\alpha\}$ whereas $\mathcal{F}_-(\alpha, y)$ is a regular function of α in the lower-half of $\alpha-$plane i.e. in the region $\mathfrak{Im}\{\alpha\} < \mathfrak{Im}\{k_{eff} \cos\theta_0\}$ and the common region formed by overlapping of these two regions, is a band of analyticity (see Fig. 3.2) in which all the functions including $\mathcal{F}_l(\alpha, y)$ are analytic in which all the functions are analytic, thus, these functions are defined as

$$\mathcal{F}_+(\alpha, y) = \frac{1}{\sqrt{2\pi}} \int\limits_0^{\infty} H_z(x, y) e^{\iota \alpha x} dx,$$

(3.17)

$$\mathcal{F}_-(\alpha, y) = \frac{1}{\sqrt{2\pi}} \int\limits_{-\infty}^{-l} H_z(x, y) e^{\iota \alpha(x+l)} dx,$$

(3.18)

$$\mathcal{F}_l(\alpha, y) = \frac{1}{\sqrt{2\pi}} \int\limits_{-l}^{0} H_z(x, y) e^{\iota \alpha x} dx.$$

(3.19)

$$\mathcal{F}^{inc}(\alpha, 0) = \frac{1 - e^{-\iota l(\alpha - k_{eff} \cos\theta_0)}}{\sqrt{2\pi}\iota (\alpha - k_{eff} \cos\theta_0)}.$$

(3.20)

Use of Fourier transform (3.12)-(3.14) yields,

$$\left(\frac{d^2}{dy^2} + \gamma^2\right)\mathcal{F}(\alpha, y) = 0, \tag{3.21}$$

where $\gamma(\alpha) = \sqrt{k_{eff}^2 - \alpha^2}$.

$$\partial_y \mathcal{F}_l(\alpha, 0^+) = -\partial_y \mathcal{F}^{inc}(\alpha, 0),$$
$$\partial_y \mathcal{F}_l(\alpha, 0^-) = -\partial_y \mathcal{F}^{inc}(\alpha, 0), \tag{3.22}$$

and

$$\mathcal{F}_-(\alpha, 0^+) = \mathcal{F}_-(\alpha, 0^-) = \mathcal{F}_-(\alpha, 0),$$
$$\mathcal{F}_+(\alpha, 0^+) = \mathcal{F}_+(\alpha, 0^-) = \mathcal{F}_+(\alpha, 0),$$
$$\partial_y \mathcal{F}_-(\alpha, 0^+) = \partial_y \mathcal{F}_-(\alpha, 0^-) = \partial_y \mathcal{F}_-(\alpha, 0),$$
$$\partial_y \mathcal{F}_+(\alpha, 0^+) = \partial_y \mathcal{F}_+(\alpha, 0^-) = \partial_y \mathcal{F}_+(\alpha, 0). \tag{3.23}$$

3.4 Modelling of Wiener-Hopf Equation

The solution of (3.21) satisfying the radiation conditions is given by

$$\mathcal{F}(\alpha, y) = \begin{cases} A_1(\alpha) e^{-\iota\gamma y} & y \geq 0, \\ A_2(\alpha) e^{\iota\gamma y} & y < 0. \end{cases} \tag{3.24}$$

Now with the aid of (3.15) and (3.22)-(3.24) the following functional Wiener-Hopf equation is computed as

$$\mathcal{F}'_+(\alpha, 0) + e^{-\iota\alpha l}\mathcal{F}'_-(\alpha, 0) + \mathcal{K}(\alpha)\tilde{\mathcal{F}}_l(\alpha, 0) = \mathcal{AG}(\alpha), \tag{3.25}$$

where $\mathcal{K}(\alpha)$ is the kernel function, which is given as

$$\mathcal{K}(\alpha) = \iota\gamma, \tag{3.26}$$

$$\tilde{\mathcal{F}}_l(\alpha, 0) = \frac{1}{2}\left[\mathcal{F}_l(\alpha, 0^+) - \mathcal{F}_l(\alpha, 0^-)\right], \tag{3.27}$$
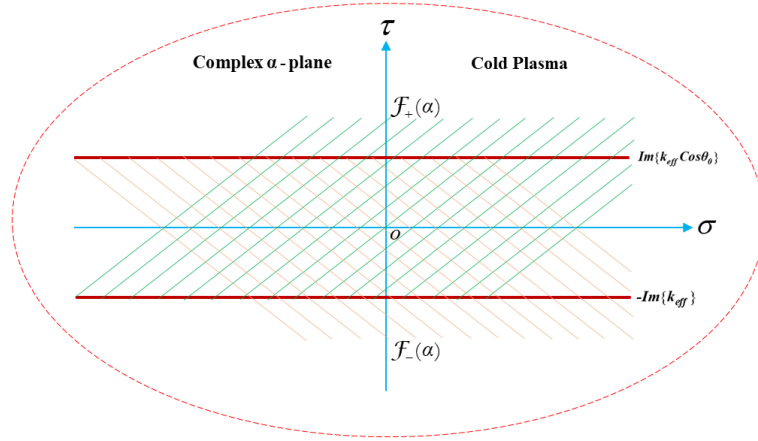
Figure 3.2: **The description of analytic continuation in the complex $\alpha-$plane.**

$$\mathcal{A} = -k_{eff} \sin \theta_0, \tag{3.28}$$

$$\mathcal{G}(\alpha) = \frac{1 - e^{-\iota\left(\alpha - k_{eff} \cos \theta_0\right)l}}{\sqrt{2\pi}\left(\alpha - k_{eff} \cos \theta_0\right)}. \tag{3.29}$$

3.5 Wiener-Hopf Procedure

The kernel factor arising from (3.25), given (3.26), is factorized as

$$\mathcal{K}(\alpha) = \iota\gamma = \mathcal{K}_{+}(\alpha)\,\mathcal{K}_{-}(\alpha), \tag{3.30}$$

The factors $\mathcal{K}_{+}$ and $\mathcal{K}_{-}$ are computed as

$$\mathcal{K}_{\pm}(\alpha) = e^{\iota\frac{\pi}{4}}\sqrt{k_{eff}\pm\alpha}, \tag{3.31}$$

and

$$\gamma(\alpha) = \gamma_{+}(\alpha)\,\gamma_{-}(\alpha), \tag{3.32}$$

$$\gamma_{+}(\alpha) = \sqrt{k_{eff} + \alpha}, \quad \gamma_{-}(\alpha) = \sqrt{k_{eff} - \alpha}. \tag{3.33}$$

The factors $\mathcal{K}_+(\alpha)$ and $\gamma_+(\alpha)$ are regular functions of α in upper-half of the $\alpha-$plane $\mathfrak{Im}\{-k_{eff}\} < \mathfrak{Im}\{\alpha\}$ whereas the factors $\mathcal{K}_-(\alpha)$ and $\gamma_-(\alpha)$ regular functions of α in the lower-half of the $\alpha-$plane $\mathfrak{Im}\{\alpha\} < \mathfrak{Im}\{k_{eff}\cos\theta_0\}$. For large $k_{eff}r$ $\left(r = \sqrt{x^2 + y^2}\right)$, a solution in approximated form may be attained through made by Wiener-Hopf technique. Equating the terms of (3.25) with positive sign on one side of the equation and the terms with negative sign on the other side results into the same function $\mathfrak{J}(\alpha)$, say, which is a polynomial function, thus $\mathfrak{J}(\alpha)$ is an entire function. Analytic continuation (see Fig. 3.2) along with arguments involving extended form of Liouville's theorem allows to equate the function $\mathfrak{J}(\alpha)$ to zero, hence, discard of detailed calculations, we obtain the following results

$$\mathcal{F}'_+(\alpha, 0) = \frac{A\mathcal{K}_+(\alpha)}{\sqrt{2\pi}}\left(\mathcal{G}_1(\alpha) + \mathcal{T}(\alpha)\mathcal{C}_1\right), \tag{3.34}$$

$$\mathcal{F}'_-(\alpha, 0) = \frac{A\mathcal{K}_-(\alpha)}{\sqrt{2\pi}}\left(\mathcal{G}_2(-\alpha) + \mathcal{T}(-\alpha)\mathcal{C}_2\right), \tag{3.35}$$

where

$$\mathcal{G}_1(\alpha) = \frac{1}{(\alpha - k_{eff}\cos\theta_0)}\left(\frac{1}{\mathcal{K}_+(\alpha)} - \frac{1}{\mathcal{K}_+(k_{eff}\cos\theta_0)}\right) - \exp\left(-\iota l k_{eff}\cos\theta_0\right)\mathcal{R}_1(\alpha), \tag{3.36}$$

$$\mathcal{G}_2(\alpha) = \frac{\exp\left(\iota l k_{eff}\cos\theta_0\right)}{(\alpha + k_{eff}\cos\theta_0)}\left(\frac{1}{\mathcal{K}_+(\alpha)} - \frac{1}{\mathcal{K}_+(-k_{eff}\cos\theta_0)}\right) - \mathcal{R}_2(\alpha), \tag{3.37}$$

$$\mathcal{C}_1 = \mathcal{K}_+(k_{eff})\left(\frac{\mathcal{G}_2(k_{eff}) + \mathcal{K}_+(k_{eff})\mathcal{G}_1(k_{eff})\mathcal{T}(k_{eff})}{1 - \mathcal{K}_+^2(k_{eff})\mathcal{T}^2(k_{eff})}\right), \tag{3.38}$$

$$\mathcal{C}_2 = \mathcal{K}_+(k_{eff})\left(\frac{\mathcal{G}_1(k_{eff}) + \mathcal{K}_+(k_{eff})\mathcal{G}_2(k_{eff})\mathcal{T}(k_{eff})}{1 - \mathcal{K}_+^2(k_{eff})\mathcal{T}^2(k_{eff})}\right), \tag{3.39}$$

$$\mathcal{R}_{1,2}(\alpha) = \frac{E_{-1}\left[\mathcal{W}_{-1}\left(-\iota\left(k_{eff} \pm k_{eff}\cos\theta_0\right)l\right) - \mathcal{W}_{-1}\left(-\iota\left(k_{eff} + \alpha\right)l\right)\right]}{2\pi\iota\left(\alpha \mp k_{eff}\cos\theta_0\right)}, \tag{3.40}$$

$$\mathcal{T}(\alpha) = \frac{1}{2\pi\iota}E_{-1}\mathcal{W}_{-1}\left(-\iota\left(k_{eff} + \alpha\right)l\right), \tag{3.41}$$

$$E_{-1} = 2\exp\left(\iota k_{eff}l\right)(l)^{\frac{1}{2}}(\iota)^{-\frac{1}{2}}, \tag{3.42}$$

and

$$\mathcal{W}_{n-\frac{1}{2}}(p) = \int\limits_{0}^{\infty} \frac{u^n \exp{(-u)}}{u+p} du \tag{3.43}$$

$$= \Gamma(n+1) \exp\left(\frac{p}{2}\right) p^{\frac{1}{2}n-\frac{1}{2}} \mathcal{W}_{-\frac{1}{2}(n+1),\frac{1}{2}n}(p),$$

where $p = -\iota(k_{eff} + \alpha)l$ and $n = -\frac{1}{2}$. $\mathcal{W}_{m,n}$ is known as Whittaker function.

From (3.24) and (3.25), the diffracted field in transformed domain is given as follows :

$$\mathcal{F}(\alpha, y) = -\frac{1}{\mathcal{K}(\alpha)} \left[\mathcal{F}'_+(\alpha, 0) + \mathcal{F}'_l(\alpha, 0) + e^{-\iota\alpha l}\mathcal{F}'_-(\alpha, 0) \right] e^{-\iota\gamma|y|}, \tag{3.44}$$

where

$$\mathcal{F}'_l(\alpha, 0) = -\mathcal{A}\mathcal{G}(\alpha), \text{ and } \mathcal{A} = -k_{eff}\sin\theta_0. \tag{3.45}$$

The diffracted field in the $xy-$plane is obtained by application of inverse Fourier integral transform of $\mathcal{F}(\alpha, y)$ that is defined as

$$H_z(x, y) = \frac{1}{\sqrt{2\pi}} \int\limits_{-\infty}^{\infty} \mathcal{F}(\alpha, y) e^{-\iota\alpha x - \iota\gamma|y|} d\alpha. \tag{3.46}$$

Inserting (3.44) in (3.46), we obtain

$$H_z(x, y) = -\frac{1}{\sqrt{2\pi}} \int\limits_{-\infty}^{\infty} \frac{1}{\mathcal{K}(\alpha)} \left[\mathcal{F}'_+(\alpha, 0) + \mathcal{F}'_l(\alpha, 0) + e^{-\iota\alpha l}\mathcal{F}'_-(\alpha, 0) \right] e^{-\iota\alpha x - \iota\gamma|y|} d\alpha,$$

$$\tag{3.47}$$

Now $H_z(x, y)$ comprises of two sub fields $H_z^{sep}(x, y)$ and $H_z^{inc}(x, y)$ as described by

$$H_z(x, y) = H_z^{sep}(x, y) + H_z^{int}(x, y). \tag{3.48}$$

Here, $H_z^{sep}(x, y)$ denotes the separated field and $H_z^{int}(x, y)$ denotes the interacted field. After using (3.34), (3.35) and (3.45) in (3.47), $H_z^{sep}(x, y)$ and $H_z^{int}(x, y)$ are

evaluated as follows :

$$H_z^{sep}(x,y) = -\frac{1}{2\pi} \int\limits_{-\infty}^{\infty} \frac{\mathcal{A}\mathcal{K}_+(\alpha) e^{(-\iota\alpha x - \iota\gamma|y|)}}{\mathcal{K}(\alpha)\mathcal{K}_+(k_{eff}\cos\theta_0)(\alpha - k_{eff}\cos\theta_0)} d\alpha$$
$$+ \frac{1}{2\pi} \int\limits_{-\infty}^{\infty} \frac{\mathcal{A}\exp(-\iota l(\alpha - k_{eff}\cos\theta_0))\mathcal{K}_+(-\alpha) e^{(-\iota\alpha x - \iota\gamma|y|)}}{\mathcal{K}(\alpha)\mathcal{K}_+(-k_{eff}\cos\theta_0)(\alpha - k_{eff}\cos\theta_0)} d\alpha, \quad (3.49)$$

and

$$H_z^{int}(x,y) = \frac{1}{2\pi} \int\limits_{-\infty}^{\infty} \frac{\mathcal{A}}{\mathcal{K}(\alpha)} \begin{pmatrix} \mathcal{K}_+(\alpha)\mathcal{R}_1(\alpha) e^{-\iota l k_{eff}\cos\theta_0} \\ -\mathcal{K}_+(\alpha)\mathcal{T}(\alpha)\mathcal{C}_1 \\ +\mathcal{K}_+(-\alpha)\mathcal{R}_2(-\alpha) e^{-\iota l\alpha} \\ -\mathcal{K}_+(-\alpha)\mathcal{T}(-\alpha)\mathcal{C}_2 e^{-\iota l\alpha} \end{pmatrix} e^{(-\iota\alpha x - \iota\gamma|y|)} d\alpha. \quad (3.50)$$

The separated field $H_z^{sep}(x,y)$ given by (3.49) have two parts. One presents the diffraction by the edge at $x = 0$ and other presents the diffraction by edge at $x = -l$. The interaction field $H_z^{int}(x,y)$ given by (3.50) presents the interaction of one edge upon other which is already counted by the separated field.

3.6 Acquirement of Diffracted field

The diffracted field in the far field zone now may be tackled by using the asymptotic evaluation of the integrals appearing in (3.46), (3.49) and (3.50). For this purpose, the polar coordinates as $x = r\cos\theta$, $|y| = r\sin\theta$ are introduced and following transformation helps in the deformation of contour.

$$\alpha = -k_{eff}\cos(\theta + \iota\zeta), \quad \text{for } 0 < \theta < \pi, \; -\infty < \zeta < \infty. \quad (3.51)$$

Hence, applying the method of stationary phase, (3.46) takes the form as follows :

$$H_z(x,y) = \frac{\iota k_{eff}}{\sqrt{k_{eff}r}} \mathcal{F}(-k_{eff}\cos\theta, y)\sin\theta \exp\left(\iota k_{eff}r + \iota\frac{\pi}{4}\right). \quad (3.52)$$

Similarly, after using the method of stationary phase to cope with the integrals appearing in (3.49) and (3.50), we obtain the following results following results

$$H_z^{sep}(x, y) = -\frac{1}{\sqrt{2\pi}} \frac{\iota k_{eff}}{\sqrt{k_{eff}r}} f_{sep}(-k_{eff}\cos\theta)\sin\theta\exp\left(\iota k_{eff}r + \iota\frac{\pi}{4}\right), \qquad (3.53)$$

$$H_z^{int}(x, y) = -\frac{1}{\sqrt{2\pi}} \frac{\iota k_{eff}}{\sqrt{k_{eff}r}} f_{int}(-k_{eff}\cos\theta)\sin\theta\exp\left(\iota k_{eff}r + \iota\frac{\pi}{4}\right), \qquad (3.54)$$

where

$$f_{sep}(-k_{eff}\cos\theta) = \frac{\mathcal{A}\mathcal{K}_+(-k_{eff}\cos\theta)}{\mathcal{K}(-k_{eff}\cos\theta)\mathcal{K}_+(-k_{eff}\cos\theta_0)(-k_{eff}\cos\theta - k_{eff}\cos\theta_0)}$$
$$- \frac{\mathcal{A}\exp(\iota k_{eff}(\cos\theta + \cos\theta_0)l)\mathcal{K}_+(k_{eff}\cos\theta)}{\mathcal{K}(-k_{eff}\cos\theta)\mathcal{K}_+(k_{eff}\cos\theta_0)(-k_{eff}\cos\theta - k_{eff}\cos\theta_0)}, \qquad (3.55)$$

and

$$f_{int}(-k_{eff}\cos\theta) = \frac{\mathcal{A}}{\mathcal{K}(-k_{eff}\cos\theta)}\begin{pmatrix} \mathcal{K}_+(-k_{eff}\cos\theta)\mathcal{R}_1(-k_{eff}\cos\theta)e^{\iota l k_{eff}\cos\theta_0} \\ +\mathcal{K}_+(k_{eff}\cos\theta)\mathcal{R}_2(k_{eff}\cos\theta)e^{\iota l k_{eff}\cos\theta} \\ -\mathcal{K}_+(-k_{eff}\cos\theta)\mathcal{T}(-k_{eff}\cos\theta)\mathcal{C}_1 \\ -\mathcal{K}_+(k_{eff}\cos\theta)\mathcal{T}(k_{eff}\cos\theta)\mathcal{C}_2 e^{\iota l k_{eff}\cos\theta} \end{pmatrix}. \qquad (3.56)$$

The result presented by (3.52) gives the asymptotic representation of the far field of the diffracted field as $k_{eff}r \longrightarrow \infty$. It can also be elaborated that the asymptotic expansion of $H_z(x, y)$ proves to be valid for every angle of observation in the entire space. Observation depicts that the separated field is actually the diffraction of EM-plane wave by a non-symmetric plate of finite length with one edge at $x = 0$ and other at $x = -l$. The separated field is the resultant wave field providing an insight to the physics of the problem. Whereas the interacted field appears due to the interaction with edge of plate upon the other providing no physics of the problem. The separated field provides the physical perception of diffraction phenomenon at the boundary defined for associated model. Therefore, only the separated field is taken into account while describing the diffraction phenomena at the defined boundary.

Furthermore, the interaction field appears due to dual diffraction by the two edges which has already been counted by the separated field (or diffracted field by a finite length plate). Also, extending the plate length upto infinity discards the involvement of terms appearing due to the interaction and consequently, the separated field appears to be diffracted field. Therefore, only the separated field is focused to discuss graphically in the next section.

3.7 Results and Discussion

In the presented section, the separated field versus observation angle θ under the effects of physical parameters such as the angle of incidence θ_0, the wave-number k, the length of plate l and the elements of permittivity tensor ε_1, ε_2 is elaborated graphically. Figs. 3.3, 3.4 display the variation of separated field due to angle of incidence by keeping all other parameters fixed with $l = 5$ and $l = 25$. The comparative study of Fig. 3.4 with Fig. 3.3 elaborates that large value of plate length causes the squeeze in wavelength, resulting an increase in number of oscillations and amplification of the separated field. Effects of cold plasma can be seen by comparative analysis of Figs. 3.3b, 3.4b with their respective Figs. 3.3a, 3.4a where there is no cold plasma. By observation it is depicted that presence of cold plasma has expanded the wavelength and caused of vertical shift in separated field. Figs. 3.5a, 3.5b are sketched to display the fluctuation of separated field for wave-number. For increasing wave-number, the number of oscillations of the separated field increase. This means that wave frequency moves towards the high frequency range. Figs. 3.6a, 3.6b are graphical description of separated field for variation of l in the absence and presence of cold plasma, respectively. Analysis of plot describes that extending the length of plate amplifies the separated field. The comparative study of the separated field in the presence of cold plasma with separated field in the absence of cold plasma has explored that wavelength of separated field has expanded and vertical shift is occurred. Fig. 3.7 explores the behavior of separated field for ε_1. A decay in the

separated field occurs for the ε_1. Fig. 3.8 elaborates the behavior of separated field for ε_2. The separated field gets a slight amplification for increasing values of ε_2. An enhancement in ε_2 is caused by an increase in cyclotron frequency. Consequently, magnetic Lorentz force increases and leads to an enhancement in the amplitude of separated field (field diffracted by a finite length plate).
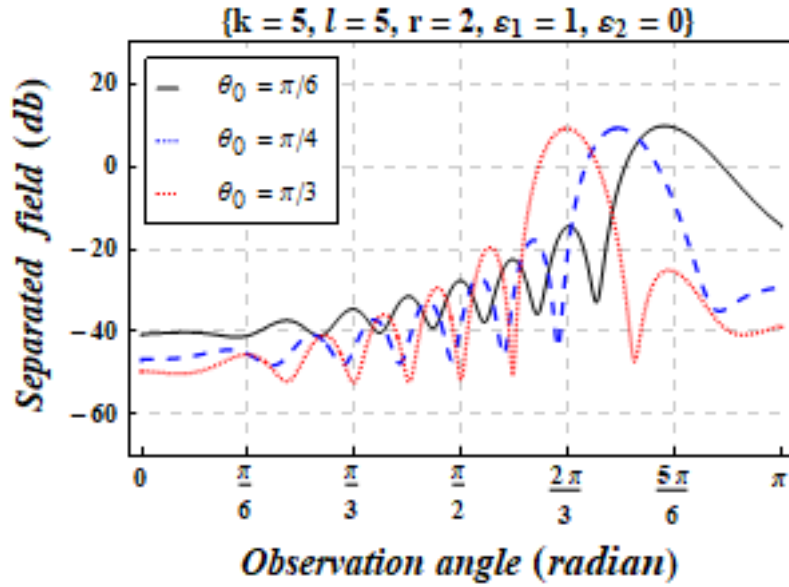
(a)
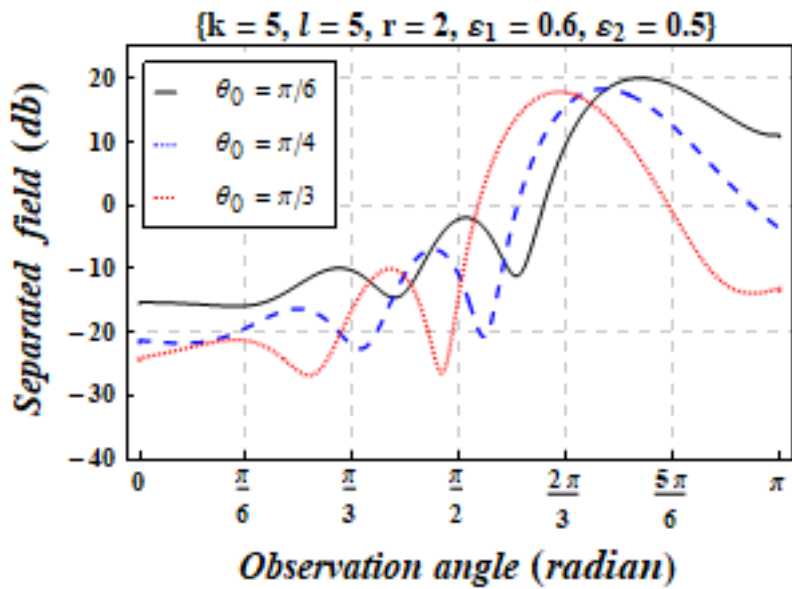
(b)

Figure 3.3: **The separated field for angle of incidence in the absence (a) and presence (b) of cold plasma when $l = 5$.**
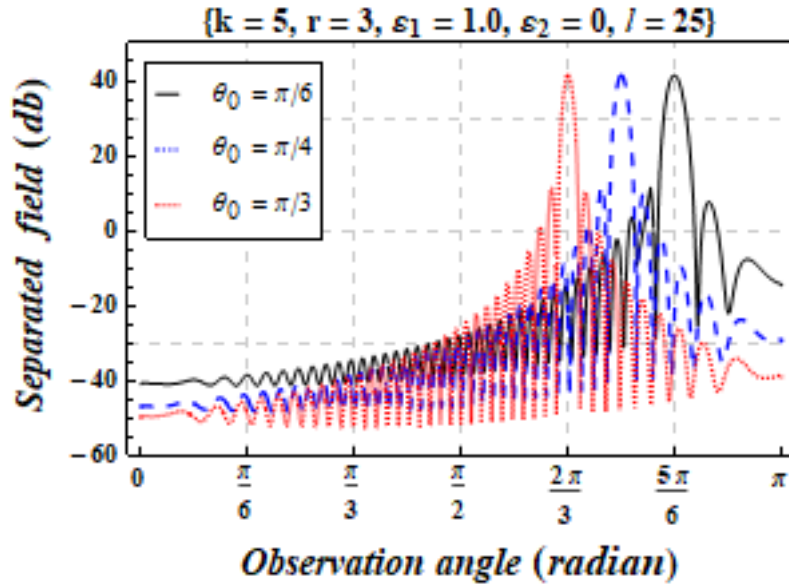
(a)
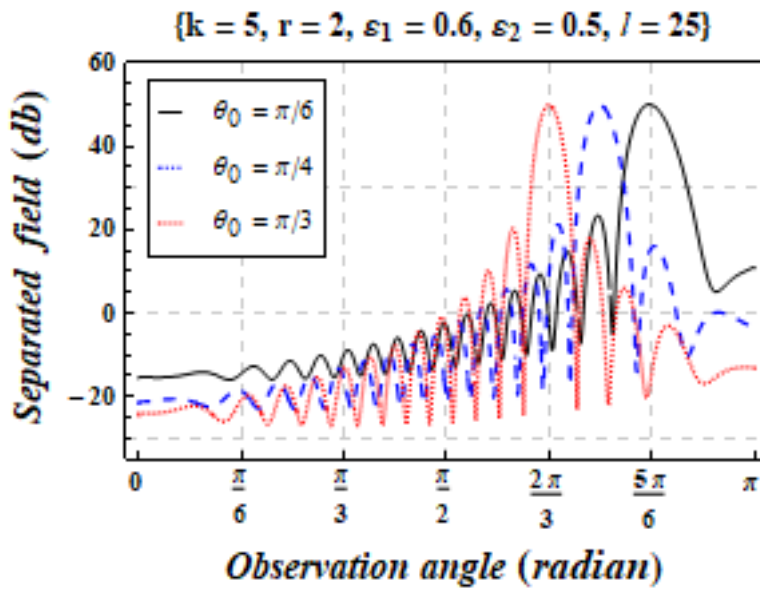
(b)

Figure 3.4: **The separated field for angle of incidence in the absence (a) and presence (b) of cold plasma when** $l = 25$.
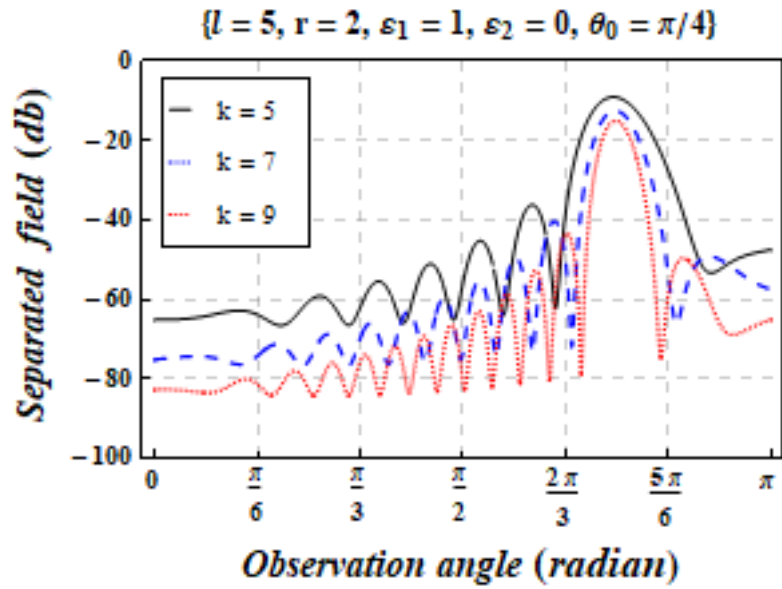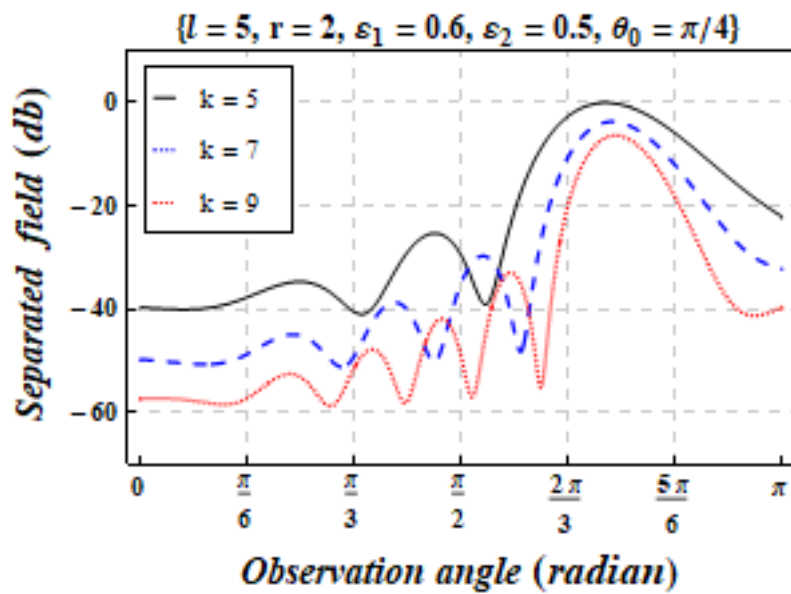
Figure 3.5: **The separated field for wave-number in the absence (a) and presence (b) of cold plasma.**

$\{k = 5, \, r = 2, \, \varepsilon_1 = 1, \, \varepsilon_2 = 0, \, \theta_0 = \pi/4\}$

(a)

$\{k = 5, \, r = 2, \, \varepsilon_1 = 0.6, \, \varepsilon_2 = 0.5, \, \theta_0 = \pi/4\}$
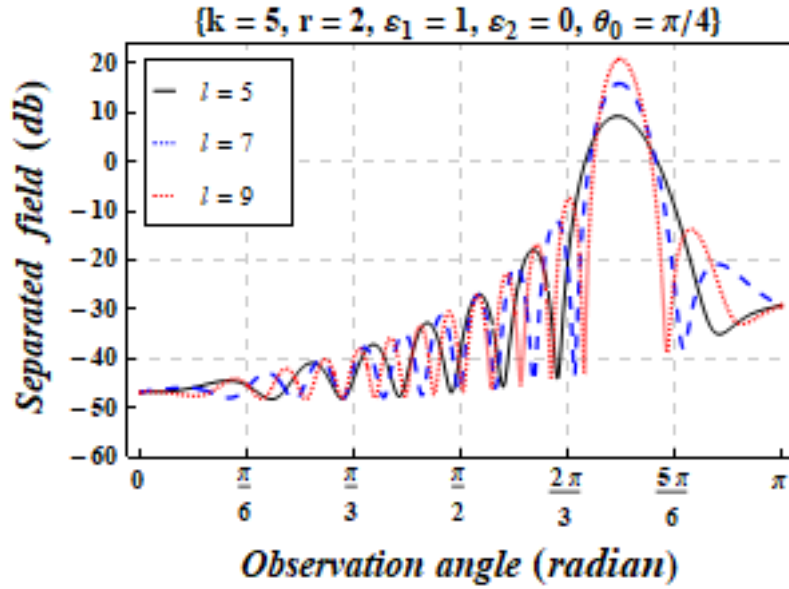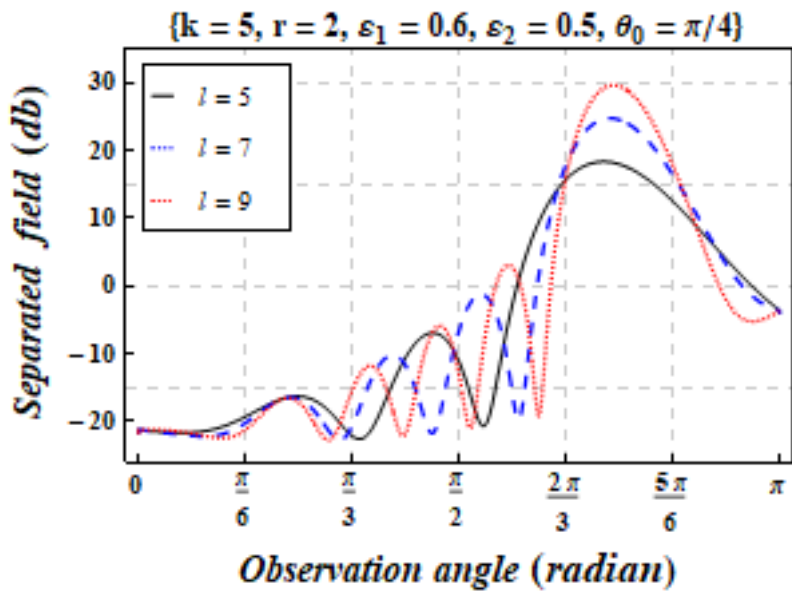
(b)

Figure 3.6: **The separated field for length of plate in the absence (a) and presence (b) of cold plasma.**
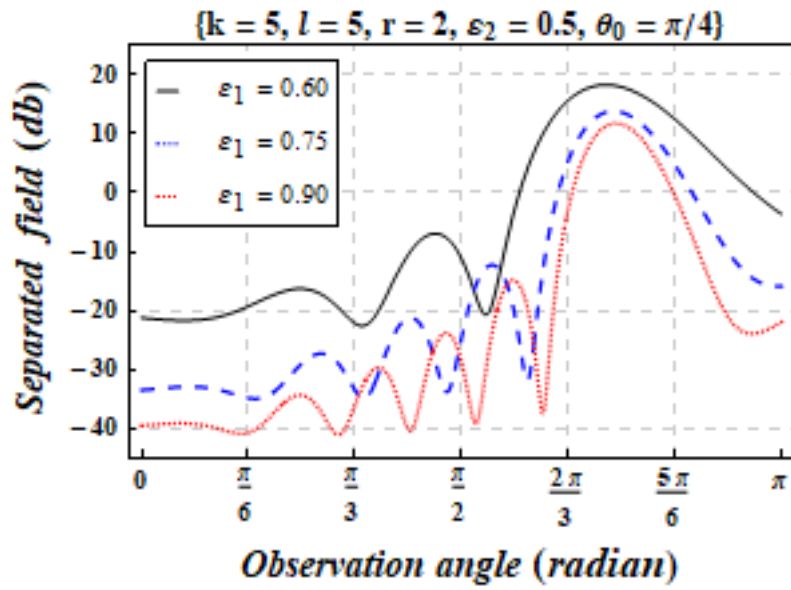
Figure 3.7: **The separated field for** ε_1.
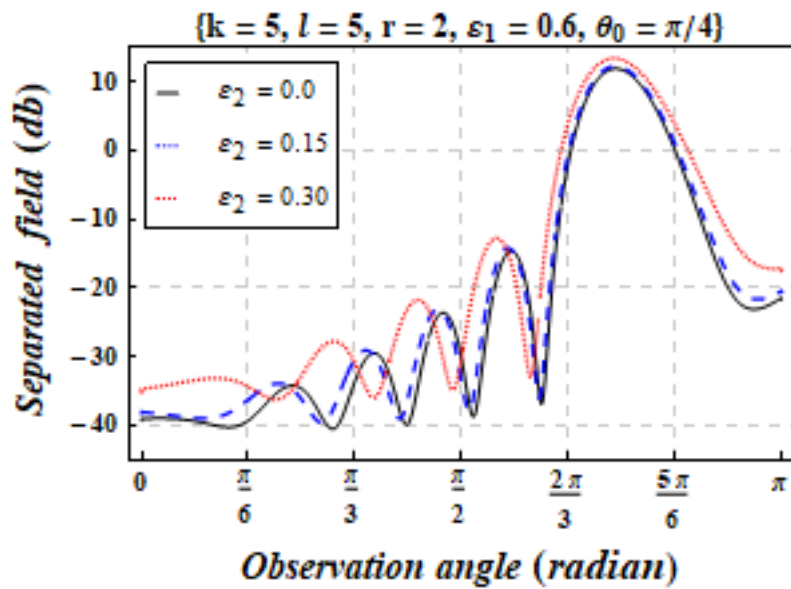
Figure 3.8: **The separated field for** ε_2.

3.8   Conclusions

This chapter has elaborated the analysis of EM-plane wave diffracted by finite plate with Neumann conditions immersed in cold plasma, rigorously. It is noticed that separated field gets affected by (a) extending the length of plate (b) keeping different angle of incidence (c) changing the wave-number (d) assigning different values to permittivity elements of cold plasma.

Chapter 4

Exact and Asymptotic Analysis of Wave Diffracted by a Finite Plate with Impedance in Cold Plasma

This chapter provides comprehensive briefing about the diffraction of electromagnetic (EM) plane wave by a non-symmetric finite plate with impedance lying in the cold plasma. Leontovich boundary conditions are assumed to consider the impedance on the both surfaces of the plate. Helmholtz equation is formulated using the Maxwell's equations with the effects of cold plasma. The Fourier transform is applied and then Wiener-Hopf equations are obtained. The method stationary phase (an asymptotic method) is used to get the result of diffracted field by a finite plate (separated field). Behavior of separated field is discussed graphically.

4.1 Modelling of the Helmholtz Equation

The dielectric permittivity tensor to count the presence of cold plasma is defined as

$$\bar{\varepsilon} = \begin{pmatrix} \varepsilon_1 & -\iota\varepsilon_2 & 0 \\ \iota\varepsilon_2 & \varepsilon_1 & 0 \\ 0 & 0 & \varepsilon_z \end{pmatrix}, \tag{4.1}$$

$$\varepsilon_1 = 1 - \left(\frac{\omega_p}{\omega}\right)^2 \left[1 - \left(\frac{\omega_c}{\omega}\right)^2\right]^{-1}, \quad \varepsilon_2 = \left(\frac{\omega_p}{\omega}\right)^2 \left[\frac{\omega}{\omega_c} - \frac{\omega_c}{\omega}\right]^{-1}, \tag{4.2}$$

and

$$\varepsilon_z = 1 - \left(\frac{\omega_p}{\omega}\right)^2, \tag{4.3}$$

with

$$\omega_p^2 = \frac{N_e e^2}{m \varepsilon_0}, \quad \omega_c = \frac{|e| \mu_0 H_{dc}}{m}. \tag{4.4}$$

It is known that Maxwell's equations are proved to be valid in cold plasma with dielectric permittivity tensor. Use of Maxwell's equation along with (4.1) gives the electric field components in terms of magnetic field which are expressed as

$$E_x = \frac{\iota \varepsilon_1}{\omega \varepsilon_0 (\varepsilon_1^2 - \varepsilon_2^2)} \frac{\partial H_z(x, y)}{\partial y} + \frac{\varepsilon_2}{\omega \varepsilon_0 (\varepsilon_1^2 - \varepsilon_2^2)} \frac{\partial H_z(x, y)}{\partial x}, \tag{4.5}$$

and

$$E_y = \frac{\varepsilon_2}{\omega \varepsilon_0 (\varepsilon_1^2 - \varepsilon_2^2)} \frac{\partial H_z(x, y)}{\partial y} - \frac{\iota \varepsilon_1}{\omega \varepsilon_0 (\varepsilon_1^2 - \varepsilon_2^2)} \frac{\partial H_z(x, y)}{\partial x}. \tag{4.6}$$

Thus, the Helmholtz's equation satisfying H_z obtained from Maxwell's equations along with electric field components (4.5) and (4.6), is computed as follows :

$$\partial_{xx} H_z(x, y) + \partial_{yy} H_z(x, y) + k_{eff}^2 H_z(x, y) = 0, \tag{4.7}$$

with propagation constant

$$k_{eff} = k\sqrt{\frac{\varepsilon_1^2 - \varepsilon_2^2}{\varepsilon_1}}, \quad k = \omega\sqrt{\varepsilon_0 \mu_0}. \tag{4.8}$$

Here, k_{eff} is dependent of k, ε_1 and ε_2, time dependence is taken to be as harmonically behaving as $\exp(-\iota \omega t)$ and will be counted as suppressed throughout the analysis.
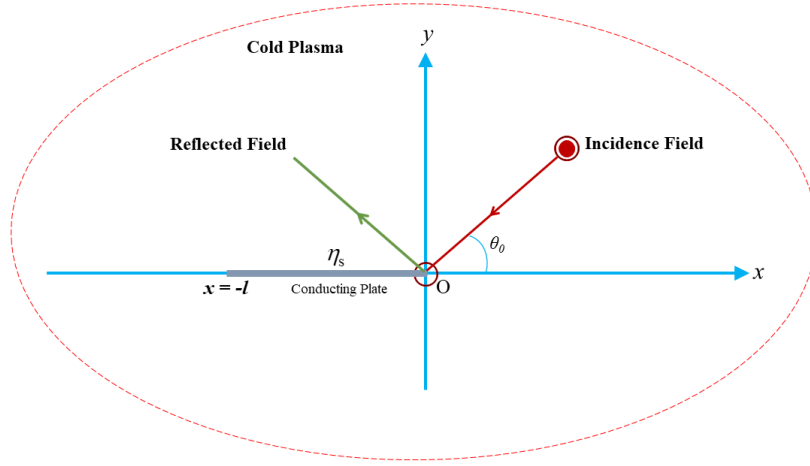
Figure 4.1: **Geometrical description of the model.**

4.2 Mathematical Modelling of the Problem

The finite non-symmetric plate with surface impedance is lying along $y = 0$ with edges at $x = -l$ and $x = 0$ as displayed in Fig. 4.1. The EM-plane wave incident on the non-symmetric finite plate is taken as

$$H_z^{inc}(x, y) = \exp\{-\iota k_{eff}(x \cos \theta_0 + y \sin \theta_0)\}, \qquad (4.9)$$

where amplitude of the magnetic field is taken 1 A/m and θ_0 is the angle of incidence with $x-$axis. Here, the total field can be expressed as follows:

$$H_z^{tot}(x, y) = H_z^{inc}(x, y) + H_z^{ref}(x, y) + H_z(x, y). \qquad (4.10)$$

Here, the function $H_z(x, y)$ is the diffracted field and $H_z^{ref}(x, y)$ denotes the reflected field, which is defined as

$$H_z^{ref}(x, y) = \left(\frac{\eta_s \sin \theta_0 - 1}{\eta_s \sin \theta_0 + 1}\right) \exp\{-\iota k_{eff}(x \cos \theta_0 - y \sin \theta_0)\}. \qquad (4.11)$$

For convenience of analyzing the model, medium is assumed to be slightly lossy as in $k_{eff} = \Re\{k_{eff}\} + \iota \Im\{k_{eff}\}$, $0 < \Im\{k_{eff}\} \ll \Re\{k_{eff}\}$ and the solution for real

k_{eff} may be achieved by assuming $\mathfrak{Im}\{k_{eff}\} \longrightarrow 0$. The boundary value problem (BVP) under consideration is elaborated in terms of the magnetic field potential and it is adequate to denote the diffracted field in the different regions. The total field $H_z^{tot}(x, y)$ in the range $x \in (-\infty, \infty)$, that satisfies the Helmholtz's equation as follows :

$$\left[\partial_{xx} + \partial_{yy} + k_{eff}^2\right] H_z^{tot}(x, y) = 0, \qquad (4.12)$$

diffracted field satisfying Helmholtz's equation obtained from (4.12) is given as follows:

$$\left[\partial_{xx} + \partial_{yy} + k_{eff}^2\right] H_z(x, y) = 0. \qquad (4.13)$$

Our focus is to evaluate the diffracted field of EM-plane wave incident on the non-symmetric plate of finite length. Same impedance is assumed on both upper and lower surface of the finite plate. Therefore, Leontovich boundary conditions are taken into account to consider the effects of impedance as

$$\partial_y H_z^{tot}(x, 0^{\mp}) - \iota \frac{\varepsilon_2}{\varepsilon_1} \partial_x H_z^{tot}(x, 0^{\mp}) = \pm \iota \frac{k_{eff}^2}{\omega \mu_0} \eta_0 \eta_s H_z^{tot}(x, 0^{\mp}), \quad \text{for } -l \leq x \leq 0, \ (4.14)$$

where $\eta_0 = \sqrt{\mu_0/\varepsilon_0}$. The continuity conditions are

$$\left.\begin{array}{ll} H_z^{tot}(x, 0^+) = H_z^{tot}(x, 0^-), & \text{for } -\infty < x < -l, \ x > 0, \\ \partial_y H_z^{tot}(x, 0^+) = \partial_y H_z^{tot}(x, 0^-), & \text{for } -\infty < x < -l, \ x > 0. \end{array}\right\} \qquad (4.15)$$

4.3 Transformation of the Problem

Now we apply the Fourier transform on the boundary value problem (BVP) with respect to variable x as

$$\mathcal{F}(\alpha, y) = \frac{1}{\sqrt{2\pi}} \int_{-\infty}^{\infty} H_z(x, y) e^{\iota \alpha x} dx$$

$$= \mathcal{F}_+(\alpha, y) + e^{-\iota \alpha l} \mathcal{F}_-(\alpha, y) + \mathcal{F}_l(\alpha, y), \qquad (4.16)$$

where $\alpha = \mathfrak{Re}\{\alpha\} + \iota\mathfrak{Im}\{\alpha\} = \sigma + \iota\tau$. The asymptotic expression of $H_z(x, y)$ for $x \longrightarrow \pm\infty$ is taken into account as

$$H_z(x, y) = \begin{cases} O\left(e^{-\mathfrak{Im}\{k_{eff}\}x}\right) & \text{for } x \longrightarrow \infty, \\ O\left(e^{\mathfrak{Im}\{k_{eff}\}x\cos\theta_0}\right) & \text{for } x \longrightarrow -\infty. \end{cases} \tag{4.17}$$

$\mathcal{F}_+(\alpha, y)$ is the regular function of α in the upper half-plane $\mathfrak{Im}\{-k_{eff}\} < \mathfrak{Im}\{\alpha\}$, $\mathcal{F}_-(\alpha, y)$ is the regular function of α in the lower half-plane $\mathfrak{Im}\{\alpha\} < \mathfrak{Im}\{k_{eff}\cos\theta_0\}$ and these both regions together generate a common region (or a band of analyticity) $\mathfrak{Im}\{-k_{eff}\} < \mathfrak{Im}\{\alpha\} < \mathfrak{Im}\{k_{eff}\cos\theta_0\}$ in which all the functions including $\mathcal{F}_l(\alpha, y)$ are analytic, these functions are defined as

$$\mathcal{F}_+(\alpha, y) = \frac{1}{\sqrt{2\pi}} \int_0^\infty H_z(x, y) e^{\iota\alpha x} dx, \tag{4.18}$$

$$\mathcal{F}_-(\alpha, y) = \frac{1}{\sqrt{2\pi}} \int_{-\infty}^{-l} H_z(x, y) e^{\iota\alpha(x+l)} dx, \tag{4.19}$$

$$\mathcal{F}_l(\alpha, y) = \frac{1}{\sqrt{2\pi}} \int_{-l}^0 H_z(x, y) e^{\iota\alpha x} dx, \tag{4.20}$$

$$\mathcal{F}^{inc}(\alpha, 0) = \frac{1 - e^{-\iota l\left(\alpha - k_{eff}\cos\theta_0\right)}}{\sqrt{2\pi}\iota(\alpha - k_{eff}\cos\theta_0)}, \tag{4.21}$$

$$\mathcal{F}^{ref}(\alpha, 0) = \frac{1}{\sqrt{2\pi}}\left(\frac{\eta_s\sin\theta_0 - 1}{\eta_s\sin\theta_0 + 1}\right)\frac{1 - e^{-\iota l\left(\alpha - k_{eff}\cos\theta_0\right)}}{\iota(\alpha - k_{eff}\cos\theta_0)}. \tag{4.22}$$

The application of Fourier transform on (4.13)-(4.15) yields,

$$\left(\frac{d^2}{dy^2} + \gamma^2\right)\mathcal{F}(\alpha, y) = 0, \tag{4.23}$$

where $\gamma(\alpha) = \sqrt{k_{eff}^2 - \alpha^2}$.

$$\partial_y\mathcal{F}^{tot}(\alpha, 0^\mp) - \alpha\frac{\varepsilon_2}{\varepsilon_1}\mathcal{F}^{tot}(\alpha, 0^\mp) = \pm\iota\frac{k_{eff}^2}{\omega\mu_0}\eta_0\eta_s\mathcal{F}^{tot}(\alpha, 0^\mp), \tag{4.24}$$

and

$$\mathcal{F}_- \left(\alpha, 0^+ \right) = \mathcal{F}_- \left(\alpha, 0^- \right) = \mathcal{F}_- \left(\alpha, 0 \right),$$

$$\mathcal{F}_+ \left(\alpha, 0^+ \right) = \mathcal{F}_+ \left(\alpha, 0^- \right) = \mathcal{F}_+ \left(\alpha, 0 \right),$$

$$\partial_y \mathcal{F}_- \left(\alpha, 0^+ \right) = \partial_y \mathcal{F}_- \left(\alpha, 0^- \right) = \partial_y \mathcal{F}_- \left(\alpha, 0 \right), \quad (4.25)$$

$$\partial_y \mathcal{F}_+ \left(\alpha, 0^+ \right) = \partial_y \mathcal{F}_+ \left(\alpha, 0^- \right) = \partial_y \mathcal{F}_+ \left(\alpha, 0 \right).$$

4.4 Modelling of Wiener-Hopf Equation

The solution of (4.23) satisfying the radiation conditions is given by

$$\mathcal{F} \left(\alpha, y \right) = \begin{cases} A_1 \left(\alpha \right) e^{-\iota \gamma y} & y \geq 0, \\ A_2 \left(\alpha \right) e^{iota\gamma y} & y < 0. \end{cases} \quad (4.26)$$

Now with the aid of (4.16), (4.24), (4.25) and (4.26), following coupled functional equations are obtained as

$$\begin{aligned} \mathcal{F}'_+ \left(\alpha, 0 \right) + e^{-\iota \alpha l} \mathcal{F}'_- \left(\alpha, 0 \right) &= \left[\mathcal{F}'_{inc}(\alpha, 0) + \mathcal{F}'_{ref} \left(\alpha, 0 \right) \right] \\ &\quad - \alpha \Big(\frac{\varepsilon_2}{\varepsilon_1} \Big) \left[\mathcal{F}_{inc}(\alpha, 0) + \mathcal{F}_{ref} \left(\alpha, 0 \right) \right] \\ &\quad - \frac{1}{2} \alpha \Big(\frac{\varepsilon_2}{\varepsilon_1} \Big) \left[\mathcal{F}_l(\alpha, 0^+) + \mathcal{F}_l \left(\alpha, 0^- \right) \right] \quad (4.27) \\ &\quad + \frac{1}{2} \Big(\iota \frac{k_{eff}^2}{\omega \mu_0} \eta_0 \eta \Big) \left[\mathcal{F}_l(\alpha, 0^+) - \mathcal{F}_l \left(\alpha, 0^- \right) \right] \\ &\quad - \frac{\iota \gamma}{2} \left[A_1(\alpha) - A_2(\alpha) \right], \end{aligned}$$

$$\mathcal{F}_{+}\left(\alpha,0\right)+e^{-\iota\alpha l}\mathcal{F}_{-}\left(\alpha,0\right)=-\frac{\alpha\left(\frac{\varepsilon_2}{\varepsilon_1}\right)}{\left(\alpha\frac{\varepsilon_2}{\varepsilon_1}\right)^2+\left(\frac{k_{eff}^2}{\omega\mu_0}\eta_0\eta_s\right)^2}\left[\mathcal{F}'_{inc}(\alpha,0)+\mathcal{F}'_{ref}\left(\alpha,0\right)\right]$$

$$+\left[\mathcal{F}'_{inc}(\alpha,0)+\mathcal{F}'_{ref}\left(\alpha,0\right)\right]$$

$$-\frac{\alpha\left(\frac{\varepsilon_2}{\varepsilon_1}\right)}{\left(\alpha\frac{\varepsilon_2}{\varepsilon_1}\right)^2+\left(\frac{k_{eff}^2}{\omega\mu_0}\eta_0\eta_s\right)^2}\left[\mathcal{F}'_l(\alpha,0^+)+\mathcal{F}'_l\left(\alpha,0^-\right)\right] \quad (4.28)$$

$$-\frac{1}{2}\frac{1}{\left(\alpha\frac{\varepsilon_2}{\varepsilon_1}\right)^2+\left(\frac{k_{eff}^2}{\omega\mu_0}\eta_0\eta_s\right)^2}\left(\iota\frac{k_{eff}^2}{\omega\mu_0}\eta_0\eta_s\right)\left[\mathcal{F}'_l(\alpha,0^+)-\mathcal{F}'_l\left(\alpha,0^-\right)\right]$$

$$+\frac{1}{2}\left[A_1(\alpha)+A_2(\alpha)\right].$$

Now we use certain approximations to attain result for high signal frequency such that $\omega\gg\omega_c$, while keeping it at the same order with ω_p, yielding the $\varepsilon_1\approx 1-(\omega_p/\omega)^2$ and $\varepsilon_2\to 0$ in the limit case. After approximations, the functional Wiener-Hopf equations are computed as follows :

$$\mathcal{F}'_{+}\left(\alpha,0\right)+e^{-\iota\alpha l}\mathcal{F}'_{-}\left(\alpha,0\right)+\mathcal{S}\left(\alpha\right)\tilde{\mathcal{F}}_l\left(\alpha,0\right)=\mathcal{F}'_{inc}(\alpha,0)+\mathcal{F}'_{ref}\left(\alpha,0\right), \quad (4.29)$$

$$\mathcal{F}_{+}\left(\alpha,0\right)+e^{-\iota\alpha l}\mathcal{F}_{-}\left(\alpha,0\right)+\mathcal{K}\left(\alpha\right)\tilde{\mathcal{F}}'_l\left(\alpha,0\right)=\mathcal{F}_{inc}(\alpha,0)+\mathcal{F}_{ref}\left(\alpha,0\right), \quad (4.30)$$

where

$$\tilde{\mathcal{F}}_l\left(\alpha,0\right)=\frac{1}{2}\left[\mathcal{F}_l\left(\alpha,0^+\right)-\mathcal{F}_l\left(\alpha,0^-\right)\right], \quad (4.31)$$

$$\tilde{\mathcal{F}}'_l\left(\alpha,0\right)=\frac{1}{2}\left[\mathcal{F}'_l\left(\alpha,0^+\right)-\mathcal{F}'_l\left(\alpha,0^-\right)\right], \quad (4.32)$$

$$A_1\left(\alpha\right)=-\tilde{\mathcal{F}}_l\left(\alpha,0\right)+\frac{\tilde{\mathcal{F}}'_l\left(\alpha,0\right)}{i\gamma\left(\alpha\right)}, \quad (4.33)$$

$$A_2\left(\alpha\right)=\tilde{\mathcal{F}}_l\left(\alpha,0\right)+\frac{\tilde{\mathcal{F}}'_l\left(\alpha,0\right)}{i\gamma\left(\alpha\right)}. \quad (4.34)$$

The kernel functions appearing in the coupled system of Wiener-Hopf equations are as follows:

$$\mathcal{S}\left(\alpha\right)=-\iota\gamma\left(\alpha\right)\mathcal{L}\left(\alpha\right), \quad (4.35)$$
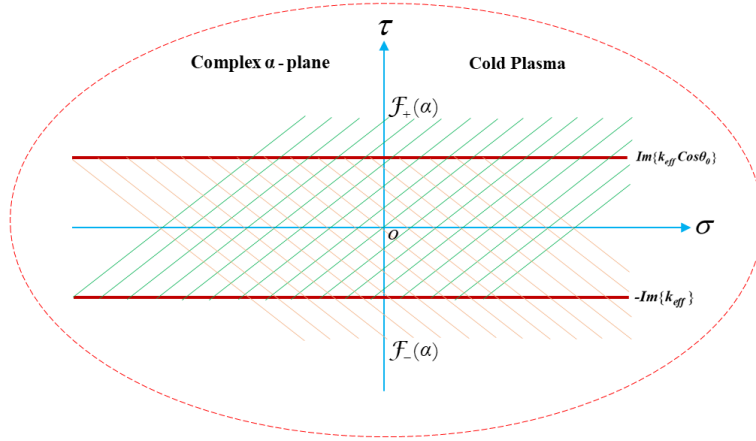
Figure 4.2: **The description of analytic continuation in the complex $\alpha-$plane.**

$$\mathcal{K}\left(\alpha\right) = \frac{\iota k}{k_{eff}^2 \eta_s} \mathcal{L}\left(\alpha\right), \tag{4.36}$$

where

$$\mathcal{L}\left(\alpha\right) = \left(1 + \frac{k_{eff}^2 \eta_s}{k\gamma\left(\alpha\right)}\right), \tag{4.37}$$

4.5   Wiener-Hopf Procedure

The objective of this model is to observe the effect of EM-wave incident (which is an ultimate result in the form of diffracted field) on a conductible plate of finite length with surface impedance in the presence of cold plasma. The functional Wiener-Hopf equations (4.29) and (4.30) for the boundary value problem are put to rigorous analysis through Wiener-Hopf method. The salient fact of Wiener-Hopf technique is that being not a fundamentally numerical naturally that's why it permits an additional insight to physical and mathematical structure for diffracted field of incident EM-wave. The kernel functions arising from (4.29) and (4.30) presented by (4.35) and (4.36) are decomposed as

$$\mathcal{S}\left(\alpha\right) = \mathcal{S}_+\left(\alpha\right)\mathcal{S}_-\left(\alpha\right), \tag{4.38}$$

$$\mathcal{K}\left(\alpha\right) = \mathcal{K}_{+}\left(\alpha\right)\mathcal{K}_{-}\left(\alpha\right), \tag{4.39}$$

and the factors appearing in (4.38) and (4.39) are given as follows :

$$\mathcal{S}_{\pm}\left(\alpha\right) = e^{-\iota\frac{\pi}{4}}\gamma_{\pm}\left(\alpha\right)\mathcal{L}_{\pm}, \tag{4.40}$$

$$\mathcal{K}_{\pm}\left(\alpha\right) = \frac{e^{\iota\frac{\pi}{4}}\sqrt{k}}{k_{eff}\sqrt{\eta_s}}\mathcal{L}_{\pm}\left(\alpha\right). \tag{4.41}$$

Furthermore, the product decomposition of the function $\mathcal{L}(\alpha)$ appearing in (4.35) and (4.36), presented by (4.37), is made as

$$\mathcal{L}\left(\alpha\right) = \mathcal{L}_{+}\left(\alpha\right)\mathcal{L}_{-}\left(\alpha\right), \tag{4.42}$$

where

$$\mathcal{L}_{\pm}\left(\alpha\right) = \left(1 \pm \frac{\iota k_{eff}\sqrt{\eta_s}}{\sqrt{k}\gamma_{\pm}\left(\alpha\right)}\right), \tag{4.43}$$

and

$$\gamma_{\pm}\left(\alpha\right) = \sqrt{k_{eff} \pm \alpha}. \tag{4.44}$$

The factors with subscript of $+$ are regular functions of α in upper-half of $\alpha-$plane $(\mathcal{I}m\left\{-k_{eff}\right\} < \mathcal{I}m\left\{\alpha\right\})$ whereas the factors with subscript of - are regular functions of α in the lower-half $\alpha-$plane $(\mathcal{I}m\left\{\alpha\right\} < \mathcal{I}m\left\{k\right\})$. Now plugging the (4.21) and (4.22) in both (4.29) and (4.30), we get

$$\mathcal{F}'_{+}\left(\alpha,0\right) + e^{-\iota\alpha l}\mathcal{F}'_{-}\left(\alpha,0\right) + \mathcal{S}\left(\alpha\right)\tilde{\mathcal{F}}_{l}\left(\alpha,0\right) = \mathcal{A}\mathcal{G}(\alpha), \tag{4.45}$$

$$\mathcal{F}_{+}\left(\alpha,0\right) + e^{-\iota\alpha l}\mathcal{F}_{-}\left(\alpha,0\right) + \mathcal{K}\left(\alpha\right)\tilde{\mathcal{F}}'_{l}\left(\alpha,0\right) = \mathcal{A}'\mathcal{G}'(\alpha), \tag{4.46}$$

where

$$\mathcal{A} = \left[\left(\frac{\eta_s\sin\theta_0 - 1}{\eta_s\sin\theta_0 + 1}\right) - 1\right]k_{eff}\sin\theta_0, \tag{4.47}$$

$$\mathcal{A}' = -\left[\left(\frac{\eta_s\sin\theta_0 - 1}{\eta_s\sin\theta_0 + 1}\right) + 1\right]\iota. \tag{4.48}$$

$$\mathcal{G}(\alpha) = \mathcal{G}'(\alpha) = \frac{1 - e^{-\iota l (\alpha - k_{eff} \cos \theta_0)}}{\sqrt{2\pi} \left(\alpha - k_{eff} \cos \theta_0 \right)} \tag{4.49}$$

Inserting $\tilde{\mathcal{F}}_l (\alpha, 0)$ and $\tilde{\mathcal{F}}'_l (\alpha, 0)$ explicitly from (4.45) and (4.46) into (4.33) and (4.34), we get

$$\begin{aligned} A_1 (\alpha) = {} & \frac{1}{\mathcal{S}(\alpha)} \left\{ \mathcal{F}'_+ (\alpha, 0) + e^{-\iota \alpha l} \mathcal{F}'_- (\alpha, 0) - \mathcal{A} \mathcal{G}(\alpha) \right\} \\ & - \frac{1}{\iota \gamma (\alpha) \mathcal{K}(\alpha)} \left\{ \mathcal{F}_+ (\alpha, 0) + e^{-\iota \alpha l} \mathcal{F}_- (\alpha, 0) - \mathcal{A}' \mathcal{G}'(\alpha) \right\}, \end{aligned} \tag{4.50}$$

$$\begin{aligned} A_2 (\alpha) = {} & -\frac{1}{\mathcal{S}(\alpha)} \left\{ \mathcal{F}'_+ (\alpha, 0) + e^{-\iota \alpha l} \mathcal{F}'_- (\alpha, 0) - \mathcal{A} \mathcal{G}(\alpha) \right\} \\ & - \frac{1}{\iota \gamma (\alpha) \mathcal{K}(\alpha)} \left\{ \mathcal{F}_+ (\alpha, 0) + e^{-\iota \alpha l} \mathcal{F}_- (\alpha, 0) - \mathcal{A}' \mathcal{G}'(\alpha) \right\}, \end{aligned} \tag{4.51}$$

The Wiener-Hopf equations presented by (4.45) and (4.46) are derived through the general theory of Wiener-Hopf procedure and the solution for large $k_{eff} r$ $\left(r = \sqrt{x^2 + y^2} \right)$ may be obtained in an approximate form through the analysis made by using Wiener-Hopf technique. Now equating the terms of (4.45) and (4.46) with subscript of positive sign on one side of the equation and the terms with subscript of negative sign on the other side give us consequently the same function $\mathcal{J}(\alpha)$, say, which is a polynomial function, so is an entire function. Analytic continuation (see Fig. 4.2) along with arguments involving extended form of Liouville's theorem allows to equate the function $\mathcal{J}(\alpha)$ to zero, thus, we obtain the following results

$$\mathcal{F}'_+ (\alpha, 0) = \frac{\mathcal{A} \mathcal{S}_+ (\alpha)}{\sqrt{2\pi}} \left(\mathcal{G}_1 (\alpha) + \mathcal{T}(\alpha) \mathcal{C}_1 \right), \tag{4.52}$$

$$\mathcal{F}'_- (\alpha, 0) = \frac{\mathcal{A} \mathcal{S}_- (\alpha)}{\sqrt{2\pi}} \left(\mathcal{G}_2 (-\alpha) + \mathcal{T}(-\alpha) \mathcal{C}_2 \right), \tag{4.53}$$

$$\mathcal{F}_+ (\alpha, 0) = \frac{\mathcal{A}' \mathcal{K}_+ (\alpha)}{\sqrt{2\pi}} \left(\mathcal{G}'_1 (\alpha) + \mathcal{T}'(\alpha) \mathcal{C}'_1 \right), \tag{4.54}$$

$$\mathcal{F}_- (\alpha, 0) = \frac{\mathcal{A}' \mathcal{K}_- (\alpha)}{\sqrt{2\pi}} \left(\mathcal{G}'_2 (-\alpha) + \mathcal{T}'(-\alpha) \mathcal{C}'_2 \right), \tag{4.55}$$

where

$$\mathcal{G}_1\left(\alpha\right) = \frac{1}{\left(\alpha - k_{eff}\cos\theta_0\right)}\left(\frac{1}{\mathcal{S}_+\left(\alpha\right)} - \frac{1}{\mathcal{S}_+\left(k_{eff}\cos\theta_0\right)}\right) - e^{-\iota l k_{eff}\cos\theta_0}\mathcal{R}_1\left(\alpha\right), \quad (4.56)$$

$$\mathcal{G}_2\left(\alpha\right) = \frac{e^{\iota l k_{eff}\cos\theta_0}}{\left(\alpha + k_{eff}\cos\theta_0\right)}\left(\frac{1}{\mathcal{S}_+\left(\alpha\right)} - \frac{1}{\mathcal{S}_+\left(-k_{eff}\cos\theta_0\right)}\right) - \mathcal{R}_2\left(\alpha\right), \quad (4.57)$$

$$\mathcal{C}_1 = \mathcal{S}_+\left(k_{eff}\right)\left(\frac{\mathcal{G}_2\left(k_{eff}\right) + \mathcal{S}_+\left(k_{eff}\right)\mathcal{G}_1\left(k_{eff}\right)\mathcal{T}\left(k_{eff}\right)}{1 - \mathcal{S}_+^2\left(k_{eff}\right)\mathcal{T}^2\left(k_{eff}\right)}\right), \quad (4.58)$$

$$\mathcal{C}_2 = \mathcal{S}_+\left(k_{eff}\right)\left(\frac{\mathcal{G}_1\left(k_{eff}\right) + \mathcal{S}_+\left(k_{eff}\right)\mathcal{G}_2\left(k_{eff}\right)\mathcal{T}\left(k_{eff}\right)}{1 - \mathcal{S}_+^2\left(k_{eff}\right)\mathcal{T}^2\left(k_{eff}\right)}\right), \quad (4.59)$$

$$\mathcal{G}_1'\left(\alpha\right) = \frac{1}{\left(\alpha - k_{eff}\cos\theta_0\right)}\left(\frac{1}{\mathcal{K}_+\left(\alpha\right)} - \frac{1}{\mathcal{K}_+\left(k_{eff}\cos\theta_0\right)}\right) - e^{-\iota l k_{eff}\cos\theta_0}\mathcal{R}_1\left(\alpha\right), \quad (4.60)$$

$$\mathcal{G}_2'\left(\alpha\right) = \frac{e^{\iota l k_{eff}\cos\theta_0}}{\left(\alpha + k_{eff}\cos\theta_0\right)}\left(\frac{1}{\mathcal{K}_+\left(\alpha\right)} - \frac{1}{\mathcal{K}_+\left(-k_{eff}\cos\theta_0\right)}\right) - \mathcal{R}_2\left(\alpha\right), \quad (4.61)$$

$$\mathcal{C}_1' = \mathcal{K}_+\left(k_{eff}\right)\left(\frac{\mathcal{G}_2\left(k_{eff}\right) + \mathcal{K}_+\left(k_{eff}\right)\mathcal{G}_1\left(k_{eff}\right)\mathcal{T}\left(k_{eff}\right)}{1 - \mathcal{K}_+^2\left(k_{eff}\right)\mathcal{T}^2\left(k_{eff}\right)}\right), \quad (4.62)$$

$$\mathcal{C}_2' = \mathcal{K}_+\left(k_{eff}\right)\left(\frac{\mathcal{G}_1\left(k_{eff}\right) + \mathcal{K}_+\left(k_{eff}\right)\mathcal{G}_2\left(k_{eff}\right)\mathcal{T}\left(k_{eff}\right)}{1 - \mathcal{K}_+^2\left(k_{eff}\right)\mathcal{T}^2\left(k_{eff}\right)}\right), \quad (4.63)$$

$$\mathcal{R}_{1,2}\left(\alpha\right) = \frac{E_{-1}\left[\mathcal{W}_{-1}\left(-\iota l\left(k_{eff}\pm k_{eff}\cos\theta_0\right)\right) - \mathcal{W}_{-1}\left(-\iota l\left(k_{eff}+\alpha\right)\right)\right]}{2\pi\iota\left(\alpha\mp k_{eff}\cos\theta_0\right)}, \quad (4.64)$$

$$\mathcal{T}\left(\alpha\right) = \frac{1}{2\pi\iota}E_{-1}\mathcal{W}_{-1}\left(-\iota\left(k_{eff}+\alpha\right)l\right), \quad (4.65)$$

$$E_{-1} = 2\exp\left(\iota k_{eff}l\right)\left(l\right)^{\frac{1}{2}}\left(\iota\right)^{-\frac{1}{2}}, \quad (4.66)$$

and

$$\begin{aligned}\mathcal{W}_{n-\frac{1}{2}}\left(s\right) &= \int_0^\infty \frac{v^n\exp\left(-v\right)}{v+s}du \\ &= \Gamma\left(n+1\right)\exp\left(\frac{s}{2}\right)s^{\frac{1}{2}n-\frac{1}{2}}\mathcal{W}_{-\frac{1}{2}\left(n+1\right),\frac{1}{2}n}\left(s\right).\end{aligned} \quad (4.67)$$

Here, $\mathcal{W}_{m,n}$ is named as Whittaker function and $s = -\iota\left(k_{eff}+\alpha\right)l$, $n = -\frac{1}{2}$.

Now plugging the (4.52)-(4.55) along with (4.47)-(4.49) in (4.50) and (4.51) gives us

61

the following result :

$$
\left.\begin{array}{c} A_1\left(\alpha\right) \\ A_2\left(\alpha\right) \end{array}\right\} = \frac{\mathcal{A}sgn\left(y\right)}{\sqrt{2\pi}\mathcal{S}\left(\alpha\right)} \left\{ \begin{array}{c} \mathcal{S}_+\left(\alpha\right)\mathcal{G}_1\left(\alpha\right) + \mathcal{S}_+\left(\alpha\right)\mathcal{T}\left(\alpha\right)\mathcal{C}_1 \\ +e^{-\iota\alpha l}\mathcal{S}_-\left(\alpha\right)\mathcal{G}_2\left(-\alpha\right) \\ +e^{-\iota\alpha l}\mathcal{S}_-\left(\alpha\right)\mathcal{T}\left(-\alpha\right)\mathcal{C}_2 \\ -\frac{1-e^{-\iota l\left(\alpha-k_{eff}\cos\theta_0\right)}}{\left(\alpha-k_{eff}\cos\theta_0\right)} \end{array} \right\}
$$
$$
- \frac{\mathcal{A}'}{\sqrt{2\pi}\iota\gamma\left(\alpha\right)\mathcal{K}\left(\alpha\right)} \left\{ \begin{array}{c} \mathcal{K}_+\left(\alpha\right)\mathcal{G}'_1\left(\alpha\right) + \mathcal{K}_+\left(\alpha\right)\mathcal{T}\left(\alpha\right)\mathcal{C}'_1 \\ +e^{-\iota\alpha l}\mathcal{K}_-\left(\alpha\right)\mathcal{G}'_2\left(-\alpha\right) \\ +e^{-\iota\alpha l}\mathcal{K}_-\left(\alpha\right)\mathcal{T}\left(-\alpha\right)\mathcal{C}'_2 \\ -\frac{1-e^{-\iota l\left(\alpha-k_{eff}\cos\theta_0\right)}}{\left(\alpha-k_{eff}\cos\theta_0\right)} \end{array} \right\},
$$

(4.68)

The diffraction of EM-wave field obtained by the use of inverse Fourier transform of (4.26) is defined as

$$
\begin{aligned}
H_z(x,y) &= \frac{1}{\sqrt{2\pi}} \int_{-\infty}^{\infty} \mathcal{F}\left(\alpha,y\right)e^{-\iota\alpha x}d\alpha \\
&= \frac{1}{\sqrt{2\pi}} \int_{-\infty}^{\infty} \left\{ \begin{array}{c} A_1\left(\alpha\right) \\ A_2\left(\alpha\right) \end{array} \right\} e^{-\iota\alpha x - \iota\gamma|y|}d\alpha.
\end{aligned}
$$

(4.69)

where $A_1\left(\alpha\right)$ and $A_2\left(\alpha\right)$ are given by (4.68). Substitution of (4.68) into (4.69) and splitting up the diffracted field function $H_z(x,y)$ into two functions $H_z^{sep}(x,y)$ and $H_z^{int}(x,y)$ as described by

$$
H_z(x,y) = H_z^{sep}(x,y) + H_z^{int}(x,y),
$$

(4.70)

where

$$H_z^{sep}(x,y) = \frac{sgn(y)}{2\pi} \int\limits_{-\infty}^{\infty} \frac{1}{\mathcal{S}(\alpha)} \left(\begin{array}{c} -\dfrac{\mathcal{A}\mathcal{S}_+(\alpha)}{(\alpha-k_{eff}\cos\theta_0)\mathcal{S}_+(k_{eff}\cos\theta_0)} \\[3mm] +\dfrac{\mathcal{A}\mathcal{S}_-(\alpha)e^{-\iota l(\alpha-k_{eff}\cos\theta_0)}}{(\alpha-k_{eff}\cos\theta_0)\mathcal{S}_+(-k_{eff}\cos\theta_0)} \end{array} \right) e^{(-\iota\alpha x - \iota\gamma|y|)} d\alpha$$

$$+ \frac{1}{2\pi} \int\limits_{-\infty}^{\infty} \frac{1}{\iota\gamma(\alpha)\mathcal{K}(\alpha)} \left(\begin{array}{c} \dfrac{\mathcal{A}'\mathcal{K}_+(\alpha)}{(\alpha-k_{eff}\cos\theta_0)\mathcal{K}_+(k_{eff}\cos\theta_0)} \\[3mm] -\dfrac{\mathcal{A}'\mathcal{K}_-(\alpha)e^{-\iota l(\alpha-k_{eff}\cos\theta_0)}}{(\alpha-k_{eff}\cos\theta_0)\mathcal{K}_+(-k_{eff}\cos\theta_0)} \end{array} \right) e^{(-\iota\alpha x - \iota\gamma|y|)} d\alpha,$$

$$\tag{4.71}$$

and

$$H_z^{int}(x,y) = \frac{sgn(y)}{2\pi} \int\limits_{-\infty}^{\infty} \frac{\mathcal{A}}{\mathcal{S}(\alpha)} \left(\begin{array}{c} -\mathcal{S}_+(\alpha)\mathcal{R}_1(\alpha)e^{-\iota l k_{eff}\cos\theta_0} \\[2mm] +\mathcal{S}_+(\alpha)\mathcal{T}(\alpha)\mathcal{C}_1 \\[2mm] -\mathcal{S}_+(-\alpha)\mathcal{R}_2(-\alpha)e^{-\iota l\alpha} \\[2mm] +\mathcal{S}_+(-\alpha)\mathcal{T}(-\alpha)\mathcal{C}_2 e^{-\iota l\alpha} \end{array} \right) e^{(-\iota\alpha x - \iota\gamma|y|)} d\alpha$$

$$+ \frac{1}{2\pi} \int\limits_{-\infty}^{\infty} \frac{\mathcal{A}'}{\iota\gamma(\alpha)\mathcal{K}(\alpha)} \left(\begin{array}{c} \mathcal{K}_+(\alpha)\mathcal{R}_1(\alpha)e^{-\iota l k_{eff}\cos\theta_0} \\[2mm] -\mathcal{K}_+(\alpha)\mathcal{T}(\alpha)\mathcal{C}_1' \\[2mm] +\mathcal{K}_+(-\alpha)\mathcal{R}_2(-\alpha)e^{-\iota l\alpha} \\[2mm] -\mathcal{K}_+(-\alpha)\mathcal{T}(-\alpha)\mathcal{C}_2' e^{-\iota l\alpha} \end{array} \right) e^{(-\iota\alpha x - \iota\gamma|y|)} d\alpha.$$

$$\tag{4.72}$$

In above (4.71) $H_z^{sep}(x,y)$ has two integrals in which the integrand with kernel function $\mathcal{S}(\alpha)$ has two parts one for the edge $x=0$ and other for edge $x=-l$, similarly, integrand with kernel function $\mathcal{K}(\alpha)$ has two parts one for the edge $x=0$ and other for edge $x=-l$, so evaluation of integrals will give the diffracted field for $x=0$ as well as for $x=-l$ whereas $H_z^{int}(x,y)$ presented by (4.71) also have two integrands corresponding to two kernels $\mathcal{S}(\alpha)$ and $\mathcal{K}(\alpha)$. Each integrand with its respective kernel functions $\mathcal{S}(\alpha)$ and $\mathcal{K}(\alpha)$ have two parts and on evaluating the integrals, one will give the interaction field due extremity $x=0$ of plate and other for the interaction field due to extremity $x=-l$ of plate.

4.6 Acquirement of Diffracted Field

In the far field zone, the diffracted field now may be evaluated asymptotically. For this purpose, the polar coordinates as $x = r \cos \theta$, $|y| = r \sin \theta$ are introduced and following transformation helps in the deformation of contour.

$$\alpha = -k_{eff} \cos (\theta + \iota \zeta), \quad \text{for } 0 < \theta < \pi \quad -\infty < \zeta < \infty. \tag{4.73}$$

Now applying the method of stationary phase for large $k_{eff}r$, (4.69) takes the following form

$$H_z(r, \theta) = \frac{\iota k_{eff}}{\sqrt{k_{eff}r}} \left\{ \begin{array}{c} A_1 \left(-k_{eff} \cos \theta\right) \\ A_2 \left(-k_{eff} \cos \theta\right) \end{array} \right\} \sin \theta \exp \left(ik_{eff}r + \iota \frac{\pi}{4} \right). \tag{4.74}$$

Similarly, integrals involved in (4.71) and (4.73) are evaluated asymptotically using method of stationary phase as

$$H_z^{sep}(r, \theta) = \frac{1}{\sqrt{2\pi}} \frac{\iota k_{eff}}{\sqrt{k_{eff}r}} \Big\{ - sgn(\theta) \, \psi^{sep} \left(-k_{eff} \cos \theta\right) \\ + \phi^{sep} \left(-k_{eff} \cos \theta\right) \Big\} \sin \theta \exp \left(\iota k_{eff}r + \iota \frac{\pi}{4} \right), \tag{4.75}$$

and

$$H_z^{int}(r, \theta) = \frac{1}{\sqrt{2\pi}} \frac{\iota k_{eff}}{\sqrt{k_{eff}r}} \Big\{ - sgn(\theta) \, \psi^{int} \left(-k_{eff} \cos \theta\right) \\ + \phi^{int} \left(-k_{eff} \cos \theta\right) \Big\} \sin \theta \exp \left(\iota k_{eff}r + \iota \frac{\pi}{4} \right), \tag{4.76}$$

where

$$\psi^{sep} \left(-k_{eff} \cos \theta\right) = \frac{\mathcal{A}\mathcal{S}_+ \left(-k_{eff} \cos \theta\right)}{\mathcal{S} \left(-k_{eff} \cos \theta\right) \left(-k_{eff} \cos \theta - k_{eff} \cos \theta_0\right) \mathcal{S}_+ \left(k_{eff} \cos \theta_0\right)} \\ - \frac{\mathcal{A}\mathcal{S}_- \left(-k_{eff} \cos \theta\right) e^{-\iota l \left(-k_{eff} \cos \theta - k_{eff} \cos \theta_0\right)}}{\mathcal{S} \left(-k_{eff} \cos \theta\right) \left(-k_{eff} \cos \theta - k_{eff} \cos \theta_0\right) \mathcal{S}_+ \left(-k_{eff} \cos \theta_0\right)}, \tag{4.77}$$

and

$$\phi^{sep}\left(-k_{eff}\cos\theta\right) = \frac{\mathcal{A}'\mathcal{K}_+\left(-k_{eff}\cos\theta\right)}{\iota\gamma\left(-k_{eff}\cos\theta\right)\mathcal{K}\left(-k_{eff}\cos\theta\right)\left(-k_{eff}\cos\theta-k_{eff}\cos\theta_0\right)\mathcal{K}_+\left(k_{eff}\cos\theta_0\right)}$$
$$-\frac{\mathcal{A}'\mathcal{K}_-\left(k_{eff}\cos\theta\right)e^{-\iota l\left(-k_{eff}\cos\theta-k_{eff}\cos\theta_0\right)}}{\iota\gamma\left(-k_{eff}\cos\theta\right)\mathcal{K}\left(-k_{eff}\cos\theta\right)\left(-k_{eff}\cos\theta-k_{eff}\cos\theta_0\right)\mathcal{K}_+\left(-k_{eff}\cos\theta_0\right)},$$

(4.78)

$$\psi^{int}\left(-k_{eff}\cos\theta\right) = \frac{\mathcal{A}}{\mathcal{S}\left(-k_{eff}\cos\theta\right)}\begin{pmatrix} \mathcal{S}_+\left(-k_{eff}\cos\theta\right)\mathcal{R}_1\left(-k_{eff}\cos\theta\right)e^{-\iota l k_{eff}\cos\theta_0} \\ -\mathcal{S}_+\left(-k_{eff}\cos\theta\right)\mathcal{T}\left(-k_{eff}\cos\theta\right)\mathcal{C}_1 \\ +\mathcal{S}_-\left(-k_{eff}\cos\theta\right)\mathcal{R}_2\left(k_{eff}\cos\theta\right)e^{\iota l k_{eff}\cos\theta} \\ -\mathcal{S}_-\left(-k_{eff}\cos\theta\right)\mathcal{T}\left(k_{eff}\cos\theta\right)\mathcal{C}_2 e^{\iota l k_{eff}\cos\theta} \end{pmatrix},$$

(4.79)

$$\phi^{int}\left(-k_{eff}\cos\theta\right) = \frac{\mathcal{A}'}{\mathcal{K}\left(-k_{eff}\cos\theta\right)}\begin{pmatrix} \mathcal{K}_+\left(-k_{eff}\cos\theta\right)\mathcal{R}_1\left(-k_{eff}\cos\theta\right)e^{\iota l k_{eff}\cos\theta_0} \\ -\mathcal{K}_+\left(-k_{eff}\cos\theta\right)\mathcal{T}\left(-k_{eff}\cos\theta\right)\mathcal{C}_1' \\ +\mathcal{K}_-\left(-k_{eff}\cos\theta\right)\mathcal{R}_2\left(k_{eff}\cos\theta\right)e^{\iota l k_{eff}\cos\theta} \\ -\mathcal{K}_-\left(-k_{eff}\cos\theta\right)\mathcal{T}\left(k_{eff}\cos\theta\right)\mathcal{C}_2' e^{\iota l k_{eff}\cos\theta} \end{pmatrix}.$$

(4.80)

The result given by (4.75) presents the diffracted field evaluated asymptotically for $k_{eff}r \longrightarrow \infty$. In fact, it is the asymptotic form of $H_z(x,y)$ valid for all observation angles in the entire region. It is observed that the wave field diffracted by the extremities $x=0$ and $x=-l$ of the plate plus the additional involvement of the geometrical wave field results into the separated field. The separated field being the resultant wave field will regard a physical perception to the model. But on the other hand, the interacted field appearing due to the interaction of one edge upon other regards no physics of the model, separately. The separated field provides the physical perception of diffraction phenomenon at the boundary defined for the associated model. Therefore, only the separated field is taken into account to discussion. Furthermore, the interaction field generated as a result of double diffraction of EM-plane wave by two edges is already counted by the separated field. Also the extending the plate length upto infinity discards the contribution resulting from the interaction terms

and consequently, the separated field appears to be diffracted field. Therefore, only the separated field is focused to discuss graphically in the next section.

4.7   Results and Discussion

This section is devoted to elaborate the impact of physical parameters like angle of incidence θ_0, wave-number k, plate length l, surface impedance η_s and permittivity element ε_1 on separated field of EM-wave against observation angle in the absence and presence of cold plasma. In Figs. 4.3a, 4.3b, sketch of separated field for three different angles of incidence is displayed while keeping values of all other parameters fixed. The observation predicts that separated field intensity gets sharp peaks at observation angles $\theta = 2\pi/3, 3\pi/4, 5\pi/6$ indicating the reflection of EM-wave for respective angles of incidence $\theta_0 = \pi/3, \pi/4, \pi/6$. The structure of non-symmetric finite plate under consideration over here may work for physical aspect of scattering mechanism at these particular values of observation angles. The maximum sharp peak occurs at observation angle $\theta = 3\pi/4$ for its respective incidence angle $\theta_0 = \pi/4$ in both the cases i.e. in the absence and presence of cold plasma. However, wavelength expands in the presence of cold plasma. Figs. 4.4a, 4.4b are sketched to display behavior of separated field for incremental trend of wave-number k. This means that wave frequency excites to the high frequency range. In Figs. 4.5a, 4.5b, oscillations of the separated field increase due to increasing the length of plate. According to observation, it is found that separated field in the far away region from the origin, after the sharp peak, coincides even for three different values of length. One can observe by comparing Figs. 4.4b, 4.5b with 4.4a, 4.5a, respectively, that presence of cold plasma has expanded the wavelength of separated field. This means that cold plasma helps in controlling the dispersion of diffracted waves. Figs. 4.6a, 4.6b have shown the behavior of separated field for three different values of surface impedance in the absence and presence of cold plasma, respectively. Observation describes that separated field for real value of surface impedance (surface resistance)

is more fluctuated than for the pure imaginary (surface reactance) and imaginary values (both surface resistance and surface reactance) of surface impedance. On comparing Fig. 4.6b with Fig. 4.6a, it is found that cold plasma has reduced the downward fluctuation of separated field. Fig. 4.7 is sketched to show the behavior of separated field for ε_1. The slight variation in separated field has been depicted for ε_1. Since $\varepsilon_1 \approx 1 - (\omega_p/\omega)^2$ (for signal with high frequency) so an increase in ε_1 while keeping the number density of ions and electrons fixed in cold plasma, that's why separated field gets slightly oscillated for increasing ε_1. The electrons oscillate about cold ionic centers due to electric field of high frequency signal and these oscillating electrons scatter enormously due to increasing amplitude of the separated field. On observing all the plots, it can be elaborated that separated field shows nullity around observation angle of 0.
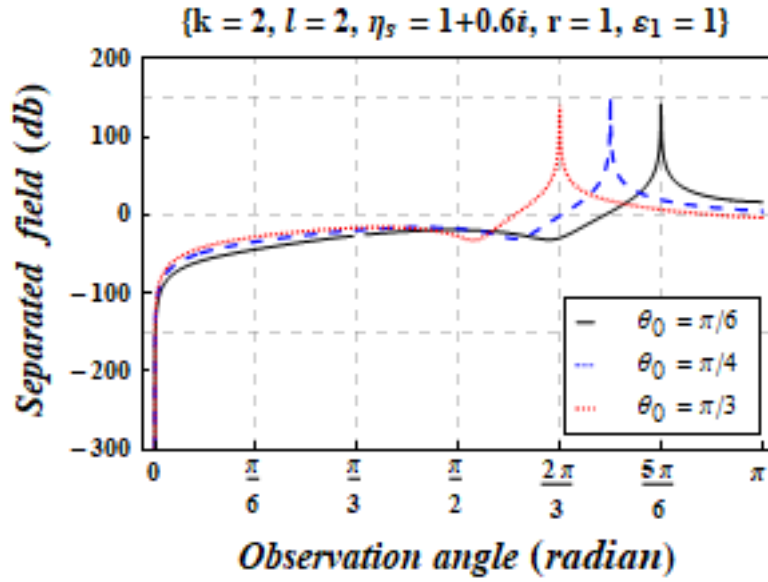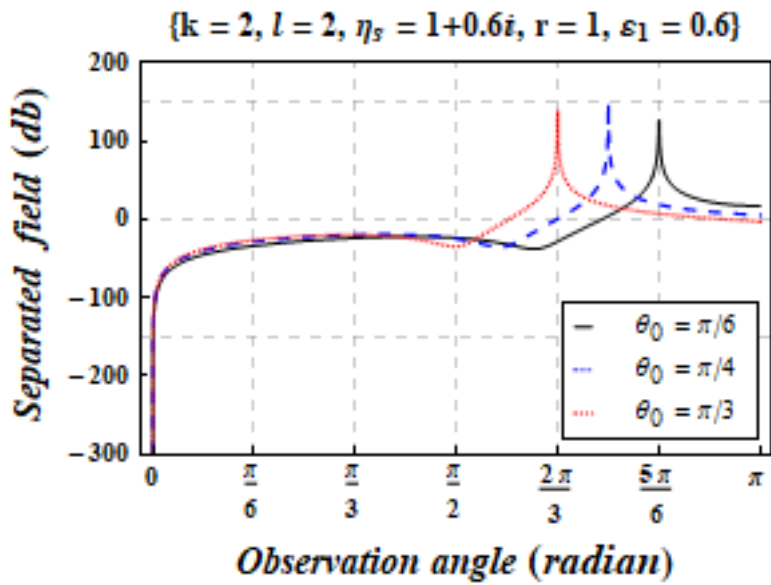
Figure 4.3: **The separated field for angle of incidence in the absence (a) and presence (b) of cold plasma.**

$\{l = 2, \eta_s = 1{+}0.6i, \text{r} = 1, \varepsilon_1 = 1, \theta_0 = \pi/3\}$

(a)

$\{l = 2, \eta_s = 1{+}0.6i, \text{r} = 1, \varepsilon_1 = 0.6, \theta_0 = \pi/3\}$

(b)

Figure 4.4: **The separated field for wave-number in the absence (a) and presence (b) of cold plasma.**
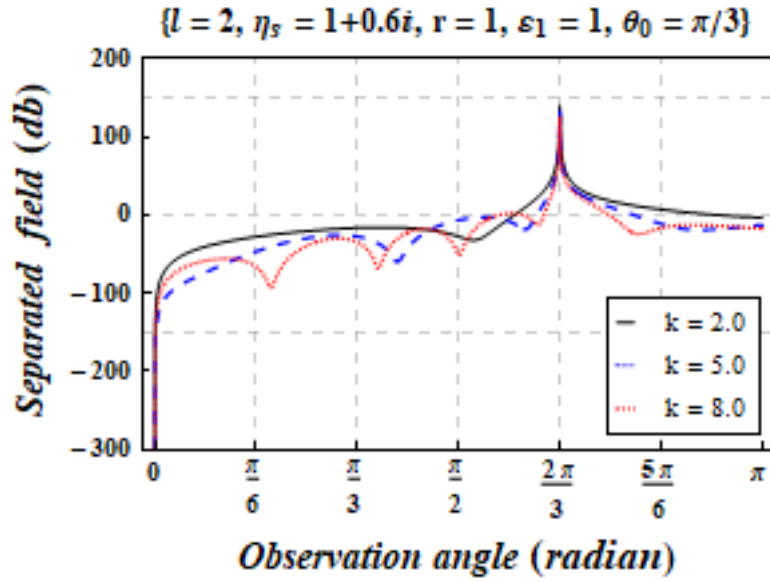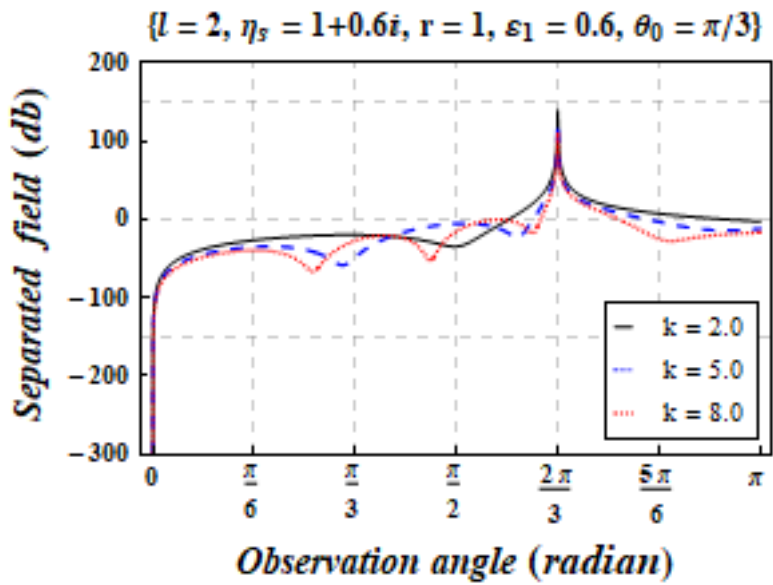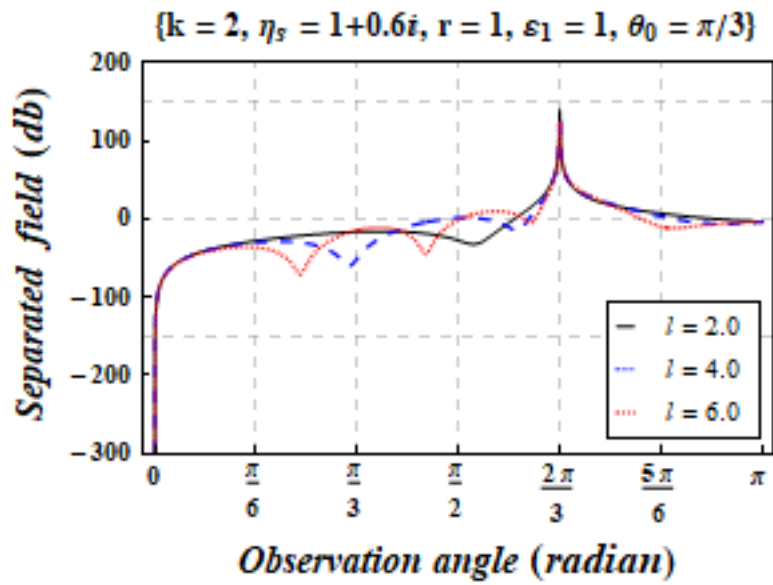
(a)
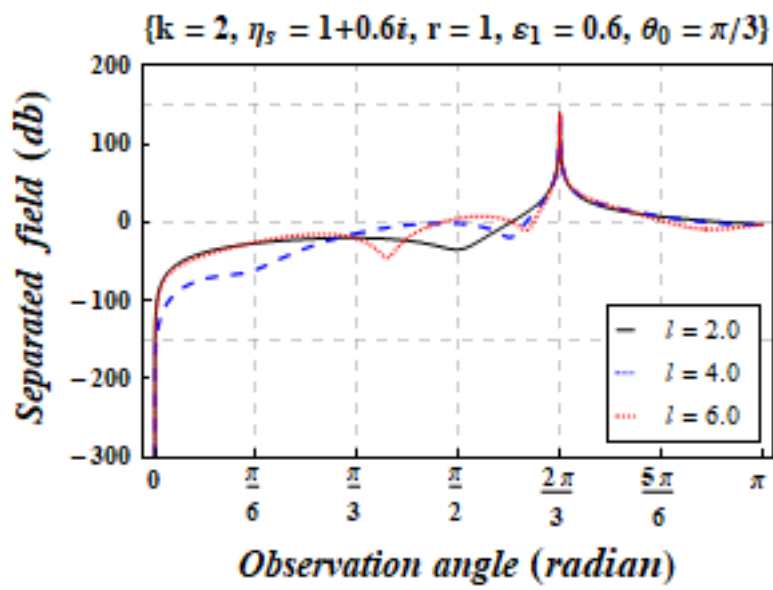
(b)

Figure 4.5: **The separated field for length of plate in the absence (a) and presence (b) of cold plasma.**
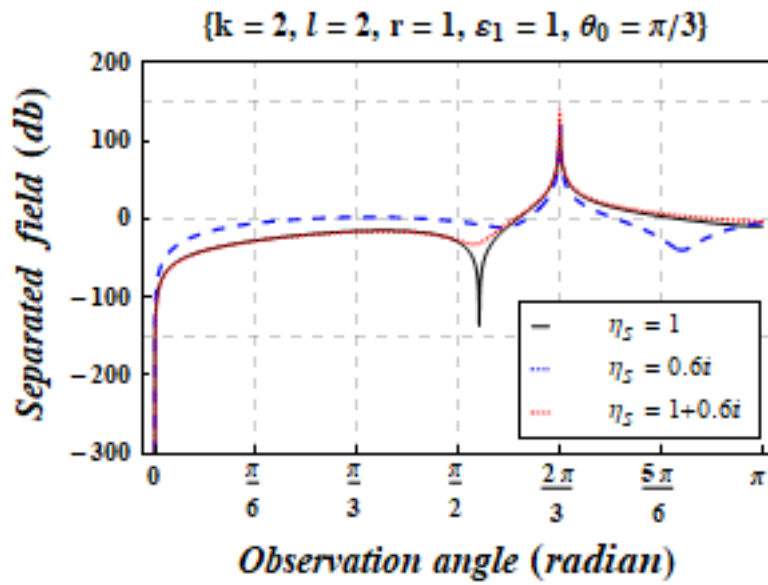
(a)
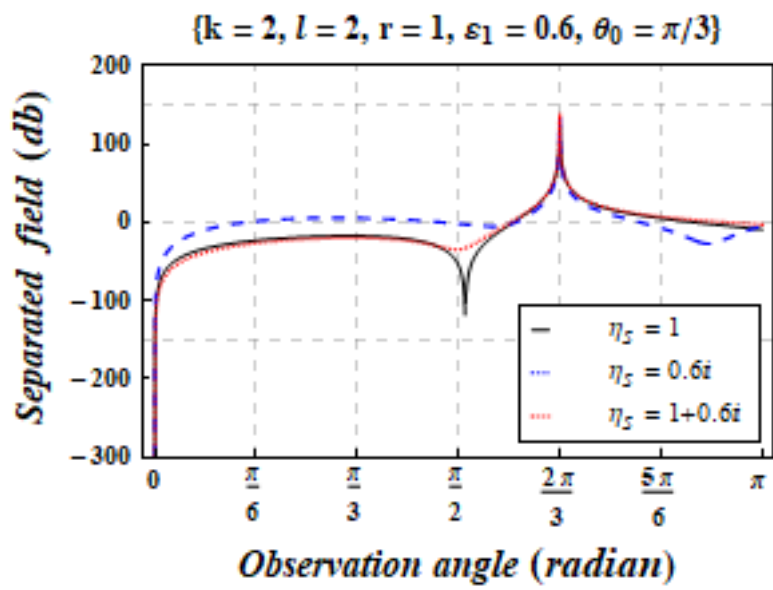
(b)

Figure 4.6: **The separated field for surface impedance in the absence (a) and presence (b) of cold plasma.**

71
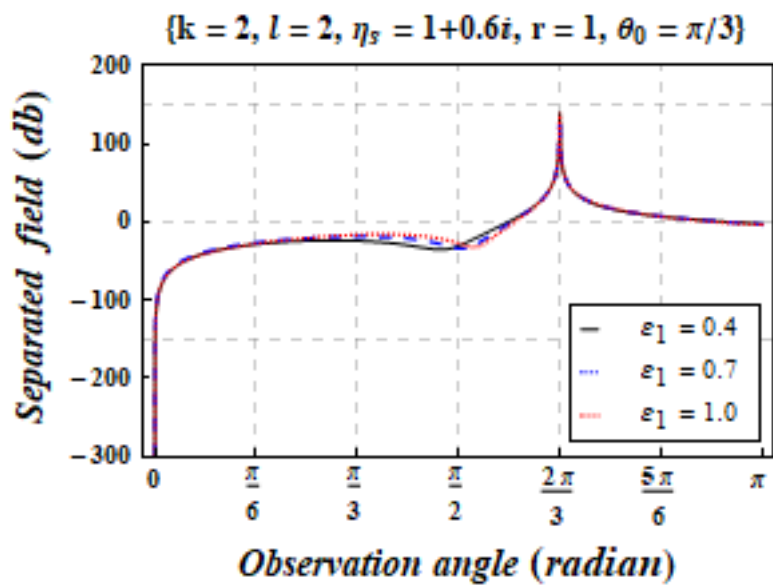
Figure 4.7: **The separated field for** ε_1.

4.8 Conclusions

The chapter has investigated the EM-plane wave diffracted by a plate of non-symmetric length with surface impedance in the presence of cold plasma. The observation depicts that diffraction of EM- plane wave is affected by (a) extending the length of the plate (b) changing the angles of incidence (c) changing the wave-number (d) changing values of surface impedance and (e) permittivity of cold plasma.

Chapter 5

Calculation of Diffraction by an Impedance Finite Symmetric Plate in Cold Plasma Using Wiener-Hopf Technique

This chapter elaborates the analysis of diffraction of electromagnetic (EM) plane wave by a plate of finite length symmetrically located in cold plasma. The impedance is assumed on the upper and lower surface of the plate, therefore Leontovich boundary conditions are assumed to consider the effects of impedance. Helmholtz's equation is formulated using the Maxwell's equations with the effects of cold plasma. The Fourier transform is applied and then Wiener-Hopf equations are obtained. The modified stationary phase method is used to get the result of diffracted field by finite symmetric plate (separated field). Graphical analysis of separated field for physical parameters in the presence and absence of cold plasma is discussed, comprehensively.

5.1 Modelling of the Helmholtz Equation

The tensor of dielectric permittivity to consider the presence of cold plasma is defined as

$$\bar{\varepsilon} = \varepsilon_0 \begin{pmatrix} \varepsilon_1 & -\iota\varepsilon_2 & 0 \\ \iota\varepsilon_2 & \varepsilon_1 & 0 \\ 0 & 0 & \varepsilon_z \end{pmatrix}, \tag{5.1}$$

$$\varepsilon_1 = 1 - \left(\frac{\omega_p}{\omega}\right)^2 \left[1 - \left(\frac{\omega_c}{\omega}\right)^2\right]^{-1}, \quad \varepsilon_2 = \left(\frac{\omega_p}{\omega}\right)^2 \left[\frac{\omega}{\omega_c} - \frac{\omega_c}{\omega}\right]^{-1}, \tag{5.2}$$

and

$$\varepsilon_z = 1 - \left(\frac{\omega_p}{\omega}\right)^2, \tag{5.3}$$

with

$$\omega_p^2 = \frac{N_e e^2}{m\varepsilon_0}, \quad \omega_c = \frac{|e|\,\mu_0 H_{dc}}{m}. \tag{5.4}$$

It is known that Maxwell's equations are proved to be valid in cold plasma with dielectric permittivity tensor, thus the electric field components in terms of magnetic field with presence of cold plasma can be evaluated with the aid of Maxwell's equation along with (5.1), given by

$$E_x = \frac{\iota\varepsilon_1}{\omega\varepsilon_0\left(\varepsilon_1^2 - \varepsilon_2^2\right)} \frac{\partial H_z\left(x,y\right)}{\partial y} + \frac{\varepsilon_2}{\omega\varepsilon_0\left(\varepsilon_1^2 - \varepsilon_2^2\right)} \frac{\partial H_z\left(x,y\right)}{\partial x}, \tag{5.5}$$

and

$$E_y = \frac{\varepsilon_2}{\omega\varepsilon_0\left(\varepsilon_1^2 - \varepsilon_2^2\right)} \frac{\partial H_z\left(x,y\right)}{\partial y} - \frac{\iota\varepsilon_1}{\omega\varepsilon_0\left(\varepsilon_1^2 - \varepsilon_2^2\right)} \frac{\partial H_z\left(x,y\right)}{\partial x}. \tag{5.6}$$

Thus, the Helmholtz's equation satisfying H_z obtained from Maxwell's equations with the use of electric field components (5.5) and (5.6), is computed as follows :

$$\partial_{xx} H_z\left(x,y\right) + \partial_{yy} H_z\left(x,y\right) + k_{eff}^2 H_z\left(x,y\right) = 0, \tag{5.7}$$
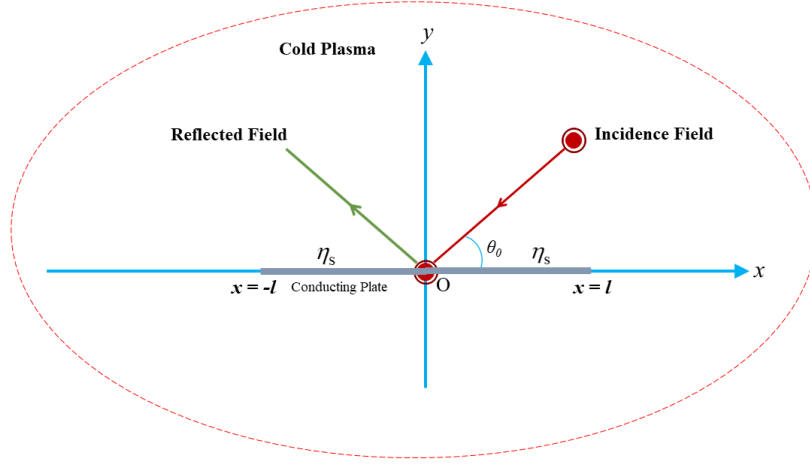
Figure 5.1: **Geometrical description of the model.**

with the propagation constant

$$k_{eff} = k\sqrt{\frac{\varepsilon_1^2 - \varepsilon_2^2}{\varepsilon_1}}, \quad k = \omega\sqrt{\varepsilon_0\mu_0}. \tag{5.8}$$

Here, k_{eff} is dependent of k, ε_1 and ε_2, harmonic time dependence $\exp(-\iota\omega t)$ is assumed and will be suppressed throughout the analysis.

5.2   Mathematical Modelling of the Problem

A symmetric plate of finite length with impedance loaded is located along $y = 0$ with edges at $x = -l$ and $x = l$ as displayed in Fig. 5.1. The incident field is taken as

$$H_z^{inc}(x, y) = \exp\{-\iota k_{eff}(x\cos\theta_0 + y\sin\theta_0)\}. \tag{5.9}$$

Here, the amplitude of magnetic field is taken as 1 A/m and θ_0 is the angle of incidence with $x-$axis. Here, the total field can be expressed as follows:

$$H_z^{tot}(x, y) = H_z^{inc}(x, y) + H_z^{ref}(x, y) + H_z(x, y), \tag{5.10}$$

where $H_z(x, y)$ is the diffracted field and $H_z^{ref}(x, y)$ denotes the reflected field, which is defined as

$$H_z^{ref}(x, y) = \left(\frac{\eta_s \sin \theta_0 - 1}{\eta_s \sin \theta_0 + 1} \right) \exp\{-\iota k_{eff}(x \cos \theta_0 - y \sin \theta_0)\}. \qquad (5.11)$$

For the convenience of analysis, medium for the present model is assumed to be slightly lossy as in $k_{eff} = \Re\{k_{eff}\} + \iota \Im\{k_{eff}\}$, $0 < \Im\{k_{eff}\} \ll \Re\{k_{eff}\}$ and the solution for real k_{eff} may be achieved by assuming $\Im\{k_{eff}\} \longrightarrow 0$. The boundary value problem (BVP) under consideration is expressed in terms of the magnetic field and it is adequate to denote the diffracted field in the different regions. The total field $H_z^{tot}(x, y)$ in the range $x \in (-\infty, \infty)$, that satisfies the Helmholtz's equation as follows :

$$\left[\partial_{xx} + \partial_{yy} + k_{eff}^2 \right] H_z^{tot}(x, y) = 0, \qquad (5.12)$$

diffracted field satisfying Helmholtz's equation extracted from (5.12) is given as follows:

$$\left[\partial_{xx} + \partial_{yy} + k_{eff}^2 \right] H_z(x, y) = 0. \qquad (5.13)$$

Our focus is to evaluate the diffracted field of EM-plane wave incident on a symmetric plate of finite length under the effects of cold plasma. Impedance considered on both surfaces of the finite plate is same. Therefore, Leontovich boundary conditions are as follows :

$$\partial_y H_z^{tot}(x, 0^{\mp}) - \iota \frac{\varepsilon_2}{\varepsilon_1} \partial_x H_z^{tot}(x, 0^{\mp}) = \pm \iota \frac{k_{eff}^2}{\omega \mu_0} \eta_0 \eta_s H_z^{tot}(x, 0^{\mp}), \quad \text{for } |x| \leq l, \quad (5.14)$$

where $\eta_0 = \sqrt{\mu_0/\varepsilon_0}$. The continuity conditions are

$$\begin{aligned} H_z^{tot}(x, 0^+) &= H_z^{tot}(x, 0^-), \ -\infty < x < -l, \ l < x < \infty, \\ \partial_y H_z^{tot}(x, 0^+) &= \partial_y H_z^{tot}(x, 0^-), \ -\infty < x < -l, \ l < x < \infty. \end{aligned} \qquad (5.15)$$

5.3   Transformation of the Problem

Now we apply the Fourier transform on the boundary value problem (BVP) with respect to variable x as

$$\mathcal{F}(\alpha, y) = \frac{1}{\sqrt{2\pi}} \int\limits_{-\infty}^{\infty} H_z(x, y) e^{\iota\alpha x} dx \tag{5.16}$$

$$= e^{\iota\alpha l} \mathcal{F}_+(\alpha, y) + e^{-\iota\alpha l} \mathcal{F}_-(\alpha, y) + \mathcal{F}_l(\alpha, y),$$

where $\alpha = \mathfrak{Re}\{\alpha\} + \iota\mathfrak{Im}\{\alpha\} = \sigma + \iota\tau$. The asymptotic expression of $H_z(x, y)$ for $x \longrightarrow \pm\infty$ is taken into account as

$$H_z(x, y) = \begin{cases} O\left(e^{-\mathfrak{Im}\{k_{eff}\}x}\right) & \text{for } x \longrightarrow \infty, \\ O\left(e^{\mathfrak{Im}\{k_{eff}\}x\cos\theta_0}\right) & \text{for } x \longrightarrow -\infty. \end{cases} \tag{5.17}$$

$\mathcal{F}_+(\alpha, y)$ is the regular function of α in the upper-half plane $\mathfrak{Im}\{-k_{eff}\} < \mathfrak{Im}\{\alpha\}$, $\mathcal{F}_-(\alpha, y)$ is the regular function of α in the lower-half plane $\mathfrak{Im}\{\alpha\} < \mathfrak{Im}\{k_{eff}\cos\theta_0\}$ and both these regions generate a band of analyticity (common region) in which all the functions including $\mathcal{F}_l(\alpha, y)$ are analytic, therefore

$$\mathcal{F}_+(\alpha, y) = \frac{1}{\sqrt{2\pi}} \int\limits_{l}^{\infty} H_z(x, y) e^{\iota\alpha(x-l)} dx, \tag{5.18}$$

$$\mathcal{F}_-(\alpha, y) = \frac{1}{\sqrt{2\pi}} \int\limits_{-\infty}^{-l} H_z(x, y) e^{\iota\alpha(x+l)} dx, \tag{5.19}$$

$$\mathcal{F}_l(\alpha, y) = \frac{1}{\sqrt{2\pi}} \int\limits_{-l}^{l} H_z(x, y) e^{\iota\alpha x} dx, \tag{5.20}$$

$$\mathcal{F}^{inc}(\alpha, 0) = \frac{e^{\iota l\left(\alpha - k_{eff}\cos\theta_0\right)} - e^{-\iota l\left(\alpha - k_{eff}\cos\theta_0\right)}}{\sqrt{2\pi}\iota\left(\alpha - k_{eff}\cos\theta_0\right)}, \tag{5.21}$$

$$\mathcal{F}^{ref}(\alpha, 0) = \frac{1}{\sqrt{2\pi}}\left(\frac{\eta_s \sin\theta_0 - 1}{\eta_s \sin\theta_0 + 1}\right) \frac{e^{\iota l\left(\alpha - k_{eff}\cos\theta_0\right)} - e^{-\iota l\left(\alpha - k_{eff}\cos\theta_0\right)}}{\iota\left(\alpha - k_{eff}\cos\theta_0\right)}. \tag{5.22}$$

78

The application of Fourier transform on (5.13)-(5.15) yields,

$$\left(\frac{d^2}{dy^2} + \gamma^2\right)\mathcal{F}(\alpha, y) = 0,\tag{5.23}$$

where $\gamma(\alpha) = \sqrt{k_{eff}^2 - \alpha^2}$.

$$\partial_y \mathcal{F}^{tot}(\alpha, 0^\mp) - \alpha \frac{\varepsilon_2}{\varepsilon_1}\mathcal{F}^{tot}(\alpha, 0^\mp) = \pm\iota\frac{k_{eff}^2}{\omega\mu_0}\eta_0\eta_s\mathcal{F}^{tot}(\alpha, 0^\mp),\tag{5.24}$$

and

$$\begin{aligned}
\mathcal{F}_-(\alpha, 0^+) &= \mathcal{F}_-(\alpha, 0^-) = \mathcal{F}_-(\alpha, 0),\\
\mathcal{F}_+(\alpha, 0^+) &= \mathcal{F}_+(\alpha, 0^-) = \mathcal{F}_+(\alpha, 0),\\
\partial_y\mathcal{F}_-(\alpha, 0^+) &= \partial_y\mathcal{F}_-(\alpha, 0^-) = \partial_y\mathcal{F}_-(\alpha, 0),\\
\partial_y\mathcal{F}_+(\alpha, 0^+) &= \partial_y\mathcal{F}_+(\alpha, 0^-) = \partial_y\mathcal{F}_+(\alpha, 0).
\end{aligned}\tag{5.25}$$

5.4   Modelling of Wiener-Hopf Equation

The solution of (5.23) satisfying the radiation conditions is given by

$$\mathcal{F}(\alpha, y) = \begin{cases} A_1(\alpha)\,e^{-\iota\gamma y} & y \geq 0,\\[2mm] A_2(\alpha)\,e^{\iota\gamma y} & y < 0. \end{cases}\tag{5.26}$$

Now with the aid of (5.16), (5.24), (5.25) and (5.26), following coupled functional equations are obtained as

$$\begin{aligned}
e^{\iota\alpha l}\mathcal{F}'_+(\alpha, 0) + e^{-\iota\alpha l}\mathcal{F}'_-(\alpha, 0) = {}& \left[\mathcal{F}'_{inc}(\alpha, 0) + \mathcal{F}'_{ref}(\alpha, 0)\right]\\
& -\alpha\big(\frac{\varepsilon_2}{\varepsilon_1}\big)\left[\mathcal{F}_{inc}(\alpha, 0) + \mathcal{F}_{ref}(\alpha, 0)\right]\\
& -\frac{1}{2}\alpha\big(\frac{\varepsilon_2}{\varepsilon_1}\big)\left[\mathcal{F}_l(\alpha, 0^+) + \mathcal{F}_l(\alpha, 0^-)\right]\\
& +\frac{1}{2}\big(\iota\frac{k_{eff}^2}{\omega\mu_0}\eta_0\eta\big)\left[\mathcal{F}_l(\alpha, 0^+) - \mathcal{F}_l(\alpha, 0^-)\right]\\
& -\frac{\iota\gamma}{2}\left[A_1(\alpha) - A_2(\alpha)\right],
\end{aligned}\tag{5.27}$$

$$e^{\iota\alpha l}\mathcal{F}_+\left(\alpha,0\right) + e^{-\iota\alpha l}\mathcal{F}_-\left(\alpha,0\right) = -\frac{\alpha\left(\frac{\varepsilon_2}{\varepsilon_1}\right)}{(\alpha\frac{\varepsilon_2}{\varepsilon_1})^2 + \left(\frac{k_{eff}^2}{\omega\mu_0}\eta_0\eta\right)^2}\left[\mathcal{F}'_{inc}(\alpha,0) + \mathcal{F}'_{ref}\left(\alpha,0\right)\right]$$

$$+\left[\mathcal{F}'_{inc}(\alpha,0) + \mathcal{F}'_{ref}\left(\alpha,0\right)\right]$$

$$-\frac{\alpha\left(\frac{\varepsilon_2}{\varepsilon_1}\right)}{(\alpha\frac{\varepsilon_2}{\varepsilon_1})^2 + \left(\frac{k_{eff}^2}{\omega\mu_0}\eta_0\eta\right)^2}\left[\mathcal{F}'_l(\alpha,0^+) + \mathcal{F}'_l\left(\alpha,0^-\right)\right]$$

$$-\frac{1}{2}\frac{1}{(\alpha\frac{\varepsilon_2}{\varepsilon_1})^2 + \left(\frac{k_{eff}^2}{\omega\mu_0}\eta_0\eta\right)^2}\left(\iota\frac{k_{eff}^2}{\omega\mu_0}\eta_0\eta\right)\left[\mathcal{F}'_l(\alpha,0^+) - \mathcal{F}'_l\left(\alpha,0^-\right)\right]$$

$$+\frac{1}{2}\left[A_1(\alpha) + A_2(\alpha)\right].$$

$$(5.28)$$

For high frequency signal, we use certain approximations such that $\omega \gg \omega_c$, while keeping it at the same order with ω_p, yielding the $\varepsilon_1 \approx 1 - (\omega_p/\omega)^2$ and $\varepsilon_2 \to 0$ in the limit case. After approximations, the system of Wiener-Hopf functional equations are computed as follows :

$$e^{\iota\alpha l}\mathcal{F}'_+\left(\alpha,0\right) + e^{-\iota\alpha l}\mathcal{F}'_-\left(\alpha,0\right) + \mathcal{S}\left(\alpha\right)\tilde{\mathcal{F}}_l\left(\alpha,0\right) = \mathcal{F}'_{inc}(\alpha,0) + \mathcal{F}'_{ref}\left(\alpha,0\right), \quad (5.29)$$

$$e^{\iota\alpha l}\mathcal{F}_+\left(\alpha,0\right) + e^{-\iota\alpha l}\mathcal{F}_-\left(\alpha,0\right) + \mathcal{K}\left(\alpha\right)\tilde{\mathcal{F}}'_l\left(\alpha,0\right) = \mathcal{F}_{inc}(\alpha,0) + \mathcal{F}_{ref}\left(\alpha,0\right), \quad (5.30)$$

where

$$\tilde{\mathcal{F}}_l\left(\alpha,0\right) = \frac{1}{2}\left[\mathcal{F}_l\left(\alpha,0^+\right) - \mathcal{F}_l\left(\alpha,0^-\right)\right], \quad (5.31)$$

$$\tilde{\mathcal{F}}'_l\left(\alpha,0\right) = \frac{1}{2}\left[\mathcal{F}'_l\left(\alpha,0^+\right) - \mathcal{F}'_l\left(\alpha,0^-\right)\right], \quad (5.32)$$

$$A_1\left(\alpha\right) = -\tilde{\mathcal{F}}_l\left(\alpha,0\right) + \frac{\tilde{\mathcal{F}}'_l\left(\alpha,0\right)}{\iota\gamma\left(\alpha\right)}, \quad (5.33)$$

$$A_2\left(\alpha\right) = \tilde{\mathcal{F}}_l\left(\alpha,0\right) + \frac{\tilde{\mathcal{F}}'_l\left(\alpha,0\right)}{\iota\gamma\left(\alpha\right)}. \quad (5.34)$$

The kernel factors appearing in the coupled system of Wiener-Hopf equations are as follows:

$$\mathcal{S}\left(\alpha\right) = -\iota\gamma\left(\alpha\right)\mathcal{L}\left(\alpha\right), \quad (5.35)$$
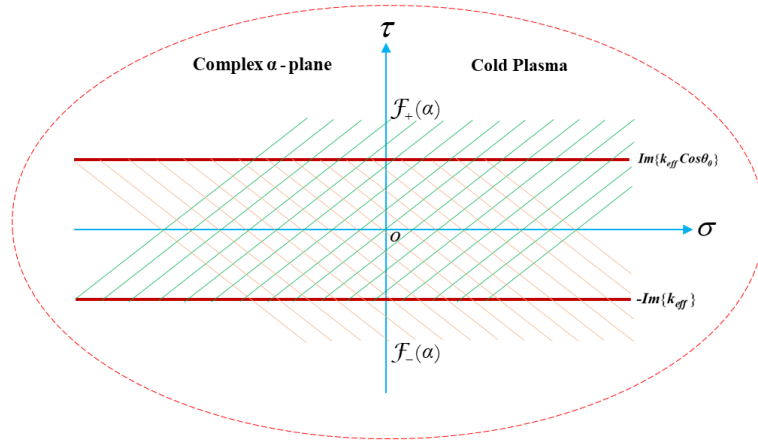
Figure 5.2: **The description of analytic continuation in the complex $\alpha-$plane.**

$$\mathcal{K}\left(\alpha\right) = \frac{\iota k}{k_{eff}^2 \eta_s} \mathcal{L}\left(\alpha\right), \tag{5.36}$$

where

$$\mathcal{L}\left(\alpha\right) = \left(1 + \frac{k_{eff}^2 \eta_s}{k\gamma\left(\alpha\right)}\right), \tag{5.37}$$

5.5   Wiener-Hopf Procedure

The main objective of this model is to observe the effect of cold plasma on diffracted field of EM-wave incident on a conductible plate of finite length with impedance loaded. The functional Wiener-Hopf equations (5.29) and (5.30) for the boundary value problem are put to rigorous analysis through Wiener-Hopf method. The salient fact of this method or analysis is that its procedure is not fundamentally numerical in nature that's why it permits an additional insight to physical and mathematical structure for diffracted field of incident EM-wave. The kernel functions arising from (5.29) and (5.30) presented by (5.35) and (5.36) are decomposed as

$$\mathcal{S}\left(\alpha\right) = \mathcal{S}_+\left(\alpha\right) \mathcal{S}_-\left(\alpha\right), \tag{5.38}$$

$$\mathcal{K}\left(\alpha\right) = \mathcal{K}_{+}\left(\alpha\right)\mathcal{K}_{-}\left(\alpha\right), \tag{5.39}$$

and the factors appearing in (5.38) and (5.39) are computed as

$$\mathcal{S}_{\pm}\left(\alpha\right) = e^{-\iota\frac{\pi}{4}}\gamma_{\pm}\left(\alpha\right)\mathcal{L}_{\pm}, \tag{5.40}$$

$$\mathcal{K}_{\pm}\left(\alpha\right) = \frac{e^{\iota\frac{\pi}{4}}\sqrt{k}}{k_{eff}\sqrt{\eta_s}}\mathcal{L}_{\pm}\left(\alpha\right). \tag{5.41}$$

Furthermore, the product decomposition of function $\mathcal{L}\left(\alpha\right)$ appearing in (5.35) and (5.36), presented by (5.37), is made as

$$\mathcal{L}\left(\alpha\right) = \mathcal{L}_{+}\left(\alpha\right)\mathcal{L}_{-}\left(\alpha\right), \tag{5.42}$$

where

$$\mathcal{L}_{\pm}\left(\alpha\right) = \left(1 \pm \frac{\iota k_{eff}\sqrt{\eta_s}}{\sqrt{k}\gamma_{\pm}\left(\alpha\right)}\right), \tag{5.43}$$

and

$$\gamma_{\pm}\left(\alpha\right) = \sqrt{k_{eff} \pm \alpha}, \tag{5.44}$$

where the factors $\mathcal{S}_{+}\left(\alpha\right)$, $\mathcal{K}_{+}\left(\alpha\right)$, $\mathcal{L}_{+}\left(\alpha\right)$ and $\gamma_{+}\left(\alpha\right)$ are regular functions of α in upper-half of $\alpha-$plane $(\mathfrak{Im}\left\{-k_{eff}\right\} < \mathfrak{Im}\left\{\alpha\right\})$ whereas the factors $\mathcal{S}_{-}\left(\alpha\right)$, $\mathcal{K}_{-}\left(\alpha\right)$, $\mathcal{L}_{-}\left(\alpha\right)$ and $\gamma_{-}\left(\alpha\right)$ are regular function of α in the lower-half of $\alpha-$plane $(\mathfrak{Im}\left\{\alpha\right\} < \mathfrak{Im}\left\{k_{eff}\cos\theta_0\right\})$. Now using (5.21) and (5.22) in both (5.29) and (5.30), we get

$$e^{\iota\alpha l}\mathcal{F}'_{+}\left(\alpha, 0\right) + e^{-\iota\alpha l}\mathcal{F}'_{-}\left(\alpha, 0\right) + \mathcal{S}\left(\alpha\right)\tilde{\mathcal{F}}_{l}\left(\alpha, 0\right) = \mathcal{A}\mathcal{G}(\alpha), \tag{5.45}$$

$$e^{\iota\alpha l}\mathcal{F}_{+}\left(\alpha, 0\right) + e^{-\iota\alpha l}\mathcal{F}_{-}\left(\alpha, 0\right) + \mathcal{K}\left(\alpha\right)\tilde{\mathcal{F}}'_{l}\left(\alpha, 0\right) = \mathcal{A}'\mathcal{G}'(\alpha) \tag{5.46}$$

where

$$\mathcal{A} = \left[\left(\frac{\eta_s\sin\theta_0 - 1}{\eta_s\sin\theta_0 + 1}\right) - 1\right]k_{eff}\sin\theta_0, \tag{5.47}$$

$$\mathcal{A}' = -\left[\left(\frac{\eta_s\sin\theta_0 - 1}{\eta_s\sin\theta_0 + 1}\right) + 1\right]\iota. \tag{5.48}$$

$$\mathcal{G}(\alpha) = \mathcal{G}'(\alpha) = \frac{e^{\iota l\left(\alpha - k_{eff}\cos\theta_0\right)} - e^{-\iota l\left(\alpha - k_{eff}\cos\theta_0\right)}}{\sqrt{2\pi}\left(\alpha - k_{eff}\cos\theta_0\right)} \tag{5.49}$$

Inserting $\tilde{\mathcal{F}}_l(\alpha, 0)$ and $\tilde{\mathcal{F}}'_l(\alpha, 0)$ explicitly from (5.45) and (5.46) into (5.33) and (5.34), we get

$$\begin{aligned}
A_1(\alpha) = {} & \frac{1}{\mathcal{S}(\alpha)}\left\{e^{\iota\alpha l}\mathcal{F}'_+(\alpha, 0) + e^{-\iota\alpha l}\mathcal{F}'_-(\alpha, 0) - \mathcal{A}\mathcal{G}(\alpha)\right\} \\
& - \frac{1}{\iota\gamma(\alpha)\mathcal{K}(\alpha)}\left\{e^{\iota\alpha l}\mathcal{F}_+(\alpha, 0) + e^{-\iota\alpha l}\mathcal{F}_-(\alpha, 0) - \mathcal{A}'\mathcal{G}'(\alpha)\right\},
\end{aligned} \tag{5.50}$$

$$\begin{aligned}
A_2(\alpha) = {} & -\frac{1}{\mathcal{S}(\alpha)}\left\{e^{\iota\alpha l}\mathcal{F}'_+(\alpha, 0) + e^{-\iota\alpha l}\mathcal{F}'_-(\alpha, 0) - \mathcal{A}\mathcal{G}(\alpha)\right\} \\
& - \frac{1}{\iota\gamma(\alpha)\mathcal{K}(\alpha)}\left\{e^{\iota\alpha l}\mathcal{F}_+(\alpha, 0) + e^{-\iota\alpha l}\mathcal{F}_-(\alpha, 0) - \mathcal{A}'\mathcal{G}'(\alpha)\right\},
\end{aligned} \tag{5.51}$$

The Wiener-Hopf equations presented by (5.45) and (5.46) are derived through the general theory of Wiener-Hopf procedure and analysis may be used to obtain a solution approximated for large $k_{eff}r$ $\left(r = \sqrt{x^2 + y^2}\right)$. Now equating the terms of (5.45) and (5.46) with positive sign on one side of the equation and the terms with negative sign on the other side give us consequently the same function, say $\mathcal{J}(\alpha)$ which is a polynomial function so is an entire function. Analytic continuation (see Fig. 5.2) along with arguments of extended form of Liouville's theorem allows the polynomial function $\mathcal{J}(\alpha)$ to equate to zero, precluding the detailed calculations, thus we obtain the following results

$$\mathcal{F}'_+(\alpha, 0) = \frac{\mathcal{A}\mathcal{S}_+(\alpha)}{\sqrt{2\pi}}\left(\mathcal{G}_1(\alpha) + \mathcal{T}(\alpha)\mathcal{C}_1\right), \tag{5.52}$$

$$\mathcal{F}'_-(\alpha, 0) = \frac{\mathcal{A}\mathcal{S}_-(\alpha)}{\sqrt{2\pi}}\left(\mathcal{G}_2(-\alpha) + \mathcal{T}(-\alpha)\mathcal{C}_2\right), \tag{5.53}$$

$$\mathcal{F}_+(\alpha, 0) = \frac{\mathcal{A}'\mathcal{K}_+(\alpha)}{\sqrt{2\pi}}\left(\mathcal{G}'_1(\alpha) + \mathcal{T}'(\alpha)\mathcal{C}'_1\right), \tag{5.54}$$

$$\mathcal{F}_-(\alpha, 0) = \frac{\mathcal{A}'\mathcal{K}_-(\alpha)}{\sqrt{2\pi}}\left(\mathcal{G}'_2(-\alpha) + \mathcal{T}'(-\alpha)\mathcal{C}'_2\right), \tag{5.55}$$

where

$$\mathcal{G}_1(\alpha) = \frac{e^{-\iota l k_{eff}\cos\theta_0}}{(\alpha - k_{eff}\cos\theta_0)}\left(\frac{1}{\mathcal{S}_+(\alpha)} - \frac{1}{\mathcal{S}_+(k_{eff}\cos\theta_0)}\right) - e^{\iota l k_{eff}\cos\theta_0}\mathcal{R}_1(\alpha), \quad (5.56)$$

$$\mathcal{G}_2(\alpha) = \frac{e^{\iota l k_{eff}\cos\theta_0}}{(\alpha + k_{eff}\cos\theta_0)}\left(\frac{1}{\mathcal{S}_+(\alpha)} - \frac{1}{\mathcal{S}_+(-_{eff}\cos\theta_0)}\right) - e^{-\iota l k_{eff}\cos\theta_0}\mathcal{R}_2(\alpha), \quad (5.57)$$

$$\mathcal{C}_1 = \mathcal{S}_+(k_{eff})\left(\frac{\mathcal{G}_2(k_{eff}) + \mathcal{S}_+(k_{eff})\mathcal{G}_1(k_{eff})\mathcal{T}(k_{eff})}{1 - \mathcal{S}_+^2(k_{eff})\mathcal{T}^2(k_{eff})}\right), \quad (5.58)$$

$$\mathcal{C}_2 = \mathcal{S}_+(k_{eff})\left(\frac{\mathcal{G}_1(k_{eff}) + \mathcal{S}_+(k_{eff})\mathcal{G}_2(k_{eff})\mathcal{T}(k_{eff})}{1 - \mathcal{S}_+^2(k_{eff})\mathcal{T}^2(k_{eff})}\right), \quad (5.59)$$

$$\mathcal{G}_1'(\alpha) = \frac{e^{-\iota l k_{eff}\cos\theta_0}}{(\alpha - k_{eff}\cos\theta_0)}\left(\frac{1}{\mathcal{K}_+(\alpha)} - \frac{1}{\mathcal{K}_+(k_{eff}\cos\theta_0)}\right) - e^{\iota l k_{eff}\cos\theta_0}\mathcal{R}_1(\alpha), \quad (5.60)$$

$$\mathcal{G}_2'(\alpha) = \frac{e^{\iota l k_{eff}\cos\theta_0}}{(\alpha + k_{eff}\cos\theta_0)}\left(\frac{1}{\mathcal{K}_+(\alpha)} - \frac{1}{\mathcal{K}_+(-k_{eff}\cos\theta_0)}\right) - e^{-\iota l k_{eff}\cos\theta_0}\mathcal{R}_2(\alpha),$$
$$(5.61)$$

$$\mathcal{C}_1' = \mathcal{K}_+(k_{eff})\left(\frac{\mathcal{G}_2(k_{eff}) + \mathcal{K}_+(k_{eff})\mathcal{G}_1(k_{eff})\mathcal{T}(k_{eff})}{1 - \mathcal{K}_+^2(k_{eff})\mathcal{T}^2(k_{eff})}\right), \quad (5.62)$$

$$\mathcal{C}_2' = \mathcal{K}_+(k_{eff})\left(\frac{\mathcal{G}_1(k_{eff}) + \mathcal{K}_+(k_{eff})\mathcal{G}_2(k_{eff})\mathcal{T}(k_{eff})}{1 - \mathcal{K}_+^2(k_{eff})\mathcal{T}^2(k_{eff})}\right), \quad (5.63)$$

$$\mathcal{R}_{1,2}(\alpha) = \frac{E_{-1}\left[\mathcal{W}_{-1}(-\iota l(k_{eff} \pm k_{eff}\cos\theta_0)) - \mathcal{W}_{-1}(-\iota l(k_{eff} + \alpha))\right]}{2\pi i\iota(\alpha \mp k_{eff}\cos\theta_0)}, \quad (5.64)$$

$$\mathcal{T}(\alpha) = \frac{1}{2\pi\iota}E_{-1}\mathcal{W}_{-1}(-\iota(k_{eff} + \alpha)l), \quad (5.65)$$

$$E_{-1} = 2\exp(\iota k_{eff}l)(l)^{\frac{1}{2}}(\iota)^{-\frac{1}{2}}, \quad (5.66)$$

and

$$\mathcal{W}_{n-\frac{1}{2}}(s) = \int_0^\infty \frac{v^n \exp(-v)}{v+s}du$$
$$= \Gamma(n+1)\exp\left(\frac{s}{2}\right)s^{\frac{1}{2}n-\frac{1}{2}}\mathcal{W}_{-\frac{1}{2}(n+1),\frac{1}{2}n}(s). \quad (5.67)$$

Here, $\mathcal{W}_{m,n}$ is named as Whittaker function and $s = -\iota(k_{eff}+\alpha)l$, $n = -\frac{1}{2}$.

Now substitution of (5.52-5.55) along with (5.49) in (5.45) and (5.46) gives us the

following result :

$$
\left.\begin{array}{c} A_1\left(\alpha\right) \\ A_2\left(\alpha\right) \end{array}\right\} = \frac{\mathcal{A}sgn\left(y\right)}{\sqrt{2\pi}\mathcal{S}\left(\alpha\right)} \left\{ \begin{array}{c} e^{\iota\alpha l}\mathcal{S}_+\left(\alpha\right)\mathcal{G}_1\left(\alpha\right) + e^{\iota\alpha l}\mathcal{S}_+\left(\alpha\right)\mathcal{T}\left(\alpha\right)\mathcal{C}_1 \\ + e^{-\iota\alpha l}\mathcal{S}_-\left(\alpha\right)\mathcal{G}_2\left(-\alpha\right) \\ + e^{-\iota\alpha l}\mathcal{S}_-\left(\alpha\right)\mathcal{T}\left(-\alpha\right)\mathcal{C}_2 \\ -\frac{e^{\iota l\left(\alpha - k_{eff}\cos\theta_0\right)} - e^{-\iota l\left(\alpha - k_{eff}\cos\theta_0\right)}}{\left(\alpha - k_{eff}\cos\theta_0\right)} \end{array} \right\}
$$
$$
- \frac{\mathcal{A}'}{\sqrt{2\pi}\iota\gamma\left(\alpha\right)\mathcal{K}\left(\alpha\right)} \left\{ \begin{array}{c} e^{\iota\alpha l}\mathcal{K}_+\left(\alpha\right)\mathcal{G}_1'\left(\alpha\right) + e^{\iota\alpha l}\mathcal{K}_+\left(\alpha\right)\mathcal{T}\left(\alpha\right)\mathcal{C}_1' \\ + e^{-\iota\alpha l}\mathcal{K}_-\left(\alpha\right)\mathcal{G}_2'\left(-\alpha\right) \\ + e^{-\iota\alpha l}\mathcal{K}_-\left(\alpha\right)\mathcal{T}\left(-\alpha\right)\mathcal{C}_2' \\ -\frac{e^{\iota l\left(\alpha - k_{eff}\cos\theta_0\right)} - e^{-\iota l\left(\alpha - k_{eff}\cos\theta_0\right)}}{\left(\alpha - k_{eff}\cos\theta_0\right)} \end{array} \right\}. \tag{5.68}
$$

The diffraction of EM-wave field obtained by the application of inverse Fourier transform of (5.26) is defined as

$$
\begin{aligned}
H_z(x,y) &= \frac{1}{\sqrt{2\pi}} \int\limits_{-\infty}^{\infty} \mathcal{F}\left(\alpha,y\right) e^{-\iota\alpha x} d\alpha \\
&= \frac{1}{\sqrt{2\pi}} \int\limits_{-\infty}^{\infty} \left\{ \begin{array}{c} A_1\left(\alpha\right) \\ A_2\left(\alpha\right) \end{array} \right\} e^{-\iota\alpha x - \iota\gamma|y|} d\alpha.
\end{aligned} \tag{5.69}
$$

where $A_1\left(\alpha\right)$ and $A_2\left(\alpha\right)$ are given by (5.68). Substitution of (5.68) into (5.69) and splitting up the diffracted field function $H_z(x,y)$ into two parts as mentioned below :

$$
H_z(x,y) = H_z^{sep}(x,y) + H_z^{int}(x,y), \tag{5.70}
$$

where

$$H_z^{sep}(x,y) = \frac{sgn(y)}{2\pi} \int\limits_{-\infty}^{\infty} \frac{1}{\mathcal{S}(\alpha)} \begin{pmatrix} -\frac{\mathcal{A}\mathcal{S}_+(\alpha)e^{\iota l\left(\alpha-k_{eff}\cos\theta_0\right)}}{\left(\alpha-k_{eff}\cos\theta_0\right)\mathcal{S}_+\left(k_{eff}\cos\theta_0\right)} \\ +\frac{\mathcal{A}\mathcal{S}_-(\alpha)e^{-\iota l\left(\alpha-k_{eff}\cos\theta_0\right)}}{\left(\alpha-k_{eff}\cos\theta_0\right)\mathcal{S}_+\left(-k_{eff}\cos\theta_0\right)} \end{pmatrix} e^{\left(-\iota\alpha x-\iota\gamma|y|\right)}d\alpha$$

$$+ \frac{1}{2\pi} \int\limits_{-\infty}^{\infty} \frac{1}{\iota\gamma(\alpha)\mathcal{K}(\alpha)} \begin{pmatrix} \frac{\mathcal{A}'\mathcal{K}_+(\alpha)e^{\iota l\left(\alpha-k_{eff}\cos\theta_0\right)}}{\left(\alpha-k_{eff}\cos\theta_0\right)\mathcal{K}_+\left(k_{eff}\cos\theta_0\right)} \\ -\frac{\mathcal{A}'\mathcal{K}_-(\alpha)e^{-\iota l\left(\alpha-k_{eff}\cos\theta_0\right)}}{\left(\alpha-k_{eff}\cos\theta_0\right)\mathcal{K}_+\left(-k_{eff}\cos\theta_0\right)} \end{pmatrix} e^{\left(-\iota\alpha x-\iota\gamma|y|\right)}d\alpha,$$

(5.71)

and

$$H_z^{int}(x,y) = \frac{sgn(y)}{2\pi} \int\limits_{-\infty}^{\infty} \frac{\mathcal{A}}{\mathcal{S}(\alpha)} \begin{pmatrix} -\mathcal{S}_+(\alpha)\mathcal{R}_1(\alpha)e^{\iota l(\alpha+k_{eff}\cos\theta_0)} \\ +\mathcal{S}_+(\alpha)\mathcal{T}(\alpha)\mathcal{C}_1 e^{\iota\alpha l} \\ -\mathcal{S}_+(-\alpha)\mathcal{R}_2(-\alpha)e^{-\iota l(\alpha+k_{eff}\cos\theta_0)} \\ +\mathcal{S}_+(-\alpha)\mathcal{T}(-\alpha)\mathcal{C}_2 e^{-\iota\alpha l} \end{pmatrix} e^{\left(-\iota\alpha x-\iota\gamma|y|\right)}d\alpha$$

$$+ \frac{1}{2\pi} \int\limits_{-\infty}^{\infty} \frac{\mathcal{A}'}{\iota\gamma(\alpha)\mathcal{K}(\alpha)} \begin{pmatrix} \mathcal{K}_+(\alpha)\mathcal{R}_1(\alpha)e^{\iota l(\alpha+k_{eff}\cos\theta_0)} \\ -\mathcal{K}_+(\alpha)\mathcal{T}(\alpha)\mathcal{C}_1' e^{\iota\alpha l} \\ +\mathcal{K}_+(-\alpha)\mathcal{R}_2(-\alpha)e^{-\iota l(\alpha+k_{eff}\cos\theta_0)} \\ -\mathcal{K}_+(-\alpha)\mathcal{T}(-\alpha)\mathcal{C}_2' e^{-\iota\alpha l} \end{pmatrix} e^{\left(-\iota\alpha x-\iota\gamma|y|\right)}d\alpha.$$

(5.72)

In above (5.71) $H_z^{sep}(x,y)$ has two integrals in which the integrand with kernel function $\mathcal{S}(\alpha)$ has two parts one for the edge $x = l$ and other for edge $x = -l$, similarly, integrand with kernel function $\mathcal{K}(\alpha)$ has two parts one for the edge $x = 0$ and other for edge $x = -l$, so evaluation of integrals will give the diffracted field for $x = l$ as well as for $x = -l$ whereas $H_z^{int}(x,y)$ presented by (5.72) also have two integrands with kernels $\mathcal{S}(\alpha)$ and $\mathcal{K}(\alpha)$. Each integrand with its respective kernel functions $\mathcal{S}(\alpha)$ and $\mathcal{K}(\alpha)$ have two parts and on evaluating the integrals, one will give the interaction field due extremity $x = 0$ of plate and other for the interaction field due to extremity $x = -l$ of plate.

5.6 Acquirement of Diffracted Field

Now the diffracted field in the far field zone may be evaluated asymptotically. For this purpose, the polar coordinates as $x = r \cos \theta$, $|y| = r \sin \theta$ are introduced and following transformation helps in the deformation of contour.

$$\alpha = -k_{eff} \cos (\theta + \iota \zeta), \quad \text{for } 0 < \theta < \pi, \; -\infty < \zeta < \infty. \tag{5.73}$$

Now applying the method of stationary phase (an asymptotic method) for large $k_{eff} r$, (5.69) takes the following form

$$H_z(r, \theta) = \frac{\iota k_{eff}}{\sqrt{k_{eff} r}} \left\{ \begin{array}{c} A_1 \left(-k_{eff} \cos \theta\right) \\ A_2 \left(-k_{eff} \cos \theta\right) \end{array} \right\} \sin \theta \exp \left(\iota k_{eff} r + \iota \frac{\pi}{4}\right). \tag{5.74}$$

Similarly, integrals appearing in (5.71) and (5.72) are evaluated asymptotically using method of stationary phase and results are obtained as

$$\begin{aligned} H_z^{sep}(r, \theta) = \frac{1}{\sqrt{2\pi}} \frac{\iota k_{eff}}{\sqrt{k_{eff} r}} \Big\{ &- sgn(\theta) \, \psi^{sep} \left(-k_{eff} \cos \theta\right) \\ &+ \phi^{sep} \left(-k_{eff} \cos \theta\right) \Big\} \sin \theta \exp \left(\iota k_{eff} r + \iota \frac{\pi}{4}\right), \end{aligned} \tag{5.75}$$

and

$$\begin{aligned} H_z^{int}(r, \theta) = \frac{1}{\sqrt{2\pi}} \frac{\iota k_{eff}}{\sqrt{k_{eff} r}} \Big\{ &- sgn(\theta) \, \psi^{int} \left(-k_{eff} \cos \theta\right) \\ &+ \phi^{int} \left(-k_{eff} \cos \theta\right) \Big\} \sin \theta \exp \left(\iota k_{eff} r + \iota \frac{\pi}{4}\right), \end{aligned} \tag{5.76}$$

where

$$\begin{aligned} \psi^{sep} \left(-k_{eff} \cos \theta\right) = &\frac{\mathcal{A} \mathcal{S}_+ \left(-k_{eff} \cos \theta\right) e^{\iota l \left(-k_{eff} \cos \theta - k_{eff} \cos \theta_0\right)}}{\mathcal{S} \left(-k_{eff} \cos \theta\right) \left(-k_{eff} \cos \theta - k_{eff} \cos \theta_0\right) \mathcal{S}_+ \left(k_{eff} \cos \theta_0\right)} \\ &- \frac{\mathcal{A} \mathcal{S}_- \left(-k_{eff} \cos \theta\right) e^{-\iota l \left(-k_{eff} \cos \theta - k_{eff} \cos \theta_0\right)}}{\mathcal{S} \left(-k_{eff} \cos \theta\right) \left(-k_{eff} \cos \theta - k_{eff} \cos \theta_0\right) \mathcal{S}_+ \left(-k_{eff} \cos \theta_0\right)}, \end{aligned} \tag{5.77}$$

and

$$\phi^{sep}\left(-k_{eff}\cos\theta\right)=\frac{\mathcal{A}'\mathcal{K}_+\left(-k_{eff}\cos\theta\right)e^{-\iota l\left(-k_{eff}\cos\theta-k_{eff}\cos\theta_0\right)}}{\iota\gamma\left(-k_{eff}\cos\theta\right)\mathcal{K}\left(-k_{eff}\cos\theta\right)\left(-k_{eff}\cos\theta-k_{eff}\cos\theta_0\right)\mathcal{K}_+\left(k_{eff}\cos\theta_0\right)}$$

$$-\frac{\mathcal{A}'\mathcal{K}_-\left(k_{eff}\cos\theta\right)e^{-\iota l\left(-k_{eff}\cos\theta-k_{eff}\cos\theta_0\right)}}{\iota\gamma\left(-k_{eff}\cos\theta\right)\mathcal{K}\left(-k_{eff}\cos\theta\right)\left(-k_{eff}\cos\theta-k_{eff}\cos\theta_0\right)\mathcal{K}_+\left(-k_{eff}\cos\theta_0\right)},$$

$$(5.78)$$

$$\psi^{int}\left(-k_{eff}\cos\theta\right)=\frac{\mathcal{A}}{\mathcal{S}\left(-k_{eff}\cos\theta\right)}$$

$$\times\begin{pmatrix}\mathcal{S}_+\left(-k_{eff}\cos\theta\right)\mathcal{R}_1\left(-k_{eff}\cos\theta\right)e^{-\iota l(-k_{eff}\cos\theta+k_{eff}\cos\theta_0)}\\-\mathcal{S}_+\left(-k_{eff}\cos\theta\right)\mathcal{T}\left(-k_{eff}\cos\theta\right)\mathcal{C}_1 e^{-\iota l k_{eff}\cos\theta}\\+\mathcal{S}_-\left(-k_{eff}\cos\theta\right)\mathcal{R}_2\left(k_{eff}\cos\theta\right)e^{-\iota l(-k_{eff}\cos\theta-k_{eff}\cos\theta_0)}\\-\mathcal{S}_-\left(-k_{eff}\cos\theta\right)\mathcal{T}\left(k_{eff}\cos\theta\right)\mathcal{C}_2 e^{\iota l k_{eff}\cos\theta}\end{pmatrix},$$

$$(5.79)$$

$$\phi^{int}\left(-k_{eff}\cos\theta\right)=\frac{\mathcal{A}'}{\mathcal{K}\left(-k_{eff}\cos\theta\right)}$$

$$\times\begin{pmatrix}\mathcal{K}_+\left(-k_{eff}\cos\theta\right)\mathcal{R}_1\left(-k_{eff}\cos\theta\right)e^{\iota l(-k_{eff}\cos\theta+k_{eff}\cos\theta_0)}\\-\mathcal{K}_+\left(-k_{eff}\cos\theta\right)\mathcal{T}\left(-k_{eff}\cos\theta\right)\mathcal{C}_1'e^{-\iota l k_{eff}\cos\theta}\\+\mathcal{K}_-\left(-k_{eff}\cos\theta\right)\mathcal{R}_2\left(k_{eff}\cos\theta\right)e^{-\iota l(-k_{eff}\cos\theta+k_{eff}\cos\theta_0)}\\-\mathcal{K}_-\left(-k_{eff}\cos\theta\right)\mathcal{T}\left(k_{eff}\cos\theta\right)\mathcal{C}_2'e^{\iota l k_{eff}\cos\theta}\end{pmatrix}.$$

$$(5.80)$$

The result given by (5.74) presents the diffracted field evaluated asymptotically for $k_{eff}r\longrightarrow\infty$. In fact, it is the asymptotic form of $H_z(x,y)$ valid for all observation angles in the entire region. It is observed that the wave field diffracted by the extremities $x=l$ and $x=-l$ of the plate plus the additional involvement of the geometrical wave field results into the separated field. The separated field being the resultant wave field will regard a physical perception to the model. But on the other hand, the interacted field appearing due to the interaction of one edge upon other regards no physics of the model, separately. The separated field provides the physical perception of diffraction phenomenon at the boundary defined for the associated model.

Therefore, only the separated field is taken into account to discussion. Furthermore, the interaction field generated as a result of double diffraction of EM-plane wave by two edges is already counted by the separated field. Also the extending the plate length upto infinity discards the contribution resulting from the interaction terms and consequently, the separated field appears to be diffracted field. Therefore, only the separated field is focused to discuss graphically in the next section.

5.7   Results and Discussion

This section highlights the impact of pertinent parameters like angle of incidence θ_0, wave-number k, plate length l, surface impedance η_s and permittivity element ε_1 on separated field of EM-wave against observation angle in the absence and presence of cold plasma. In Figs. 5.3a, 5.3b, sketch of separated field for three different angles of incidence is visualized while keeping values of all other parameters fixed. The observation predicts that separated field intensity gets sharp peaks at observation angles $\theta = 2\pi/3, 3\pi/4, 5\pi/6$ indicating the reflection of EM-wave for respective angles of incidence $\theta_0 = \pi/3, \pi/4, \pi/6$. The structure of finite length symmetric plate under consideration over here may work for physical aspect of scattering mechanism at these particular values of observation angles. The maximum sharp peak occurs at observation angle $\theta = 3\pi/4$ for its respective incidence angle $\theta_0 = \pi/4$ in both the cases i.e. in the absence and presence of cold plasma. However, wavelength expands in the presence of cold plasma. Figs. 5.4a, 5.4b are sketched to display behavior of separated field for incremental trend of wave-number k. This means that wave frequency excites to the high frequency range. On observing the sketches, it is found that number of oscillations increase here due to the symmetric plate as compared to the non-symmetric plate in previous chapter. In Figs. 5.5a, 5.5b, oscillations of the separated field increase due to increasing the length of plate. According to observation, it is found that separated field in the far away region from the origin, after the sharp peak, coincides even for three different values of length. One can observe by

comparing Figs. 5.4b, 5.5b with 5.4a, 5.5a, respectively, that presence of cold plasma has expanded the wavelength of separated field. Figs. 5.6a, 5.6b have shown the behavior of separated field for three different values of surface impedance in the absence and presence of cold plasma, respectively. Observation describes that separated field for real value (surface resistance) of surface impedance is more fluctuated than for the pure imaginary (surface reactance) and imaginary value (both surface resistance and surface reactance) of surface impedance. Fig. 5.7 is sketched to show the behavior of separated field for ε_1. The drastic effects on separated field have been predicted due presence of cold plasma. Since $\varepsilon_1 \approx 1 - (\omega_p/\omega)^2$ (for signal with high frequency) so an increase in ε_1 while keeping the number density of ions and electrons fixed in cold plasma, that's why separated field gets oscillated with increasing behavior of ε_1. The electrons oscillate about cold ionic centers due to electric field of high frequency signal and these oscillating electrons scatter enormously due to increasing amplitude of the separated field. The separated field shows the nullity around the observation angle of 0 for all physical parameters corresponding to the present model.
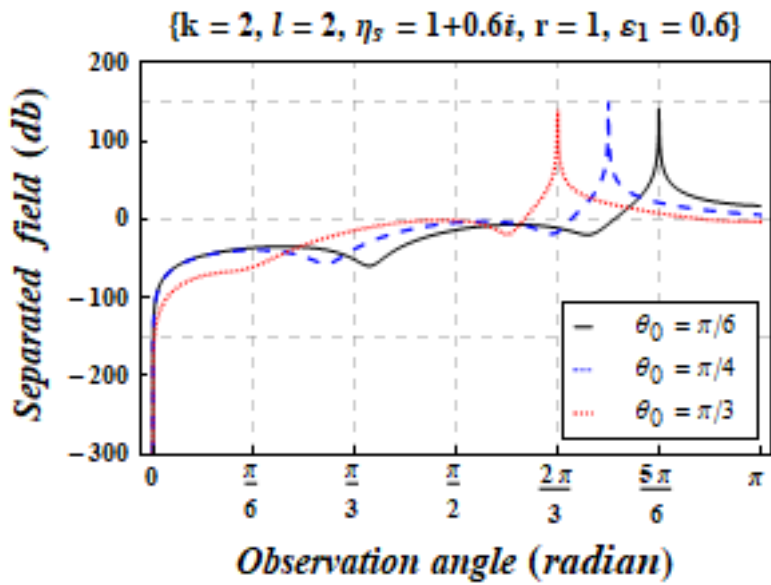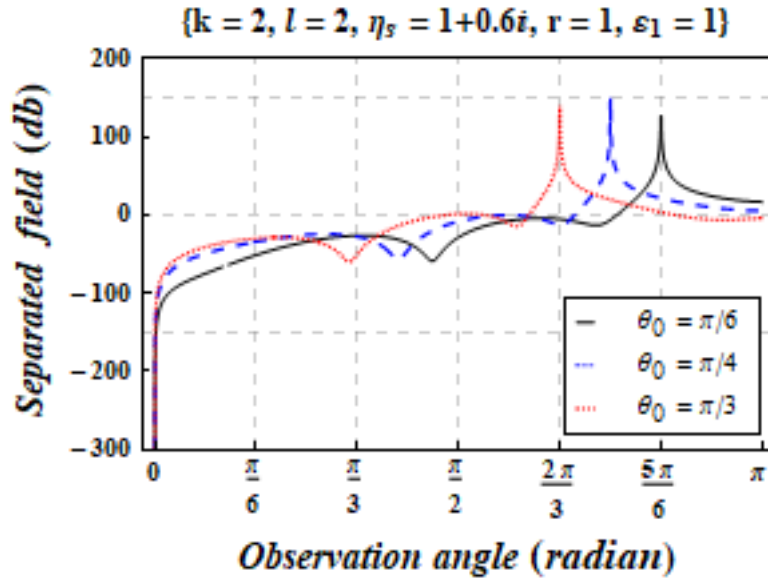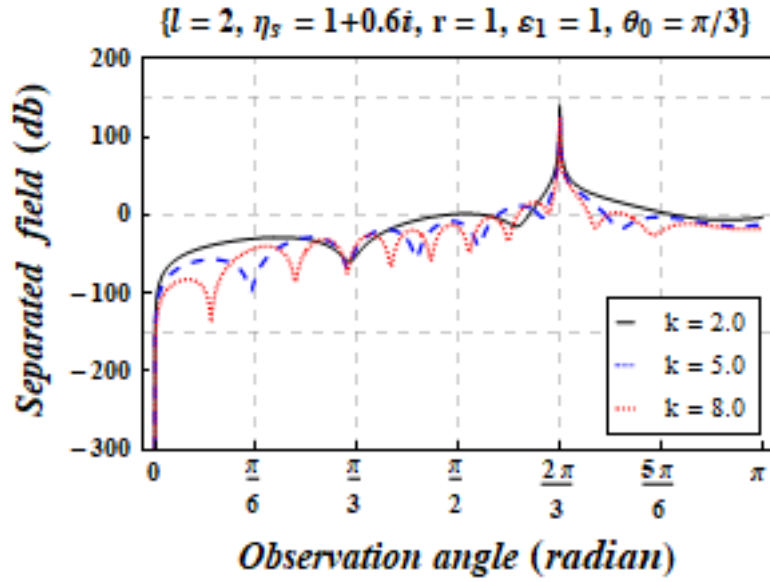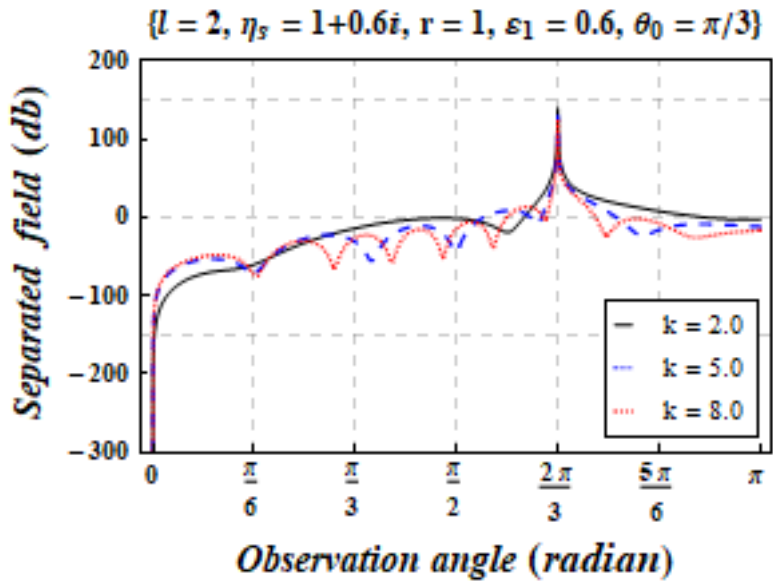
{k = 2, l = 2, η_s = 1+0.6i, r = 1, ε_1 = 1}

(a)

{k = 2, l = 2, η_s = 1+0.6i, r = 1, ε_1 = 0.6}

(b)

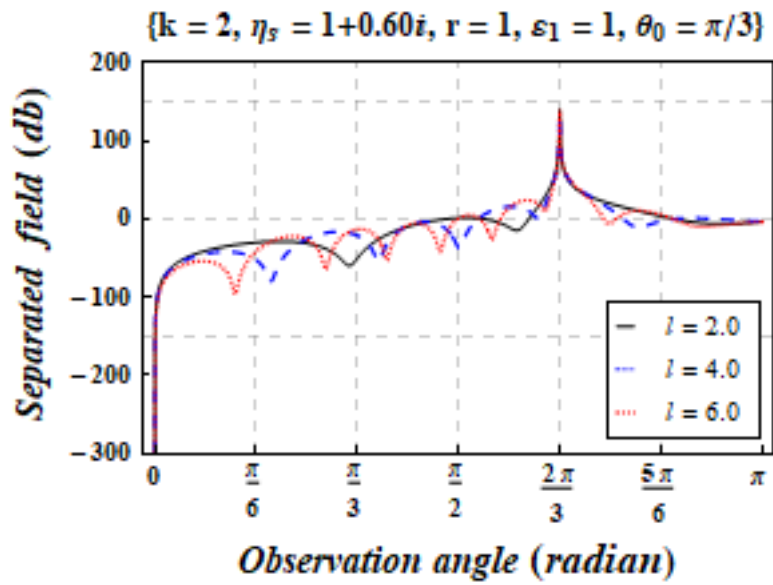Figure 5.3: **The separated field for angle of incidence in the absence (a) and presence (b) of cold plasma.**
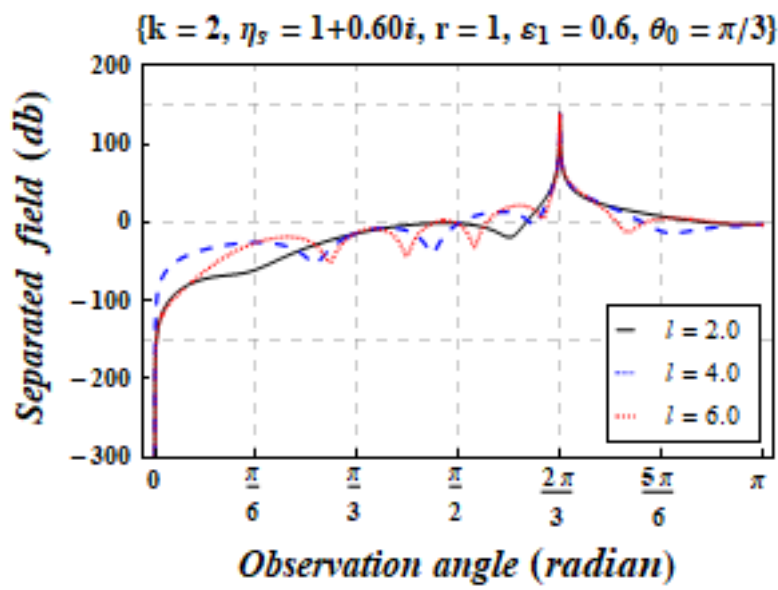
(a)

(b)

Figure 5.4: **The separated field for wave-number in the absence (a) and presence (b) of cold plasma.**
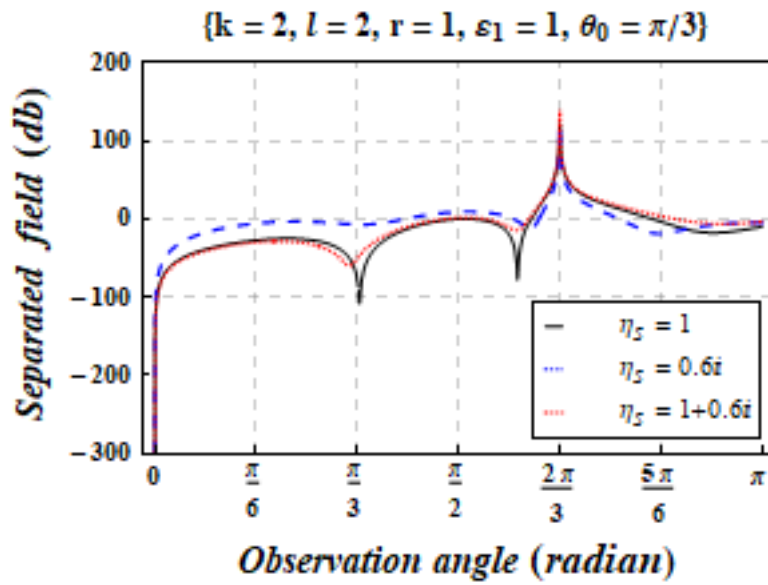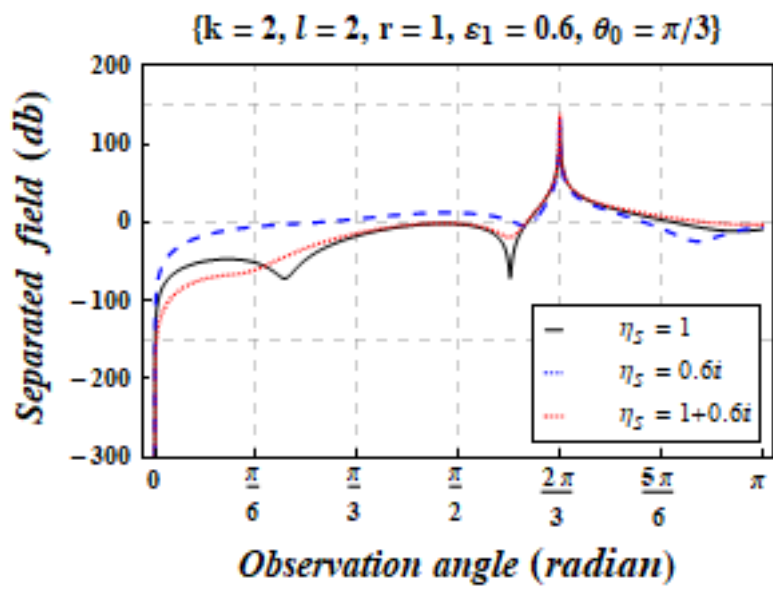
(a)

(b)

Figure 5.5: **The separated field for length of plate in the absence (a) and presence (b) of cold plasma.**

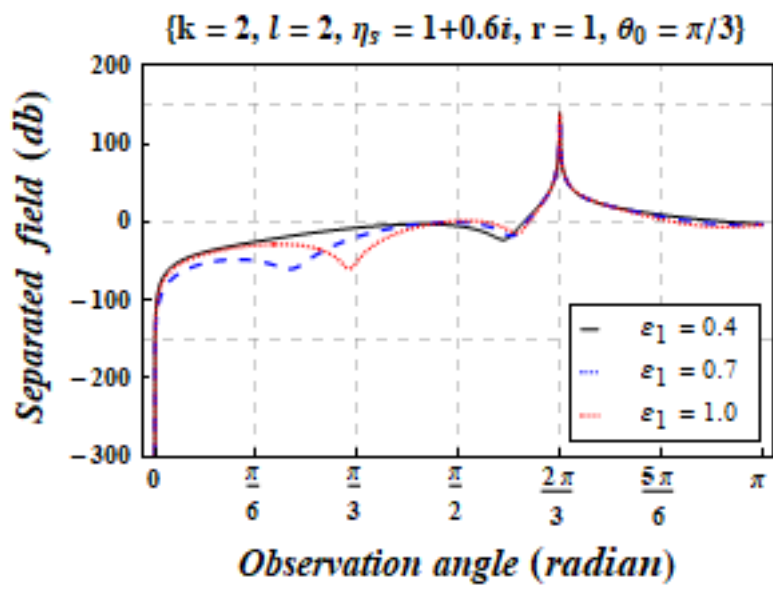Figure 5.6: **The separated field for surface impedance in the absence (a) and presence (b) of cold plasma.**

94

Figure 5.7: **The separated field for** ε_1.

5.8 Conclusions

This chapter has elaborated about the EM-plane wave incident on a plate of finite symmetric length (which ultimately gives the diffracted field) with surface impedance in the presence of the cold plasma. It has been observed that diffraction of EM-plane wave by the plate of finite symmetric length undergoes the variation due to (a) extending the plate length (b) different angles of incidence (c) increasing the wave-number (d) different values of surface impedance and (e) permittivity of cold plasma.

Chapter 6

Wiener-Hopf Analysis of Diffracted Wave in Cold Plasma by an Impedance Slit of Finite Width

Present chapter elaborates the analysis of diffraction of electromagnetic (EM) plane wave by a slit of finite width under the effects of cold plasma. The impedance is imposed on the slit and to consider the effects of impedance, Leontovich boundary conditions are assumed. Helmholtz's equation is formulated using the Maxwell's equations with the effects of cold plasma. The Fourier transform is applied and then Wiener-Hopf equations are obtained. The method of stationary phase is used to get the result of diffracted field due to slit of finite width (separated field). Graphical analysis of separated field is discussed comprehensively.

6.1 Modelling of the Helmholtz Equation

The tensor of dielectric permittivity to consider the effects of cold plasma is defined as

$$\bar{\varepsilon} = \varepsilon_0 \begin{pmatrix} \varepsilon_1 & -\iota\varepsilon_2 & 0 \\ \iota\varepsilon_2 & \varepsilon_1 & 0 \\ 0 & 0 & \varepsilon_z \end{pmatrix}, \tag{6.1}$$

$$\varepsilon_1 = 1 - \left(\frac{\omega_p}{\omega}\right)^2 \left[1 - \left(\frac{\omega_c}{\omega}\right)^2\right]^{-1}, \quad \varepsilon_2 = \left(\frac{\omega_p}{\omega}\right)^2 \left[\frac{\omega}{\omega_c} - \frac{\omega_c}{\omega}\right]^{-1}, \tag{6.2}$$

and

$$\varepsilon_z = 1 - \left(\frac{\omega_p}{\omega}\right)^2, \tag{6.3}$$

with

$$\omega_p^2 = \frac{N_e e^2}{m\varepsilon_0}, \quad \omega_c = \frac{|e|\,\mu_0 H_{dc}}{m}. \tag{6.4}$$

It is known that Maxwell's equations are proved to be valid in cold plasma with dielectric permittivity tensor, thus, the electric field components evaluated in terms of magnetic field with the effects of cold plasma with the aid of Maxwell's equations along with (6.1) are described as

$$E_x = \frac{\iota\varepsilon_1}{\omega\varepsilon_0\,(\varepsilon_1^2 - \varepsilon_2^2)} \frac{\partial H_z\,(x,y)}{\partial y} + \frac{\varepsilon_2}{\omega\varepsilon_0\,(\varepsilon_1^2 - \varepsilon_2^2)} \frac{\partial H_z\,(x,y)}{\partial x}, \tag{6.5}$$

and

$$E_y = \frac{\varepsilon_2}{\omega\varepsilon_0\,(\varepsilon_1^2 - \varepsilon_2^2)} \frac{\partial H_z\,(x,y)}{\partial y} - \frac{\iota\varepsilon_1}{\omega\varepsilon_0\,(\varepsilon_1^2 - \varepsilon_2^2)} \frac{\partial H_z\,(x,y)}{\partial x}. \tag{6.6}$$

Thus, the Helmholtz's equation satisfying H_z obtained from Maxwell's equations along with electric field components (6.5) and (6.6), is computed as follows :

$$\partial_{xx} H_z\,(x,y) + \partial_{yy} H_z\,(x,y) + k_{eff}^2 H_z\,(x,y) = 0, \tag{6.7}$$

with propagation constant

$$k_{eff} = k\sqrt{\frac{\varepsilon_1^2 - \varepsilon_2^2}{\varepsilon_1}}, \quad k = \omega\sqrt{\varepsilon_0\mu_0}. \tag{6.8}$$

Here, k_{eff} is dependent of k, ε_1 and ε_2, harmonic time dependence $\exp(-\iota\omega t)$ is assumed and will be suppressed throughout the analysis.
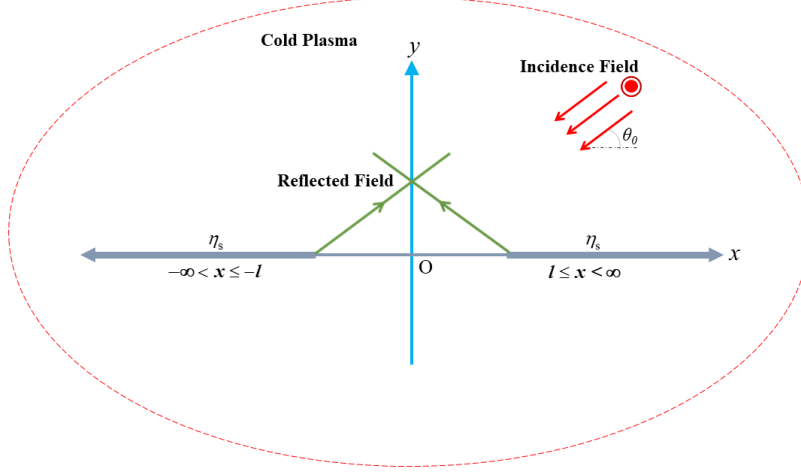
Figure 6.1: **Geometrical description of the model.**

6.2 Mathematical Modelling of the Problem

A slit of finite width with surface impedance is located symmetrically along $y = 0$ with edges at $x = -l$ and $x = l$. The wave incident at the one edge $x = -l$ of reflects back in the direction opposite to the incident field whereas the wave incident on the other edge $x = l$ of the slit reflects at an angle of $\pi - \theta_0$ with the horizontal axis as can be seen in Fig. 6.1. The incident field is taken as

$$H_z^{inc}(x, y) = \exp\{-\iota k_{eff}(x \cos \theta_0 + y \sin \theta_0)\}, \tag{6.9}$$

Here, the amplitude of magnetic field is taken as 1 A/m and θ_0 is the angle of incidence with $x-$axis. Here, the total field can be expressed as follows:

$$H_z^{tot}(x, y) = H_z^{inc}(x, y) \pm H_z^{ref}(x, y) + H_z(x, y), \text{ for } y \geq 0$$
$$H_z^{tot}(x, y) = H_z(x, y), \text{ for } y \leq 0 \tag{6.10}$$

where $H_z(x, y)$ is the diffracted field and $H_z^{ref}(x, y)$ denotes the reflected field, which is defined as

$$H_z^{ref}(x, y) = \left(\frac{\eta_s \sin \theta_0 - 1}{\eta_s \sin \theta_0 + 1} \right) \exp\{-\iota k_{eff}(x \cos \theta_0 - y \sin \theta_0)\}. \tag{6.11}$$

99

For convenience of analysis, the medium for the present model is assumed to be slightly lossy as in $k_{eff} = \mathfrak{Re}\{k_{eff}\} + \iota\mathfrak{Im}\{k_{eff}\}$, $0 < \mathfrak{Im}\{k_{eff}\} \ll \mathfrak{Re}\{k_{eff}\}$ and the solution for real k_{eff} is achieved by assuming $\mathfrak{Im}\{k_{eff}\} \longrightarrow 0$. The boundary value problem (BVP) under consideration is expressed in terms of the magnetic field potential and it is adequate to denote the diffracted field in the different regions. The total field $H_z^{tot}(x, y)$ in the range $x \in (-\infty, \infty)$, that satisfies the Helmholtz's equation as follows :

$$\left[\partial_{xx} + \partial_{yy} + k_{eff}^2\right] H_z^{tot}(x, y) = 0, \tag{6.12}$$

diffracted field satisfying Helmholtz's equation extracted from (6.12) is given as follows:

$$\left[\partial_{xx} + \partial_{yy} + k_{eff}^2\right] H_z(x, y) = 0. \tag{6.13}$$

Our focus is to evaluate the diffracted field of EM-plane wave incident on a slit of finite width. Same effects of impedance are assumed on both the surfaces. Therefore, Leontovich boundary conditions are considered as

$$\partial_y H_z^{tot}(x, 0^{\mp}) - \iota\frac{\varepsilon_2}{\varepsilon_1}\partial_x H_z^{tot}(x, 0^{\mp}) = \pm\iota\frac{k_{eff}^2}{\omega\mu_0}\eta_0\eta_s H_z^{tot}(x, 0^{\mp}), \text{ for } |x| \geq l, \tag{6.14}$$

where $\eta_0 = \sqrt{\mu_0/\varepsilon_0}$.

6.3   Transformation of the Problem

Now applying the Fourier transform on the boundary value problem (BVP) with respect to variable x as

$$\mathcal{F}(\alpha, y) = \frac{1}{\sqrt{2\pi}} \int\limits_{-\infty}^{\infty} H_z(x, y) e^{\iota\alpha x} dx$$

$$= e^{\iota\alpha l}\mathcal{F}_+(\alpha, y) + e^{-\iota\alpha l}\mathcal{F}_-(\alpha, y) + \mathcal{F}_l(\alpha, y), \tag{6.15}$$

where $\alpha = \mathfrak{Re}\{\alpha\} + \iota\mathfrak{Im}\{\alpha\} = \sigma + \iota\tau$. The asymptotic expression of $H_z(x, y)$ as $x \longrightarrow \pm\infty$ is taken into account as

$$H_z(x, y) = \begin{cases} O\left(e^{-\mathfrak{Im}\{k_{eff}\}x}\right) & \text{for } x \longrightarrow \infty, \\ O\left(e^{\mathfrak{Im}\{k_{eff}\}x\cos\theta_0}\right) & \text{for } x \longrightarrow -\infty. \end{cases} \tag{6.16}$$

$\mathcal{F}_+(\alpha, y)$ is a regular function of α lying in the upper-half of $\alpha-$plane $-\mathfrak{Im}\{k_{eff}\} < \mathfrak{Im}\{\alpha\}$, $\mathcal{F}_-(\alpha, y)$ is a regular function of α lying in the lower-half of $\alpha-$ plane $\mathfrak{Im}\{\alpha\} < \mathfrak{Im}\{k_{eff}\cos\theta_0\}$ and these together generates a band of analyticity in which all the functions including $\mathcal{F}_l(\alpha, y)$ are analytic. Now we write

$$\mathcal{F}_+(\alpha, y) = \frac{1}{\sqrt{2\pi}} \int_l^\infty H_z(x, y) e^{\iota\alpha(x-l)} dx, \tag{6.17}$$

$$\mathcal{F}_-(\alpha, y) = \frac{1}{\sqrt{2\pi}} \int_{-\infty}^{-l} H_z(x, y) e^{\iota\alpha(x+l)} dx, \tag{6.18}$$

$$\mathcal{F}_l(\alpha, y) = \frac{1}{\sqrt{2\pi}} \int_{-l}^l H_z(x, y) e^{\iota\alpha x} dx, \tag{6.19}$$

$$\mathcal{F}^{inc}(\alpha, 0) = \frac{e^{\iota l\left(\alpha - k_{eff}\cos\theta_0\right)} - e^{-\iota l\left(\alpha - k_{eff}\cos\theta_0\right)}}{\sqrt{2\pi}\iota(\alpha - k_{eff}\cos\theta_0)}, \tag{6.20}$$

$$\mathcal{F}^{ref}(\alpha, 0) = \frac{1}{\sqrt{2\pi}}\left(\frac{\eta_s\sin\theta_0 - 1}{\eta_s\sin\theta_0 + 1}\right)\frac{e^{\iota l\left(\alpha - k_{eff}\cos\theta_0\right)} - e^{-\iota l\left(\alpha - k_{eff}\cos\theta_0\right)}}{\iota(\alpha - k_{eff}\cos\theta_0)}. \tag{6.21}$$

The application of Fourier transform on (6.13)-(6.15) yields,

$$\left(\frac{d^2}{dy^2} + \gamma^2\right)\mathcal{F}(\alpha, y) = 0, \tag{6.22}$$

where $\gamma(\alpha) = \sqrt{k_{eff}^2 - \alpha^2}$.

$$\partial_y \mathcal{F}^{tot}(\alpha, 0^\mp) - \alpha\frac{\varepsilon_2}{\varepsilon_1}\mathcal{F}^{tot}(\alpha, 0^\mp) = \pm\iota\frac{k_{eff}^2}{\omega\mu_0}\eta_0\eta_s\mathcal{F}^{tot}(\alpha, 0^\mp). \tag{6.23}$$

6.4 Modelling of Wiener-Hopf Equation

The solution of (6.22) satisfying the radiation conditions is given by

$$
\mathcal{F}(\alpha, y) = \begin{cases} A_1(\alpha)\, e^{-\iota\gamma y} & y \geq 0, \\[2mm] A_2(\alpha)\, e^{\iota\gamma y} & y < 0. \end{cases} \tag{6.24}
$$

Now with the aid of (6.16), (6.23) and (6.24), following coupled functional equations are obtained as

$$
\begin{aligned}
e^{\iota\alpha l}\mathcal{F}'_+(\alpha, 0) + e^{-\iota\alpha l}\mathcal{F}'_-(\alpha, 0) &= \frac{1}{2}\big[\mathcal{F}'_{inc}(\alpha, 0) - \mathcal{F}'_{ref}(\alpha, 0)\big] \\
&\quad + \frac{1}{2}\Big(\alpha\frac{\varepsilon_2}{\varepsilon_1} + \frac{\iota k_{eff}^2}{k}\eta_s\Big)\big[\mathcal{F}_{inc}(\alpha, 0) - \mathcal{F}_{ref}(\alpha, 0)\big] \\
&\quad + \frac{1}{2}\Big(\alpha\frac{\varepsilon_2}{\varepsilon_1} + \frac{\iota k_{eff}^2}{k}\eta_s\Big)\big[\mathcal{F}_l(\alpha, 0^+) + \mathcal{F}_l(\alpha, 0^-)\big] \\
&\quad - \frac{\iota\gamma}{2}\big[A_1(\alpha) + A_2(\alpha)\big],
\end{aligned} \tag{6.25}
$$

$$
\begin{aligned}
e^{\iota\alpha l}\mathcal{F}_+(\alpha, 0) + e^{-\iota\alpha l}\mathcal{F}_-(\alpha, 0) &= -\frac{1}{2\big(\alpha\frac{\varepsilon_2}{\varepsilon_1} - \frac{\iota k_{eff}^2}{k}\eta_s\big)}\big[\mathcal{F}'_{inc}(\alpha, 0) + \mathcal{F}'_{ref}(\alpha, 0)\big] \\
&\quad + \frac{1}{2}\big[\mathcal{F}'_{inc}(\alpha, 0) + \mathcal{F}'_{ref}(\alpha, 0)\big] \\
&\quad - \frac{\alpha\big(\frac{\varepsilon_2}{\varepsilon_1}\big)}{(\alpha\frac{\varepsilon_2}{\varepsilon_1})^2 + \big(\frac{k_{eff}^2}{k}\eta_s\big)^2}\big[\mathcal{F}'_l(\alpha, 0^+) - \mathcal{F}_l(\alpha, 0^-)\big] \\
&\quad - \frac{1}{2}\frac{1}{(\alpha\frac{\varepsilon_2}{\varepsilon_1})^2 + \big(\frac{k_{eff}^2}{k}\eta_s\big)^2}\big(\iota\frac{k_{eff}^2}{k}\eta_s\big)\big[\mathcal{F}'_l(\alpha, 0^+) + \mathcal{F}'_l(\alpha, 0^-)\big] \\
&\quad + \frac{1}{2}\big[A_1(\alpha) + A_2(\alpha)\big].
\end{aligned} \tag{6.26}
$$

Here

$$
\begin{aligned}
\mathcal{F}_\pm(\alpha, 0^+) - \mathcal{F}_\pm(\alpha, 0^-) &= 2\mathcal{F}_\pm(\alpha, 0) \\
\mathcal{F}'_\pm(\alpha, 0^+) - \mathcal{F}'_\pm(\alpha, 0^-) &= 2\mathcal{F}'_\pm(\alpha, 0)
\end{aligned} \tag{6.27}
$$

To obtain the result for high frequency signal, we use the certain approximations such that $\omega \gg \omega_c$, while keeping it at the same order with ω_p, yielding the $\varepsilon_1 \approx 1 - (\omega_p/\omega)^2$ and $\varepsilon_2 \to 0$ in the limit case. After approximations, the Wiener-Hopf

functional equations are computed as follows :

$$e^{\iota\alpha l}\mathcal{F}'_+(\alpha,0) + e^{-\iota\alpha l}\mathcal{F}'_-(\alpha,0) + \mathcal{S}(\alpha)\tilde{\mathcal{F}}_l(\alpha,0) = \frac{1}{2}\left[\mathcal{F}'_{inc}(\alpha,0) - \mathcal{F}'_{ref}(\alpha,0)\right]$$
$$+ \frac{\iota k_{eff}^2\eta_s}{2k}\left[\mathcal{F}_{inc}(\alpha,0) - \mathcal{F}_{ref}(\alpha,0)\right], \tag{6.28}$$

$$e^{\iota\alpha l}\mathcal{F}_+(\alpha,0) + e^{-\iota\alpha l}\mathcal{F}_-(\alpha,0) + \mathcal{K}(\alpha)\tilde{\mathcal{F}}'_l(\alpha,0) = -\frac{\iota k}{2k_{eff}^2\eta_s}\left[\mathcal{F}'_{inc}(\alpha,0) + \mathcal{F}'_{ref}(\alpha,0)\right]$$
$$+ \frac{1}{2}\left[\mathcal{F}_{inc}(\alpha,0) + \mathcal{F}_{ref}(\alpha,0)\right], \tag{6.29}$$

where

$$\tilde{\mathcal{F}}_l(\alpha,0) = \frac{1}{2}\left[\mathcal{F}_l\left(\alpha,0^+\right) + \mathcal{F}_l\left(\alpha,0^-\right)\right], \tag{6.30}$$

$$\tilde{\mathcal{F}}'_l(\alpha,0) = \frac{1}{2}\left[\mathcal{F}'_l\left(\alpha,0^+\right) + \mathcal{F}'_l\left(\alpha,0^-\right)\right], \tag{6.31}$$

$$A_1(\alpha) = -\tilde{\mathcal{F}}_l(\alpha,0) + \frac{\tilde{\mathcal{F}}'_l(\alpha,0)}{\iota\gamma(\alpha)}, \tag{6.32}$$

$$A_2(\alpha) = -\tilde{\mathcal{F}}_l(\alpha,0) - \frac{\tilde{\mathcal{F}}'_l(\alpha,0)}{\iota\gamma(\alpha)}. \tag{6.33}$$

The kernel factors appearing in the coupled system of Wiener-Hopf equations are as follows :

$$\mathcal{S}(\alpha) = -\iota\gamma(\alpha)\mathcal{L}(\alpha), \tag{6.34}$$

$$\mathcal{K}(\alpha) = \frac{\iota k}{k_{eff}^2\eta_s}\mathcal{L}(\alpha), \tag{6.35}$$

where

$$\mathcal{L}(\alpha) = \left(1 + \frac{k_{eff}^2\eta_s}{k\gamma(\alpha)}\right), \tag{6.36}$$

6.5 Wiener-Hopf Procedure

The main objective of this model is to observe the behavior of EM-wave incident on a slit of finite width (which is an ultimate result in the form of diffracted field)
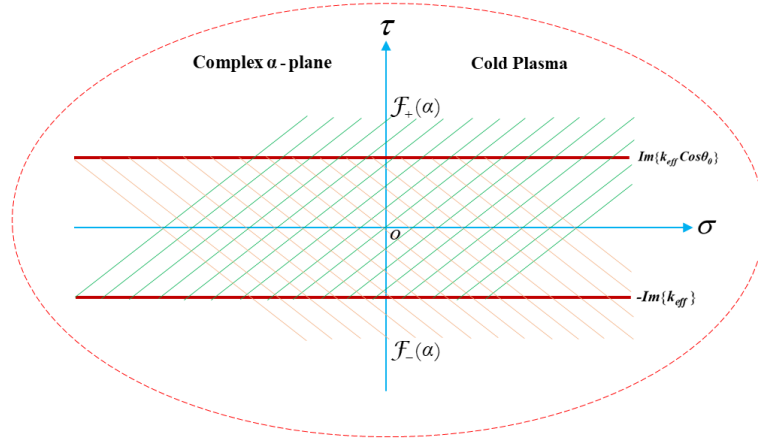
Figure 6.2: **The description of analytic continuation in the complex $\alpha-$plane.**

immersed in cold plasma. The functional Wiener-Hopf equations (6.28) and (6.29) for the boundary value problem are put to rigorous analysis through Wiener-Hopf method. The salient fact of this analysis is that its procedure is not a fundamentally numerical technique in nature that's why it predicts an additional physics of the problem and mathematical structure for diffracted field of incident EM-wave. The kernel functions arising from (6.28) and (6.29) presented by (6.34) and (6.35) are decomposed as

$$\mathcal{S}\left(\alpha\right) = \mathcal{S}_{+}\left(\alpha\right)\mathcal{S}_{-}\left(\alpha\right), \tag{6.37}$$

$$\mathcal{K}\left(\alpha\right) = \mathcal{K}_{+}\left(\alpha\right)\mathcal{K}_{-}\left(\alpha\right), \tag{6.38}$$

and the factors appearing in (6.37) and (6.38) are computed as

$$\mathcal{S}_{\pm}\left(\alpha\right) = e^{-\iota\frac{\pi}{4}}\gamma_{\pm}\left(\alpha\right)\mathcal{L}_{\pm}, \tag{6.39}$$

$$\mathcal{K}_{\pm}\left(\alpha\right) = \frac{e^{\iota\frac{\pi}{4}}\sqrt{k}}{k_{eff}\sqrt{\eta_s}}\mathcal{L}_{\pm}\left(\alpha\right). \tag{6.40}$$

Furthermore, the product decomposition of the function presented by (6.37) is formed as

$$\mathcal{L}\left(\alpha\right) = \mathcal{L}_{+}\left(\alpha\right)\mathcal{L}_{-}\left(\alpha\right), \tag{6.41}$$

where

$$\mathcal{L}_{\pm}(\alpha) = \left(1 \pm \frac{\iota k_{eff}\sqrt{\eta_s}}{\sqrt{k}\gamma_{\pm}(\alpha)}\right), \tag{6.42}$$

and

$$\gamma_{\pm}(\alpha) = \sqrt{k_{eff} \pm \alpha}, \tag{6.43}$$

where the factors with subscript $+$ are regular functions of α in upper half of complex $\alpha-$plane $(-\mathfrak{Im}\{k_{eff}\} < \mathfrak{Im}\{\alpha\})$, $\mathcal{F}_{-}(\alpha, y)$ whereas the factors with subscript $-$ are regular functions of α in the lower half of complex $\alpha-$plane $(\mathfrak{Im}\{\alpha\} < \mathfrak{Im}\{k_{eff}\cos\theta_0\})$.

Now using (6.21) and (6.22) in both (6.28) and (6.29), we get

$$e^{\iota\alpha l}\mathcal{F}'_{+}(\alpha, 0) + e^{-\iota\alpha l}\mathcal{F}'_{-}(\alpha, 0) + \mathcal{S}(\alpha)\tilde{\mathcal{F}}_l(\alpha, 0) = \mathcal{A}\mathcal{G}(\alpha), \tag{6.44}$$

$$e^{\iota\alpha l}\mathcal{F}_{+}(\alpha, 0) + e^{-\iota\alpha l}\mathcal{F}_{-}(\alpha, 0) + \mathcal{K}(\alpha)\tilde{\mathcal{F}}'_l(\alpha, 0) = \mathcal{A}'\mathcal{G}'(\alpha), \tag{6.45}$$

where

$$\mathcal{A} = \frac{1}{2}\left[-\left(1 + \frac{\eta_s\sin\theta_0 - 1}{\eta_s\sin\theta_0 + 1}\right)k_{eff}\sin\theta_0 + \frac{k_{eff}^2\eta_s}{k}\left(1 - \frac{\eta_s\sin\theta_0 - 1}{\eta_s\sin\theta_0 + 1}\right)\right], \tag{6.46}$$

$$\mathcal{A}' = \frac{1}{2}\left[\frac{\iota k\sin\theta_0}{k_{eff}\eta_s}\left(1 + \frac{\eta_s\sin\theta_0 - 1}{\eta_s\sin\theta_0 + 1}\right) + \frac{1}{\iota}\left(1 - \frac{\eta_s\sin\theta_0 - 1}{\eta_s\sin\theta_0 + 1}\right)\right], \tag{6.47}$$

$$\mathcal{G}(\alpha) = \mathcal{G}'(\alpha) = \frac{e^{\iota l\left(\alpha - k_{eff}\cos\theta_0\right)} - e^{-\iota l\left(\alpha - k_{eff}\cos\theta_0\right)}}{\sqrt{2\pi}(\alpha - k_{eff}\cos\theta_0)}. \tag{6.48}$$

Inserting $\tilde{\mathcal{F}}_l(\alpha, 0)$ and $\tilde{\mathcal{F}}'_l(\alpha, 0)$ explicitly from (6.44) and (6.45) into (6.32) and (6.33), we get

$$A_1(\alpha) = \frac{1}{\mathcal{S}(\alpha)}\left\{e^{\iota\alpha l}\mathcal{F}'_{+}(\alpha, 0) + e^{-\iota\alpha l}\mathcal{F}'_{-}(\alpha, 0) - \mathcal{A}\mathcal{G}(\alpha)\right\}$$
$$- \frac{1}{\iota\gamma(\alpha)\mathcal{K}(\alpha)}\left\{e^{\iota\alpha l}\mathcal{F}_{+}(\alpha, 0) + e^{-\iota\alpha l}\mathcal{F}_{-}(\alpha, 0) - \mathcal{A}'\mathcal{G}'(\alpha)\right\}, \tag{6.49}$$

$$A_2(\alpha) = \frac{1}{\mathcal{S}(\alpha)}\left\{e^{\iota\alpha l}\mathcal{F}'_{+}(\alpha, 0) + e^{-\iota\alpha l}\mathcal{F}'_{-}(\alpha, 0) - \mathcal{A}\mathcal{G}(\alpha)\right\}$$
$$+ \frac{1}{\iota\gamma(\alpha)\mathcal{K}(\alpha)}\left\{e^{\iota\alpha l}\mathcal{F}_{+}(\alpha, 0) + e^{-\iota\alpha l}\mathcal{F}_{-}(\alpha, 0) - \mathcal{A}'\mathcal{G}'(\alpha)\right\}, \tag{6.50}$$

The Wiener-Hopf equations presented by (6.44) and (6.45) are derived through the general theory of Wiener-Hopf procedure and an exact and asymptotic solution may be obtained for large $k_{eff}r$ $\left(r = \sqrt{x^2 + y^2}\right)$. Now equating the terms of (6.47) and (6.48) with positive sign on one side of the equation and the terms with negative sign on the other side give us consequently the same function, say $\mathcal{J}(\alpha)$, which is a polynomial function so is an entire function. Analytic continuation (see Fig. 6.2) along with arguments involving extended form of Liouville's theorem allows the function $\mathcal{J}(\alpha)$ to equate to zero, finally we obtain the following results

$$\mathcal{F}'_+(\alpha, 0) = \frac{\mathcal{A}\mathcal{S}_+(\alpha)}{\sqrt{2\pi}}\left(\mathcal{G}_1(\alpha) + \mathcal{T}(\alpha)\mathcal{C}_1\right), \tag{6.51}$$

$$\mathcal{F}'_-(\alpha, 0) = \frac{\mathcal{A}\mathcal{S}_-(\alpha)}{\sqrt{2\pi}}\left(\mathcal{G}_2(-\alpha) + \mathcal{T}(-\alpha)\mathcal{C}_2\right), \tag{6.52}$$

$$\mathcal{F}_+(\alpha, 0) = \frac{\mathcal{A}'\mathcal{K}_+(\alpha)}{\sqrt{2\pi}}\left(\mathcal{G}'_1(\alpha) + \mathcal{T}'(\alpha)\mathcal{C}'_1\right), \tag{6.53}$$

$$\mathcal{F}_-(\alpha, 0) = \frac{\mathcal{A}'\mathcal{K}_-(\alpha)}{\sqrt{2\pi}}\left(\mathcal{G}'_2(-\alpha) + \mathcal{T}'(-\alpha)\mathcal{C}'_2\right), \tag{6.54}$$

where

$$\mathcal{G}_1(\alpha) = \frac{e^{-\iota l k_{eff}\cos\theta_0}}{(\alpha - k_{eff}\cos\theta_0)}\left(\frac{1}{\mathcal{S}_+(\alpha)} - \frac{1}{\mathcal{S}_+(k_{eff}\cos\theta_0)}\right) - e^{\iota l k_{eff}\cos\theta_0}\mathcal{R}_1(\alpha), \tag{6.55}$$

$$\mathcal{G}_2(\alpha) = \frac{e^{\iota l k_{eff}\cos\theta_0}}{(\alpha + k_{eff}\cos\theta_0)}\left(\frac{1}{\mathcal{S}_+(\alpha)} - \frac{1}{\mathcal{S}_+(-k_{eff}\cos\theta_0)}\right) - e^{-\iota l k_{eff}\cos\theta_0}\mathcal{R}_2(\alpha), \tag{6.56}$$

$$\mathcal{C}_1 = \mathcal{S}_+(k_{eff})\left(\frac{\mathcal{G}_2(k_{eff}) + \mathcal{S}_+(k_{eff})\mathcal{G}_1(k_{eff})\mathcal{T}(k_{eff})}{1 - \mathcal{S}_+^2(k_{eff})\mathcal{T}^2(k_{eff})}\right), \tag{6.57}$$

$$\mathcal{C}_2 = \mathcal{S}_+(k_{eff})\left(\frac{\mathcal{G}_1(k_{eff}) + \mathcal{S}_+(k_{eff})\mathcal{G}_2(k_{eff})\mathcal{T}(k_{eff})}{1 - \mathcal{S}_+^2(k_{eff})\mathcal{T}^2(k_{eff})}\right), \tag{6.58}$$

$$\mathcal{G}'_1(\alpha) = \frac{e^{-\iota l k_{eff}\cos\theta_0}}{(\alpha - k_{eff}\cos\theta_0)}\left(\frac{1}{\mathcal{K}_+(\alpha)} - \frac{1}{\mathcal{K}_+(k_{eff}\cos\theta_0)}\right) - e^{\iota l k_{eff}\cos\theta_0}\mathcal{R}_1(\alpha), \tag{6.59}$$

$$\mathcal{G}'_2(\alpha) = \frac{e^{\iota l k_{eff}\cos\theta_0}}{(\alpha + k_{eff}\cos\theta_0)}\left(\frac{1}{\mathcal{K}_+(\alpha)} - \frac{1}{\mathcal{K}_+(-k_{eff}\cos\theta_0)}\right) - e^{-\iota l k_{eff}\cos\theta_0}\mathcal{R}_2(\alpha), \tag{6.60}$$

$$\mathcal{C}'_1 = \mathcal{K}_+\left(k_{eff}\right)\left(\frac{\mathcal{G}_2\left(k_{eff}\right) + \mathcal{K}_+\left(k_{eff}\right)\mathcal{G}_1\left(k_{eff}\right)\mathcal{T}\left(k_{eff}\right)}{1 - \mathcal{K}_+^2\left(k_{eff}\right)\mathcal{T}^2\left(k_{eff}\right)}\right), \qquad (6.61)$$

$$\mathcal{C}'_2 = \mathcal{K}_+\left(k_{eff}\right)\left(\frac{\mathcal{G}_1\left(k_{eff}\right) + \mathcal{K}_+\left(k_{eff}\right)\mathcal{G}_2\left(k_{eff}\right)\mathcal{T}\left(k_{eff}\right)}{1 - \mathcal{K}_+^2\left(k_{eff}\right)\mathcal{T}^2\left(k_{eff}\right)}\right), \qquad (6.62)$$

$$\mathcal{R}_{1,2}\left(\alpha\right) = \frac{E_{-1}\left[\mathcal{W}_{-1}\left(-\iota l\left(k_{eff} \pm k_{eff}\cos\theta_0\right)\right) - \mathcal{W}_{-1}\left(-\iota l\left(k_{eff} + \alpha\right)\right)\right]}{2\pi\iota\left(\alpha \mp k_{eff}\cos\theta_0\right)}, \qquad (6.63)$$

$$\mathcal{T}\left(\alpha\right) = \frac{1}{2\pi\iota}E_{-1}\mathcal{W}_{-1}\left(-\iota\left(k_{eff} + \alpha\right)l\right), \qquad (6.64)$$

$$E_{-1} = 2\exp\left(\iota k_{eff}l\right)\left(l\right)^{\frac{1}{2}}\left(\iota\right)^{-\frac{1}{2}}, \qquad (6.65)$$

and

$$\begin{aligned}
\mathcal{W}_{n-\frac{1}{2}}\left(s\right) &= \int_0^\infty \frac{v^n\exp\left(-v\right)}{v + s}du \\
&= \Gamma\left(n+1\right)\exp\left(\frac{s}{2}\right)p^{\frac{1}{2}n-\frac{1}{2}}\mathcal{W}_{-\frac{1}{2}\left(n+1\right),\frac{1}{2}n}\left(s\right).
\end{aligned} \qquad (6.66)$$

Here, $\mathcal{W}_{m,n}$ is named as Whittaker function and $p = -\iota\left(k_{eff} + \alpha\right)l$, $n = -\frac{1}{2}$.

Now substitution of (6.51)-(6.54) along with (6.48) in (6.49) and (6.50) gives the result as

$$
\left.\begin{array}{c} A_1\left(\alpha\right) \\ A_2\left(\alpha\right) \end{array}\right\} = \frac{\mathcal{A}}{\sqrt{2\pi}\mathcal{S}\left(\alpha\right)} \left\{ \begin{array}{c} e^{\iota\alpha l}\mathcal{S}_+\left(\alpha\right)\mathcal{G}_1\left(\alpha\right) + e^{\iota\alpha l}\mathcal{S}_+\left(\alpha\right)\mathcal{T}\left(\alpha\right)\mathcal{C}_1 \\ +e^{-\iota\alpha l}\mathcal{S}_-\left(\alpha\right)\mathcal{G}_2\left(-\alpha\right) \\ +e^{-\iota\alpha l}\mathcal{S}_-\left(\alpha\right)\mathcal{T}\left(-\alpha\right)\mathcal{C}_2 \\ -\frac{e^{\iota l\left(\alpha-k_{eff}\cos\theta_0\right)}-e^{-\iota l\left(\alpha-k_{eff}\cos\theta_0\right)}}{\left(\alpha-k_{eff}\cos\theta_0\right)} \end{array} \right\}
$$
$$
\qquad\qquad -\frac{\mathcal{A}'Sgn\left(y\right)}{\sqrt{2\pi}\iota\gamma\left(\alpha\right)\mathcal{K}\left(\alpha\right)} \left\{ \begin{array}{c} e^{\iota\alpha l}\mathcal{K}_+\left(\alpha\right)\mathcal{G}_1'\left(\alpha\right) + e^{\iota\alpha l}\mathcal{K}_+\left(\alpha\right)\mathcal{T}\left(\alpha\right)\mathcal{C}_1' \\ +e^{-\iota\alpha l}\mathcal{K}_-\left(\alpha\right)\mathcal{G}_2'\left(-\alpha\right) \\ +e^{-\iota\alpha l}\mathcal{K}_-\left(\alpha\right)\mathcal{T}\left(-\alpha\right)\mathcal{C}_2' \\ -\frac{e^{\iota l\left(\alpha-k_{eff}\cos\theta_0\right)}-e^{-\iota l\left(\alpha-k_{eff}\cos\theta_0\right)}}{\left(\alpha-k_{eff}\cos\theta_0\right)}, \end{array} \right\}
$$

(6.67)

The diffraction of EM-wave field obtained by the implementation of inverse Fourier transform of (6.24) is defined as

$$
\begin{aligned}
H_z(x,y) &= \frac{1}{\sqrt{2\pi}}\int_{-\infty}^{\infty} \mathcal{F}\left(\alpha,y\right)e^{-\iota\alpha x}d\alpha \\
&= \frac{1}{\sqrt{2\pi}}\int_{-\infty}^{\infty} \left\{ \begin{array}{c} A_1\left(\alpha\right) \\ A_2\left(\alpha\right) \end{array} \right\} e^{-\iota\alpha x-\iota\gamma|y|}d\alpha.
\end{aligned}
$$

(6.68)

where $A_1\left(\alpha\right)$ and $A_2\left(\alpha\right)$ are given by (6.67). Substitution of (6.67) into (6.68) and splitting up the diffracted field function $H_z(x,y)$ into two parts as are mentioned here

$$
H_z(x,y) = H_z^{sep}(x,y) + H_z^{int}(x,y),
$$

(6.69)

where

$$H_z^{sep}(x,y) = \frac{1}{2\pi} \int\limits_{-\infty}^{\infty} \frac{1}{\mathcal{S}(\alpha)} \left(\begin{array}{c} -\dfrac{\mathcal{A}\mathcal{S}_+(\alpha)e^{\iota l\left(\alpha - k_{eff}\cos\theta_0\right)}}{\left(\alpha - k_{eff}\cos\theta_0\right)\mathcal{S}_+\left(k_{eff}\cos\theta_0\right)} \\ +\dfrac{\mathcal{A}\mathcal{S}_-(\alpha)e^{-\iota l\left(\alpha - k_{eff}\cos\theta_0\right)}}{\left(\alpha - k_{eff}\cos\theta_0\right)\mathcal{S}_+\left(-k_{eff}\cos\theta_0\right)} \end{array} \right) e^{\left(-\iota\alpha x - \iota\gamma|y|\right)} d\alpha$$

$$+ \frac{sgn(y)}{2\pi} \int\limits_{-\infty}^{\infty} \frac{1}{\iota\gamma(\alpha)\mathcal{K}(\alpha)} \left(\begin{array}{c} \dfrac{\mathcal{A}'\mathcal{K}_+(\alpha)e^{\iota l\left(\alpha - k_{eff}\cos\theta_0\right)}}{\left(\alpha - k_{eff}\cos\theta_0\right)\mathcal{K}_+\left(k_{eff}\cos\theta_0\right)} \\ -\dfrac{\mathcal{A}'\mathcal{K}_-(\alpha)e^{-\iota l\left(\alpha - k_{eff}\cos\theta_0\right)}}{\left(\alpha - k_{eff}\cos\theta_0\right)\mathcal{K}_+\left(-k_{eff}\cos\theta_0\right)} \end{array} \right) e^{\left(-\iota\alpha x - \iota\gamma|y|\right)} d\alpha, \tag{6.70}$$

and

$$H_z^{int}(x,y) = \frac{1}{2\pi} \int\limits_{-\infty}^{\infty} \frac{\mathcal{A}}{\mathcal{S}(\alpha)} \left(\begin{array}{c} -\mathcal{S}_+(\alpha)\,\mathcal{R}_1(\alpha)\,e^{\iota l(\alpha + k_{eff}\cos\theta_0)} \\ +\mathcal{S}_+(\alpha)\,\mathcal{T}(\alpha)\,\mathcal{C}_1 e^{\iota\alpha l} \\ -\mathcal{S}_+(-\alpha)\,\mathcal{R}_2(-\alpha)\,e^{-\iota l(\alpha + k_{eff}\cos\theta_0)} \\ +\mathcal{S}_+(-\alpha)\,\mathcal{T}(-\alpha)\,\mathcal{C}_2 e^{-\iota\alpha l} \end{array} \right) e^{\left(-\iota\alpha x - \iota\gamma|y|\right)} d\alpha$$

$$+ \frac{sgn(y)}{2\pi} \int\limits_{-\infty}^{\infty} \frac{\mathcal{A}'}{\iota\gamma(\alpha)\mathcal{K}(\alpha)} \left(\begin{array}{c} \mathcal{K}_+(\alpha)\,\mathcal{R}_1(\alpha)\,e^{\iota l(\alpha + k_{eff}\cos\theta_0)} \\ -\mathcal{K}_+(\alpha)\,\mathcal{T}(\alpha)\,\mathcal{C}_1' e^{\iota\alpha l} \\ +\mathcal{K}_+(-\alpha)\,\mathcal{R}_2(-\alpha)\,e^{-\iota l(\alpha + k_{eff}\cos\theta_0)} \\ -\mathcal{K}_+(-\alpha)\,\mathcal{T}(-\alpha)\,\mathcal{C}_2' e^{-\iota\alpha l} \end{array} \right) e^{\left(-\iota\alpha x - \iota\gamma|y|\right)} d\alpha. \tag{6.71}$$

In above (6.71) $H_z^{sep}(x,y)$ has two integrals in which the integrand with kernel function $\mathcal{S}(\alpha)$ has two parts one for the edge $x = l$ and other for edge $x = -l$ of the slit, similarly, integrand with kernel function $\mathcal{K}(\alpha)$ has two parts one for the edge $x = l$ and other for edge $x = -l$, so evaluation of integrals will give the diffracted field for $x = l$ as well as for $x = -l$ whereas $H_z^{int}(x,y)$ presented by (6.72) also have two integrands with kernels $\mathcal{S}(\alpha)$ and $\mathcal{K}(\alpha)$. Each integrand with its respective kernel functions $\mathcal{S}(\alpha)$ and $\mathcal{K}(\alpha)$ have two parts and on evaluating the integrals, one will give the interaction field due extremity $x = 0$ of slit and other for the interaction field due to extremity $x = -l$ of the slit.

6.6 Acquirement of Diffracted Field

Now the diffracted field in the far field zone may be evaluated asymptotically. For this purpose, the polar coordinates as $x = r\cos\theta$, $|y| = r\sin\theta$ are introduced and following transformation helps in the deformation of contour.

$$\alpha = -k_{eff}\cos(\theta + i\zeta), \quad \text{for } 0 < \theta < \pi, \ -\infty < \zeta < \infty. \tag{6.72}$$

Now applying the method of stationary phase for large $k_{eff}r$, (6.68) takes the following form

$$H_z(r,\theta) = \frac{\iota k_{eff}}{\sqrt{k_{eff}r}} \left\{ \begin{array}{c} A_1\left(-k_{eff}\cos\theta\right) \\ A_2\left(-k_{eff}\cos\theta\right) \end{array} \right\} \sin\theta \exp\left(\iota k_{eff}r + \iota\frac{\pi}{4}\right). \tag{6.73}$$

Similarly, integrals appearing in (6.70) and (6.71) are evaluated asymptotically using the method of stationary phase as follows :

$$H_z^{sep}(r,\theta) = \frac{1}{\sqrt{2\pi}} \frac{\iota k_{eff}}{\sqrt{k_{eff}r}} \big\{ - sgn(\theta)\, \psi^{sep}\left(-k_{eff}\cos\theta\right)$$
$$+ \phi^{sep}\left(-k_{eff}\cos\theta\right) \big\} \sin\theta \exp\left(\iota k_{eff}r + \iota\frac{\pi}{4}\right), \tag{6.74}$$

and

$$H_z^{int}(r,\theta) = \frac{1}{\sqrt{2\pi}} \frac{\iota k_{eff}}{\sqrt{k_{eff}r}} \big\{ - sgn(\theta)\, \psi^{int}\left(-k_{eff}\cos\theta\right)$$
$$+ \phi^{int}\left(-k_{eff}\cos\theta\right) \big\} \sin\theta \exp\left(\iota k_{eff}r + \iota\frac{\pi}{4}\right), \tag{6.75}$$

where

$$\psi^{sep}\left(-k_{eff}\cos\theta\right) = \frac{\mathcal{A}\mathcal{S}_+\left(-k_{eff}\cos\theta\right)e^{\iota l\left(-k_{eff}\cos\theta - k_{eff}\cos\theta_0\right)}}{\mathcal{S}\left(-k_{eff}\cos\theta\right)\left(-k_{eff}\cos\theta - k_{eff}\cos\theta_0\right)\mathcal{S}_+\left(k_{eff}\cos\theta_0\right)}$$
$$- \frac{\mathcal{A}\mathcal{S}_-\left(-k_{eff}\cos\theta\right)e^{-\iota l\left(-k_{eff}\cos\theta - k_{eff}\cos\theta_0\right)}}{\mathcal{S}\left(-k_{eff}\cos\theta\right)\left(-k_{eff}\cos\theta - k_{eff}\cos\theta_0\right)\mathcal{S}_+\left(-k_{eff}\cos\theta_0\right)}, \tag{6.76}$$

and

$$\phi^{sep}\left(-k_{eff}\cos\theta\right)=\frac{\mathcal{A}'\mathcal{K}_{+}\left(-k_{eff}\cos\theta\right)e^{-\iota l\left(-k_{eff}\cos\theta-k_{eff}\cos\theta_0\right)}}{\iota\gamma\left(-k_{eff}\cos\theta\right)\mathcal{K}\left(-k_{eff}\cos\theta\right)\left(-k_{eff}\cos\theta-k_{eff}\cos\theta_0\right)\mathcal{K}_{+}\left(k_{eff}\cos\theta_0\right)}$$

$$-\frac{\mathcal{A}'\mathcal{K}_{-}\left(k_{eff}\cos\theta\right)e^{-\iota l\left(-k_{eff}\cos\theta-k_{eff}\cos\theta_0\right)}}{\iota\gamma\left(-k_{eff}\cos\theta\right)\mathcal{K}\left(-k_{eff}\cos\theta\right)\left(-k_{eff}\cos\theta-k_{eff}\cos\theta_0\right)\mathcal{K}_{+}\left(-k_{eff}\cos\theta_0\right)},$$

$$(6.77)$$

$$\psi^{int}\left(-k_{eff}\cos\theta\right)=\frac{\mathcal{A}}{\mathcal{S}\left(-k_{eff}\cos\theta\right)}$$

$$\times\begin{pmatrix}\mathcal{S}_{+}\left(-k_{eff}\cos\theta\right)\mathcal{R}_{1}\left(-k_{eff}\cos\theta\right)e^{-\iota l(-k_{eff}\cos\theta+k_{eff}\cos\theta_0)}\\ -\mathcal{S}_{+}\left(-k_{eff}\cos\theta\right)\mathcal{T}\left(-k_{eff}\cos\theta\right)\mathcal{C}_{1}e^{-\iota lk_{eff}\cos\theta}\\ +\mathcal{S}_{-}\left(-k_{eff}\cos\theta\right)\mathcal{R}_{2}\left(k_{eff}\cos\theta\right)e^{-\iota l(-k_{eff}\cos\theta-k_{eff}\cos\theta_0)}\\ -\mathcal{S}_{-}\left(-k_{eff}\cos\theta\right)\mathcal{T}\left(k_{eff}\cos\theta\right)\mathcal{C}_{2}e^{\iota lk_{eff}\cos\theta}\end{pmatrix},$$

$$(6.78)$$

$$\phi^{int}\left(-k_{eff}\cos\theta\right)=\frac{\mathcal{A}'}{\mathcal{K}\left(-k_{eff}\cos\theta\right)}$$

$$\times\begin{pmatrix}\mathcal{K}_{+}\left(-k_{eff}\cos\theta\right)\mathcal{R}_{1}\left(-k_{eff}\cos\theta\right)e^{\iota l(-k_{eff}\cos\theta+k_{eff}\cos\theta_0)}\\ -\mathcal{K}_{+}\left(-k_{eff}\cos\theta\right)\mathcal{T}\left(-k_{eff}\cos\theta\right)\mathcal{C}_{1}'e^{-\iota lk_{eff}\cos\theta}\\ +\mathcal{K}_{-}\left(-k_{eff}\cos\theta\right)\mathcal{R}_{2}\left(k_{eff}\cos\theta\right)e^{-\iota l(-k_{eff}\cos\theta+k_{eff}\cos\theta_0)}\\ -\mathcal{K}_{-}\left(-k_{eff}\cos\theta\right)\mathcal{T}\left(k_{eff}\cos\theta\right)\mathcal{C}_{2}'e^{\iota lk_{eff}\cos\theta}\end{pmatrix}.$$

$$(6.79)$$

The result given by (6.74) presents the diffracted field evaluated asymptotically for $k_{eff}r\longrightarrow\infty$. In fact, it is the asymptotic form of $H_z(x,y)$ valid for any value of observation angle in the entire space. It is observed that the wave field diffracted by the slit with edges $x=-l$ and $x=l$ yields the separated field. The separated field provides the physical perception of diffraction phenomenon at defined boundary. Therefore, only the separated field is taken into account for discussion because it describes the physical insight to the diffraction phenomenon. Furthermore, the interaction field generated as a result of double diffraction of EM-wave by two edges is already counted in the form of separated field by the slit with edges at $x=-l$

and $x = l$. Also, expanding the slit width upto infinity discards the contribution of interaction quantities and consequently, the separated field appears to be diffracted field. Therefore, only the separated field is focused to discuss graphically here in the next section.

6.7   Results and Discussion

This section elaborates the graphical behavior of separated field versus angle of observation for different physical parameters as angle of incidence θ_0, wave-number k, width of slit $2l$, surface impedance η_s and permittivity element ε_1 in the presence and absence of cold plasma. Figs. 6.3a, 6.3b display the behavior of separated field for varying values of θ_0 while keeping all other parameters fixed. The observation predicts that separated field intensity gets sharp peaks at $\theta = 2\pi/3, 3\pi/4, 5\pi/6$ indicating the reflected wave of EM-wave incident at $\theta_0 = \pi/3, \pi/4, \pi/6$, respectively. The structure of slit of finite width under consideration over here may work for physical aspect of scattering mechanism at these particular values of observation angles. The maximum sharp peak occurs at observation angle $\theta = 5\pi/6$ for respective incidence angle $\theta_0 = \pi/6$ in the absence of cold plasma but presence of cold plasma grabs this position and gives it to the observation angle $\theta = 2\pi/3$ for its respective incidence angle $\theta_0 = \pi/3$. It is also observed that separated field gets more fluctuated in the region of far away from the origin which does not happen in case of finite plate. Figs. 6.4a, 6.4b are sketched to display behavior of separated field for different values of wave-number. For increasing the wave-number, oscillations of separated field are increased. This means that wave frequency moves towards the high frequency range. In Figs. 6.5a, 6.5b, the separated field for different values of width of slit is observed. According to observation, the separated field gets more oscillated for expanding the width of slit. Figs. $4.6a, 4.6b$ show the separated field for real (surface resistance), pure imaginary (surface reactance) and imaginary values (both surface resistance and surface reactance) of surface impedance. The separated field for real and pure

imaginary surface impedance are summed up giving separated field very close to that for the real surface impedance. From the figures it can be predicted that oscillations or separated field are reduced. Fig. 6.7 is sketched to show the behavior of separated field for ε_1. It is observed that presence of cold plasma has affected the separated field drastically. Since $\varepsilon_1 \approx 1 - (\omega_p/\omega)^2$ (for signal with high frequency) so an increase in plasma permittivity ε_1 while keeping the number density of ions and electrons fixed in cold plasma, that's why separated field is predicted to be more oscillated for ε_1. The electrons oscillate about cold ionic centers due to electric field of high frequency signal and these oscillating electrons scatter enormously due to increasing oscillations of the separated field. The separated field shows the nullity around the observation angle of 0 for all physical parameters corresponding to the present model.
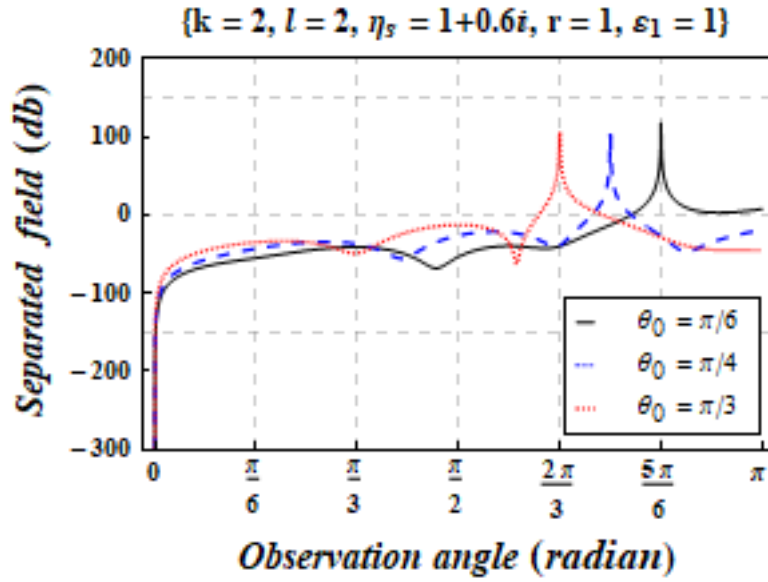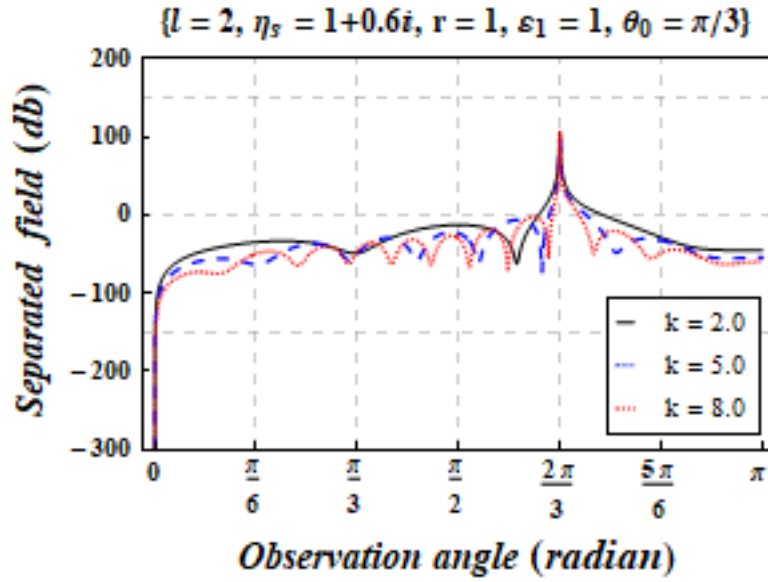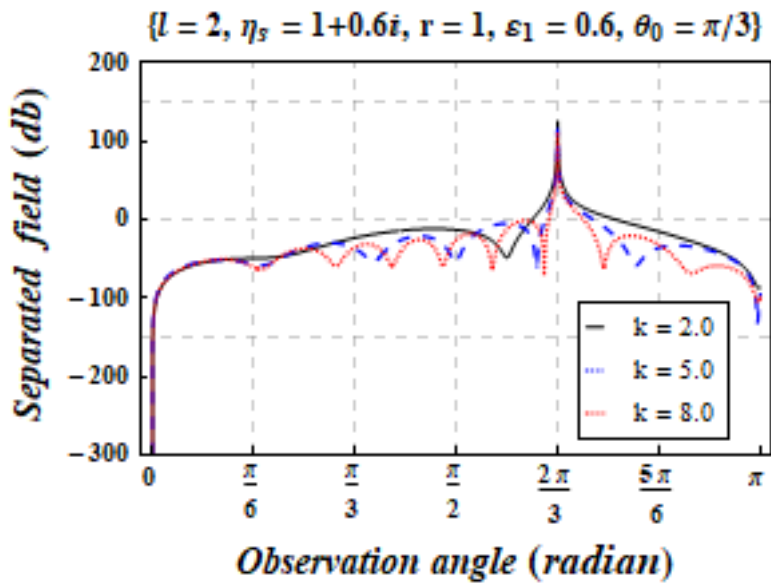
(a)
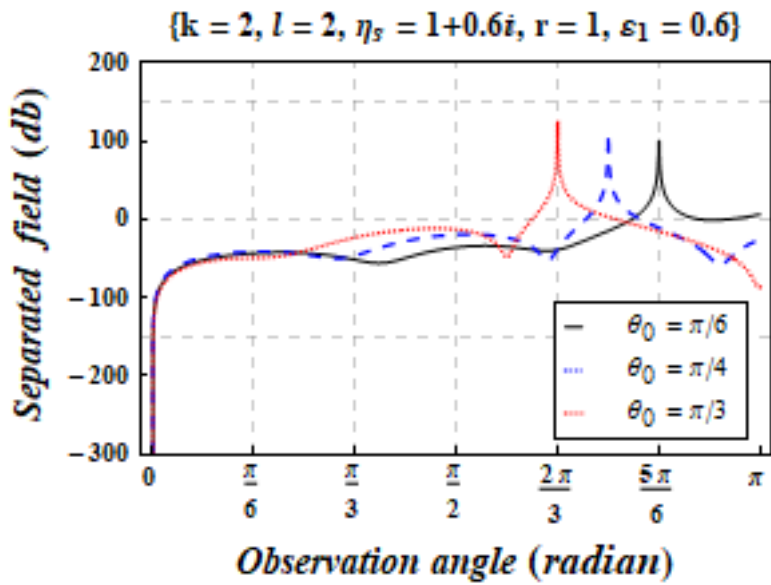
(b)

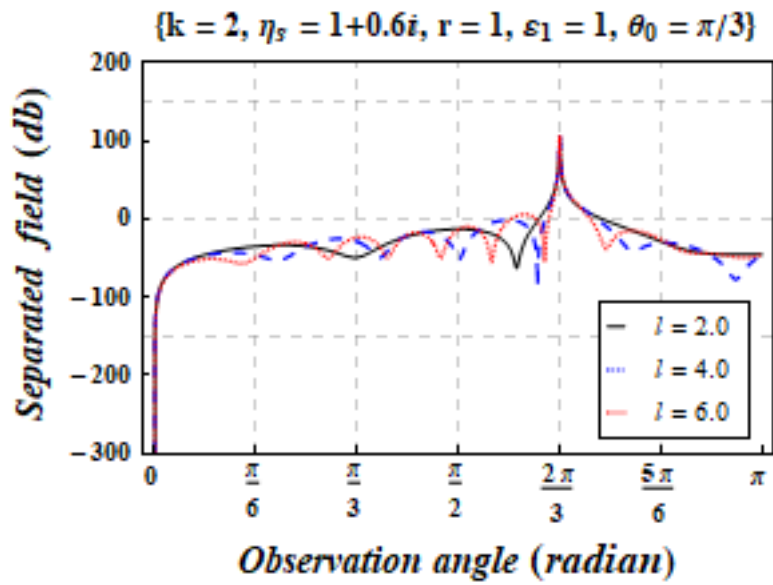Figure 6.3: **The separated field with incident angle in the absence (a) and presence (b) of cold plasma.**

{$l = 2$, $\eta_s = 1+0.6i$, r = 1, $\varepsilon_1 = 1$, $\theta_0 = \pi/3$}

(a)

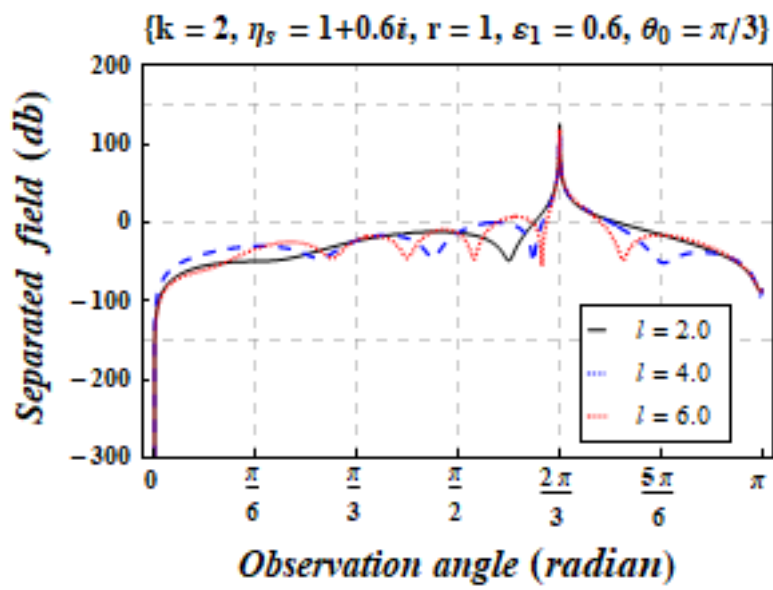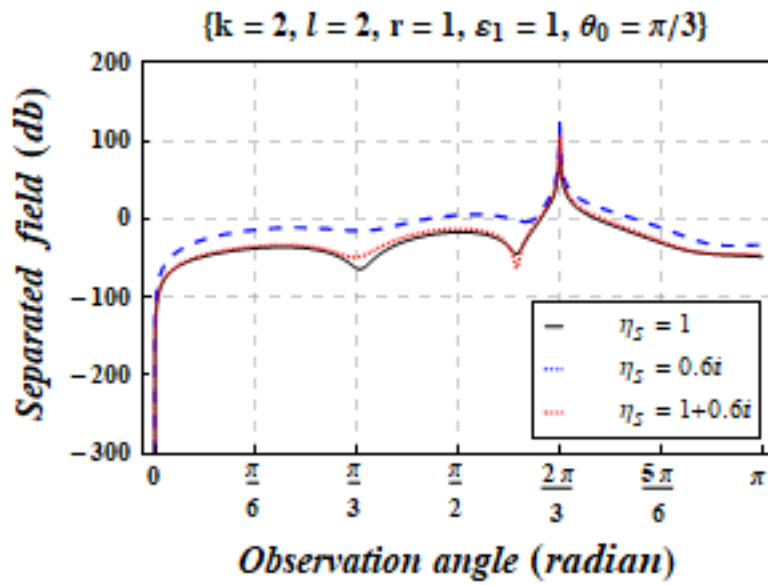{$l = 2$, $\eta_s = 1+0.6i$, r = 1, $\varepsilon_1 = 0.6$, $\theta_0 = \pi/3$}

(b)

Figure 6.4: **The separated field for wave-number in the absence (a) and presence (b) of cold plasma.**
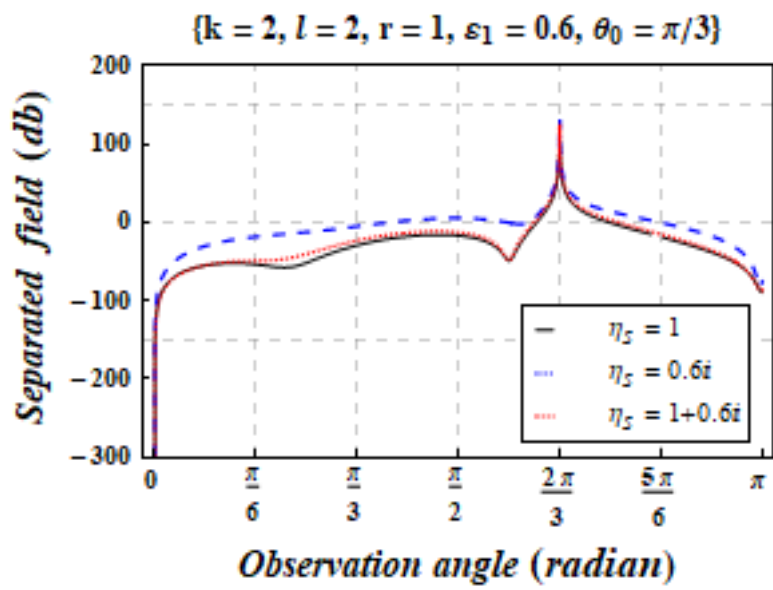
(a)

(b)

Figure 6.5: **The separated field for finite width of slit in the absence (a) and presence (b) of cold plasma.**

(a)

(b)

Figure 6.6: **The separated field for surface impedance in the absence (a) and presence (b) of cold plasma.**
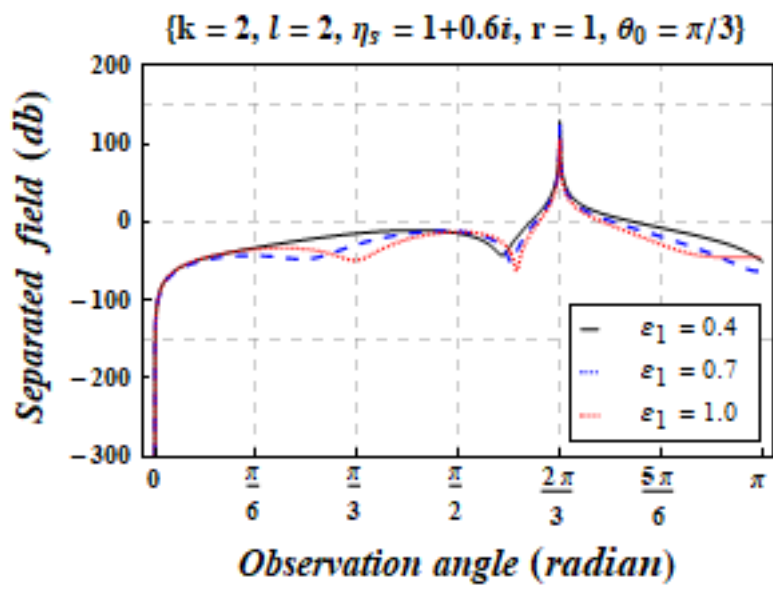
Figure 6.7: **The separated field for ε_1.**

6.8 Conclusions

The chapter has elaborated the diffraction of EM-wave by a slit of finite width with the effect of impedance in the presence of cold plasma. The observation depicts that diffraction of EM-wave has been affected due to (a) the expansion of width of the slit (b) different angles of incidence (c) the variation of wave-number (d) different values of surface impedance and (e) permittivity of cold plasma.

References

[1] H. Poincare, Sur la polarization par diffraction, Acta. Math. 16 (1892) 297–339.

[2] A. Sommerfeld, Mathematische theorie der diffraction. Math. Ann. 47 (1896) 317–374.

[3] B. Nobel, Methods Based on the Wiener–Hopf Technique, Pergamon, London, (1958).

[4] R. Mittra and S. W. Lee, Analytical Technique in the Theory of Guided Waves, Macmillan, New York, 1971.

[5] V. P. Shestopalov, The Riemann-Hilbert Method in the Theory of Diffraction and Propagation of Electromagnetic Waves, Kharkov University Press, Kharkov, 1971.

[6] Y. Okuno, Analysis Methods for Electromagnetic Wave Problems, Artech House, Boston, 1990.

[7] K. Kobayashi, Plane wave diffraction by a strip: Exact and asymptotic solutions, J. Phys. Soc. Japan, 60 (1991) 1891–1905.

[8] J. B. Lawrie and I. D. Abrahams, A brief historical perspective of Wiener–Hopf technique. Journal of Engineering Mathematics 59 (2007) 351–358.

[9] R. Nawaz, M. Ayub and Javaid, Plane wave diffraction by a finite plate with impedance boundary conditions, PloS ONE 9 (2014) 1–13.

[10] P. M. Morse and P. J. Rubenstein, The diffraction of waves by ribbon and slits, Phys. Rev. (1938) 895.

[11] P. C. Clemmow, The Plane Wave Spectrum Representation of Electromagnetic Field, Pergamon, New York, (1966).

[12] K. Hongo, Diffraction of electromagnetic plane wave by two parallel infinitely long slits in a thin conducting screen, Trans. Inst. Electronics and Comm. Engrg. in Japan 57-B (1974) 565–572.

[13] A. Imran, Q. A. Naqvi and K. Hongo, Diffraction of plane wave by two parallel slits in an infinitely long impedance plane using the method of Kobayashi potential, Progress In Electromagnetic Research 63 (2006) $107 - 123$.

[14] M. K. Tippett and R. W. Ziolkowski, A Bidirectional Wave Transformation of The Cold-Plasma Equations, Journal of Mathematical Physics 32 (1991) $488 - 492$.

[15] A. D. Avdeev, On the Special Function of the Problem of Diffraction by a Wedge in an Anisotropic-Plasma, Radio Tekhnika I Elektronika 39 (1994) $885 - 892$.

[16] S. L. Dvorak, R. W. Ziolkowski and D. G. Dudley, Ultra-Wide-Band Electromagnetic Pulse Propagation in a Homogeneous Cold Plasma, Radio Science 32 (1997) $239 - 250$.

[17] S. Yener and A. H. Serbest, Diffraction of Plane Wave by an Impedance Half-Plane in Cold Plasma, J. of Electromagn. Waves and Appl. 16 (2002) $995 - 1005$.

[18] Tufail A. Khan, M. Ayub and K. Jilani, E-polarized plane wave diffraction by an impedance loaded parallel-plate waveguide located in cold plasma, Phys. Scr 89 (2014) $01 - 09$.

[19] M. Ayub, T. A. Khan and K. Jilani, Effect of cold plasma permittivity on the radiation of the dominant TEM-wave by an impedance loaded parallel-plate waveguide radiator, Math. Meth. Appl. Sci. 39 (2015) $134 - 143$.

[20] S. Hussain, M. Ayub and G. Rasool, EM-Wave Diffraction by a Finite Plate with Dirichlet Conditions in the Ionosphere of Cold Plasma, Physics of Wave Phenomena 26 (2018) 342 − 350.

[21] C. E. Pearson, G. F. Carrier and M. Krook, Functions of a Complex Variable: Theory and Technique, McGraw-Hill, New York, (1966).

[22] E.T. Copson, Asymptotic Expansions, University Press, Cambridge, (1967).

turnitin Turnitin Originality Report

Wiener-Hopf Analysis of EM-Wave Diffraction by a Finite Plate in Cold Plasma by Sajjad Hussain .

From DRSM (DRSM L)

- Processed on 21-Dec-2020 12:30 PKT
- ID: 1479991508
- Word Count: 21580

Author: Sajjad Hussain

Similarity Index
17%
Similarity by Source

Internet Sources:
        8%
Publications:
        14%
Student Papers:
        3%

Focal Person (Turnitin)
Quaid-i-Azam University
Islamabad

sources:
1

2% match (publications)

Nawaz, Rab, Muhammad Ayub, and Akmal Javaid. "Plane Wave Diffraction by a Finite Plate with Impedance Boundary Conditions", PLoS ONE, 2014.
2

1% match (publications)

Tufail A Khan, M Ayub, K Jilani. "E-polarized plane wave diffraction by an impedance loaded parallel-plate waveguide located in cold plasma", Physica Scripta, 2014
3

1% match (Internet from 17-Jul-2020)

http://dep1.iszf.irk.ru/en/aggregator/sources/51?page=1
4

1% match (publications)

E. Kochneff. "Expansions in Jacobi Polynomials of Negative Order", Constructive Approximation, 1997
5

1% match (publications)

E. Stride. "Investigating the significance of multiple scattering in ultrasound contrast agent particle populations", IEEE Transactions on Ultrasonics Ferroelectrics and Frequency Control, 12/2005
6

1% match (Internet from 07-Sep-2010)